NTNU – Trondheim
Norwegian University of
Science and Technology

Screening of Inhibitors for Amine Degradation

Jørund Elnan

Chemical Engineering and Biotechnology
Submission date: June 2012
Supervisor: Bård Helge Hoff, IKJ
Co-supervisor: Hallvard Svendsen, IKP
Solrun Johanne Vevelstad, IKP

Norwegian University of Science and Technology
Department of Chemistry

Acknowledgments

This master's thesis was carried out at the Department of Chemistry at the Norwegian University of Science and Technology (NTNU) during the spring of 2012. This thesis is written for the subject TKJ4900 and was carried out at the Department of Chemical Engineering in the Environmental Engineering and Reactor Technology group.

I would like to thank my supervisors, Hallvard F. Svendsen and Bård H. Hoff, for giving me the opportunity to do this thesis. I would also like to thank my co-supervisor, PhD candidate Solrun Johanne Vevelstad, for supervision, help with this report and scientific discussions.

I declare that this is an independent work according to the exam regulations of the Norwegian University of Science and Technology.

Jørund Elnan
Trondheim 14.06.2012

Abstract

Hindering the degradation of amines in the CO_2-capturing process is important both for economical purposes when it comes to loss of solvent and impacts on the process, and to prevent emissions of volatile degradation compounds such as ammonia, nitrosamines and formaldehyde. To prevent the absorbent from degrading, either a non-degrading absorbent can be developed or a degradation inhibitor can be added to minimize the degradation.

The degradation inhibitors tested in this thesis are meant to inhibit the oxidative degradation that mainly occurs in the absorber. The carbamate polymerization degradation due to CO_2 and temperature has to be addressed on its own. The inhibitor screening apparatus was new, and a part of the assignment was testing this setup.

The first experiment conducted on the inhibitor screening apparatus used a gas blend of 6% O_2/2 % CO_2 (N_2 balance). This did not give enough degradation, which caused the need for rebuilding the rig. In the other experiments on the screening apparatus, a gas composition of 98 % O_2/2 % CO_2 was used to get sufficient amount of degradation for inhibitor screening. Inhibitor screening experiments were done using 150 mL of a 30 weight% (wt%) 2-aminoethanol (MEA) solution loaded with 0,4 mol CO_2/mol MEA, at 55 °C with a gas flow of 10 mL/min. To test the stability of the inhibitors at higher temperature, thermal experiments with inhibitors were conducted. 7 mL solution was filled in stainless steel cylinders and heated at 135 °C, for a period of five weeks. The solution was 30 wt% MEA loaded with 0,5 mol CO_2/mol MEA. Hydrazine was screened for inhibitory effect using a circulative closed loop apparatus because of the hazards related to this compound. The experiment was run with air, using a 30 wt% MEA solution loaded with 0,4 mol CO_2/mol MEA, at 55 °C.

Since experiments with both 6 % and 98 % oxygen were conducted, it was natural to compare the impact of oxygen concentration on the degradation products. Results indicated that 2-oxazolidinone (OZD) was preferred at the conditions with high oxygen, while N-(2-hydroxyethyl) glycine (HeGly) concentrations increased with decreasing oxygen content. The effect of metals on product composition was also investigated. The degradation compound N-(2-hydroxyethyl) imidazole (HEI) seems to be dependent on the metal concentrations, increasing in the presence of metals. For the inhibitors screened, the inhibition ranged from 23,59-67,81 %. Two compounds gave an increase in degradation. 1-hydroxyethane 1,1-diphosphonic acid (HEDP) was the only chelating agent stable at thermal conditions. The inhibitors did not appear to have a substantial effect on the carbamate polymerization.

Quantification of degradation compounds in the samples was done using liquid chromatography-mass spectrometry (LC-MS) and anion chromatography-electrochemical detector (IC-EC). Amine loss and CO_2-loading were determined using titration methods. Metal concentrations were determined using inductively coupled plasma-mass spectrometry (ICP-MS). Some analyses were done gravimetrically while

others were done volumetrically. For comparison purposes, simple density measurements were done, and the data converted according to the amine loss in the sample.

The initial intention was to use gas chromatography - mass spectrometry (GC-MS) to analyze the samples from the thermal experiments. The system was however not operable during the time available. ICP-MS analysis was not done in time for the last experiment. Ammonia analyses were not conducted in time for this thesis.

Samandrag

Å hindre degradering av aminer i CO_2-reinsing er viktig både på grunn av økonomiske faktorar som tap av amin og operasjonelle konsekvensar for prosessen, og for å hindre utslepp av flyktige degraderingsprodukt som ammoniakk, nitrosaminer og formaldehyd. For å forhindre absorbenten frå å degradere, kan anten ein ikkje-degraderande absorbent utviklast, eller ein inhibitor kan tilsetjast for å minimere degraderinga.

Degraderingsinhibitorane som er testa i denne oppgåva er først og fremst meint for å inhibere den oksidative degraderinga som føregår i absorberen. Karbamatpolymeriseringa grunna CO_2 og temperatur må sjåast på separat. Inhibitor screening apparaturen var utesta før denne oppgåva, og ein del av oppgåva var å teste denne.

Det fyrste eksperimentet utført på inhibitor screening apparaturen brukte ei gassblanding av 6 % O_2/2 % CO_2 (resten N_2). Dette gav ikkje nok degradering, noko som gav eit behov for å bygge om riggen. I dei andre eksperimenta på screening apparaturen vart ei gassblanding av 98 % O_2/2 % CO_2 nytta for å få nok degradering til å teste inhibitorar. Eksperimenta der inhibitorane vart testa brukte ei 30 vekt% løysing av 2-aminoetanol (MEA) i avionisert vatn, loada med 0,4 mol CO_2/mol MEA, ved ein temperatur på 55 °C og ein gasstraum på 10 mL/min. For å teste stabiliteten til inhibitorane ved høgare temperaturar vart termiske eksperiment med inhibitorar vart utførd i 7 mL rustfrie stålsylindrar ved 135 °C, over ein periode på fem veker. For dette vart det brukt ei 30 vekt% MEA løysing loada med 0,5 mol CO_2/mol MEA. Hydrazin vart testa for inhiberande effekt ved å bruke ein sirkulativ lukka sløyfe apparatur. Årsaka til at dette stoffet ikkje vart testa i screeningsapparaturen var at dette stoffet er ansett som eit potensielt karsinogen. Dette eksperimentet vart kjørt med luft, med ei 30 vekt% MEA løysing loada med 0,4 mol CO_2/mol MEA, og temperaturen var på 50-55 °C.

Sidan eksperiment med både 6 % og 98 % oksygen vart utførde var det naturleg å samanlikna desse resultata og sjå kva verknad oksygenkonsentrasjonen har på degraderingsprodukta. Resultata tyda på at OZD var føretrukken ved høg oksygenkonsentrasjon, medan HeGly konsentrasjonane auka med minkande oksygenkonsentrasjon. Effekten av tilsats av metaller vart òg undersøkt. Degraderingsproduktet N-(2-hydroksyetyl) imidazol HEI ser ut til auke ved tilsats av metaller. For inhibitorane som vart testa, vart degraderinga hindra med 23,59-67,81 %. To inhibitorar gav ei auke i degraderinga. Stabiliteten til dei chelaterande inhibitorane vart testa, der HEDP var den einaste som var stabil ved termiske betingingar. Ingen av inhibitorane såg ut til å ha nokon spesiell verknad på den termiske karbamatpolymeriseringa.

Kvantifisering av degraderingsprodukt vart gjort med væskekromatografi-massespektrometri (LC-MS) og ionekromatografi-elektrokjemisk detektor (IC-EC). Amintap og CO_2-innhald vart bestemd ved titreringsmetodar. Metallkonsentrasjonane vart bestemt med bruk av induktivt kopla plasma-massespektrometri (ICP-MS). Nokon

analysar vart gjort på vektbasis, medan andre vart gjort på volumbasis. For samanlikningsføremål vart enkle tettleiksmålingar gjort og dataa vart omgjorte i samsvar med amintapet i prøven.

I utgangspunktet var det meininga å bruke gasskromatografi-massespektrometri (GC-MS) for å analysere prøvane frå dei termiske eksperimenta. Dette systemet var midlertidig ute av drift, så desse analysane kunne ikkje gjennomførast. ICP-MS analysane for det siste eksperimentet vart ikkje utførte i tide for det siste eksperimentet. Kvantifisering av ammoniakk i væskefasen vart heller ikkje utført i tide for denne oppgåva.

Table of contents

Nomenclature

Eq	Equivalence factor	
h	Hours	
L	Liter	
M	Molar	mol/L
M	Mega	10^{6}
m	Molal	mol/kg
m	Milli	10^{-3}
mg	Milligram	10^{-3} g
mL	Milliliter	10^{-3} L
min	Minutes	
N	Normality	Eq/L
n	Nano	10^{-9}
ng	Nanograms	10^{-9} g
Ω	Electrical resistance	
ppm	Parts per million	10^{-6}
rpm	Rounds per minute	
µg	Microgram	10^{-6} g
wt %	Weight percent	

Abbreviations

AED	Atomic emission detector
AEHEIA	N-(2-aminoethyl)-N'-(2-hydroxyethyl) imidazolidinone
As	Arsenic
BHEOX	N, N'-bis(2-hydroxyethyl) oxalamide
CO_2	Carbon dioxide
Cr	Chromium
Cu	Copper
DEA	Diethanolamine
DEHA	Diethylhydroxylamine
DGA	Diglycolamine
ELSD	Evaporative light scattering detection
ESI	Electrospray ionization source
Fe	Iron
Fe^{2+}	Ferrous iron
Fe^{3+}	Ferric iron
FTIR	Fourier transform infrared
GC-MS	Gas chromatography-mass spectroscopy
H_2	Hydrogen gas
H^+	Proton
HCl	Hydrochloric acid

HEA	N-(2-hydroxyethyl) acetamide
HEDP	1-hydroxyethane 1,1-diphosphonic acid
HEEDA	N-(2-hydroxyethyl)ethylenediamine
HEF	N-(2-hydroxyethyl)formamide
HeGly	N-(2-hydroxyethyl)glycine
HEHEAA	N-(2-hydroxyethyl)-2-(2-hydroxyethylamino)acetamide
HEI	N-(2-hydroxyethyl)imidazole
HEIA	N-(2-hydroxyethyl)imidazolidinone
HEPO	4-(2-hydroxyethyl)piperazin-2-one
HPLC	High performance liquid chromatography
IC-EC	Ion chromatography-electrochemical detector
ICP-MS	Inductively coupled plasma mass spectrometry
IPCC	Intergovernmental panel on climate change
LC-MS	Liquid chromatography-mass spectroscopy
MDEA	N-methyl diethanolamine
MEA	2-aminoethanol
MEKO	Methylethyl ketoxime
MFC	Mass flow controller
N	Nitrogen
N_2	Nitrogen gas
NaOH	Sodium hydroxide
NDELA	N-nitrosodiethanolamine
Ni	Nickel
O	Oxygen
O_2	Oxygen gas
OH^-	Hydroxide anion
OZD	2-oxazolidinone
P	Phosphorous
RID	Refractive index detector
S	Sulfur
Se	Selenium
V	Vanadium

Introduction

Global atmospheric concentrations of CO_2, methane and nitrous oxide have since 1750 increased markedly as a result of human activity. The increase in CO_2 is primarily a result of land-use change and the use of fossil fuels. Sources of methane and nitrous oxide are mainly due to agriculture. [1]

The atmospheric concentration of CO_2 has increased from 250 ppm in pre-industrial times to 379 ppm in 2005. This exceeds by far the natural variations from the last 650 000 years (determined by ice cores). The average annual CO_2 concentration growth-rate in the period 1995-2005 was larger than the average growth rate since the measures started in 1960. From 1960-2005 the annual carbon dioxide growth rate was 1,4 ppm/year, while it in the period 1995-2005 increased to 1,9 ppm/year. Figure 1 shows the changes in carbon dioxide concentration from the last 10 000 years. [1]

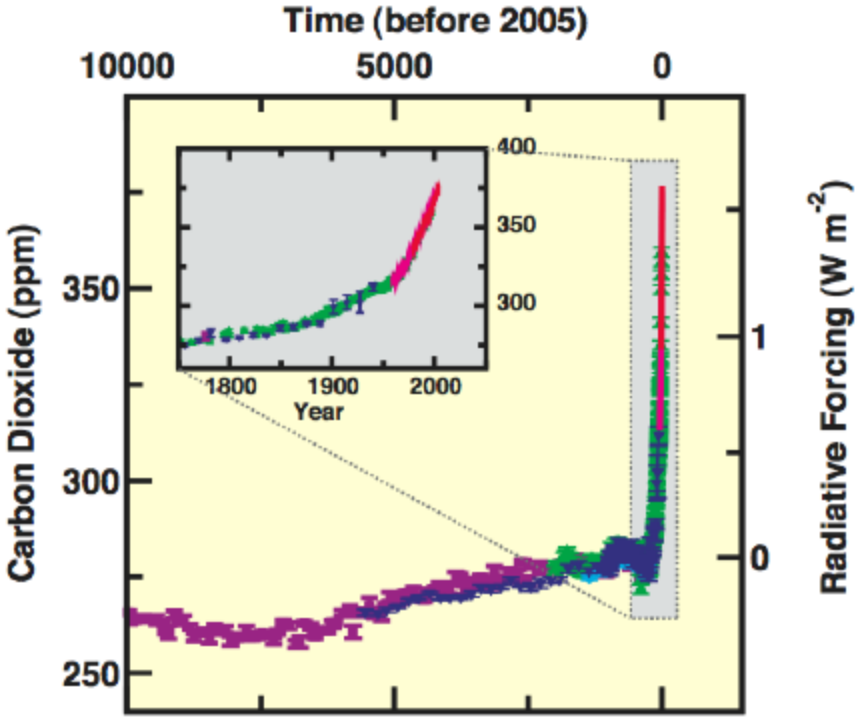

Figure 1: Changes in atmospheric CO_2 from ice-core and modern data. [1]

Radiative forcing is a term employed by the Intergovernmental Panel on Climate Change (IPCC) to denote an externally imposed perturbation in the radiative energy system of the earth's climate. This can be brought about by changes in concentrations of radiatively active species, such as CO_2 and aerosols. It can also be caused by changes in the solar irradiance on the planet, or other changes affecting the reflective properties of the planet's surface, such as land-use change. [1, 2]

The increase in radiative forcing as a result of increased greenhouse gas emissions and deforestation is believed to be the reason for the rising of the earth's average temperature since the late 19th century. This increase in temperature cause glaciers to melt, the sea levels to rise, an expansion of subtropical deserts as well as more extreme weather. The extreme weather includes heat waves, heavy rainfall and droughts. Extinction of species and differences in crop yields are other predicted results due to climate change. [1, 3]

To limit the global warming as a result of anthropogenic greenhouse gas emissions several technologies have been developed. In the case of CO_2-removal from flue gas there are multiple technologies available. These can be classified into three main groups; pre-combustion, post-combustion and oxy-fuel. [4]

The main principle in oxy-fuel technology is to use pure oxygen for the combustion instead of air. This gives a flue gas containing mainly water vapor and CO_2. By condensing the water, a CO_2-rich stream is obtained. In pre-combustion CO_2-capture, the first step is to convert the fossile fuel into CO_2 and H_2 by a steam reforming process. The CO_2 can be captured using post-combustion technology, while the H_2 is used as fuel in for example a gas turbine. Post-combustion CO_2-capturing technology is based on removing the CO_2 after the combustion. Several absorbents are being researched for absorbing CO_2 from the flue gas, among those chilled ammonia and amine absorption. Chemical absorption with amines is recognized as the most cost effective technology available today, and is applicable to already existing plants. [4, 5]

In post-combustion CO_2-capture, the combination of high temperatures, oxygen in the flue gas and dissolved metals cause the amine solution to degrade. The degradation of the amine solution lowers the concentration of amine, thus lowering the capacity of the solution. The performance of the plant can also be affected by the degradation of the amine solution due to increased viscosity, changed vapor-liquid equilibria, increased foaming and increased corrosivity. Formation and emissions of toxic volatile degradation compounds also give cause for concern. The replacement cost for lost amine in a MEA system has been estimated to 4-10% of the total cost. [6-12]

2-aminoalcohol (MEA) is considered to be the benchmark solvent in CO_2-capture because of its good properties; fast absorption rate, cheap, non-volatile. However, this solvent has its flaws. In addition to its high energy requirements in the stripping stage, the degradation and corrosivity of this solvent are important issues for industrial applications. [9, 13]

The use of inhibitors to hinder the oxidative degradation of the amine solution has been proposed as one solution for the problem. Inhibitors are compounds designed to interfere with one or more of the degradation routes to decrease the degradation. [14, 15]

1. Background and theory

In this chapter, some background and theory about the CO_2-absorption process with amines is presented. Then a review of the mechanisms for amine degradation, and earlier studies is presented. Theory of the different types of inhibitors and earlier work on inhibitors is presented in the end of this chapter.

1.1. CO_2-capture with amine absorbents

The process of capturing CO_2 from flue gas using amine absorbents is based on the reversible reaction between the sour gas and a weak base. The equilibrium reactions shown in Equation 1 and Equation 2 are the competing reactions in the process. Which of these are the preferred is dependent on the properties of the amine. These reactions are temperature dependent, and the reverse reaction is favored at higher temperatures. [16]

$$2R_1NH_2 + CO_2 \leftrightharpoons R_1NH_3^+ + R_1NHCO_2^- \quad (1)$$

$$R_1NH_2 + CO_2 + H_2O \leftrightharpoons R_1NH_3^+ + HCO_3^- \quad (2)$$

Here R_1NH_2 is an amine with R_1 and R_2 as side chains.

A simplified scheme of a CO_2-capturing process with amines is shown in Figure 2.

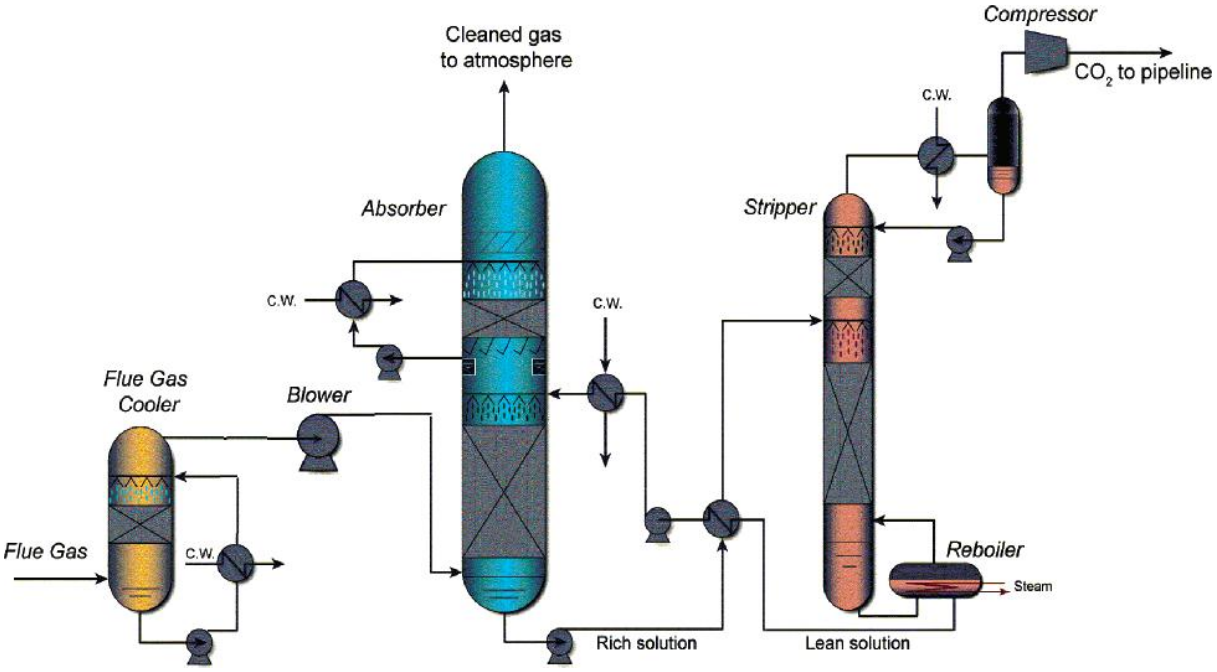

Figure 2: Scheme of a CO_2-capturing plant based on amine technology.[17]

In this process, the first stage is cooling the flue gas with water, before it is introduced to the absorber. In the absorber, the flue gas countercurrently meets an amine solution with contact via a structured packing, and the CO_2 in the flue gas reacts with the amine in the solution. The rest of the flue gas, containing mainly nitrogen and oxygen, leaves

through the top of the absorber, via a washing stage. The purpose of the washing stage is to prevent emissions of water soluble degradation compounds and amine to the atmosphere. The rich amine solution (high loading) goes via a heat exchanger, where it is heated by the stream coming from the stripping stage. The solution is pumped into the top of the stripper, where the equilibrium between CO_2 and amine is reversed using high temperature steam produced in the reboiler. The released CO_2-gas goes through the top of the column and through a condenser where water and other condensable compounds are removed. The gas is compressed and goes to a pipeline. Some of the lean amine solution (low loading) goes to the reboiler where stripping steam is produced, while the rest is transferred back to the absorber. [16]

1.2. Degradation of amine solvents

The degradation of amines in CO_2-capture is related to the conditions found in the capturing plant. Oxidative degradation mainly occurs in the absorber where typical temperatures are 40-60 °C. The carbamate polymerization occurs in the stripper and reboiler where the temperatures usually are 100-125 °C. A thermal degradation, with anaerobic cleavage of the amine bonds, does not occur in significant amounts at the conditions used today. [6, 16, 18]

1.2.1. Oxidative degradation

The oxidative degradation is a result of oxygen from the flue gas reacting with the amine at elevated temperatures. The reaction is assumed to be catalyzed by dissolved metals, and initiated by the formation of radicals. These radicals are believed to be the product of either a direct interaction between a metal ion and the amine, or by an oxidation of variable valence metal ions by dissolved oxygen. [18, 19]

1.2.1.1. Oxidative degradation mechanism

Bedell [18] proposes a mechanism where oxygen from the flue gas is reduced to radicals in a reaction (I) with metal ions. These radicals go on to react with the amine (II) to give degradation products. A scheme of this is shown in Figure 3.

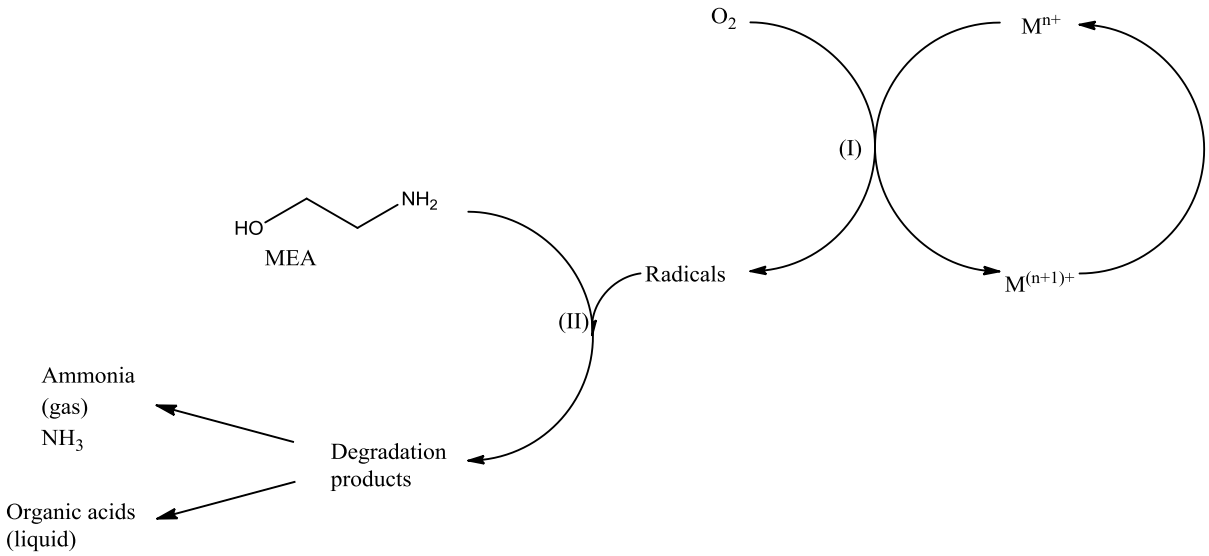

Figure 3: Amine autoxidation overall mechanism, according to Bedell and Aouini. [11, 18]

The reaction between the amine and radicals (II) is believed to go via either the electron- or hydrogen abstraction mechanism.

The electron abstraction mechanism is based on a radical (Fe^{3+} or $R^{\cdot}$) which abstract an electron from the lone pair of the amine nitrogen (I). The abstraction of the proton in α - position of the amine (II), causes a reorganization of the amine, giving a carbon centered radical. This radical can react directly with dissolved oxygen to give a peroxyl radical which decomposes into the degradation products (III). It can react also with another radical to give molecular products (IV). An example of this mechanism with MEA is shown in Figure 4. [20-22]

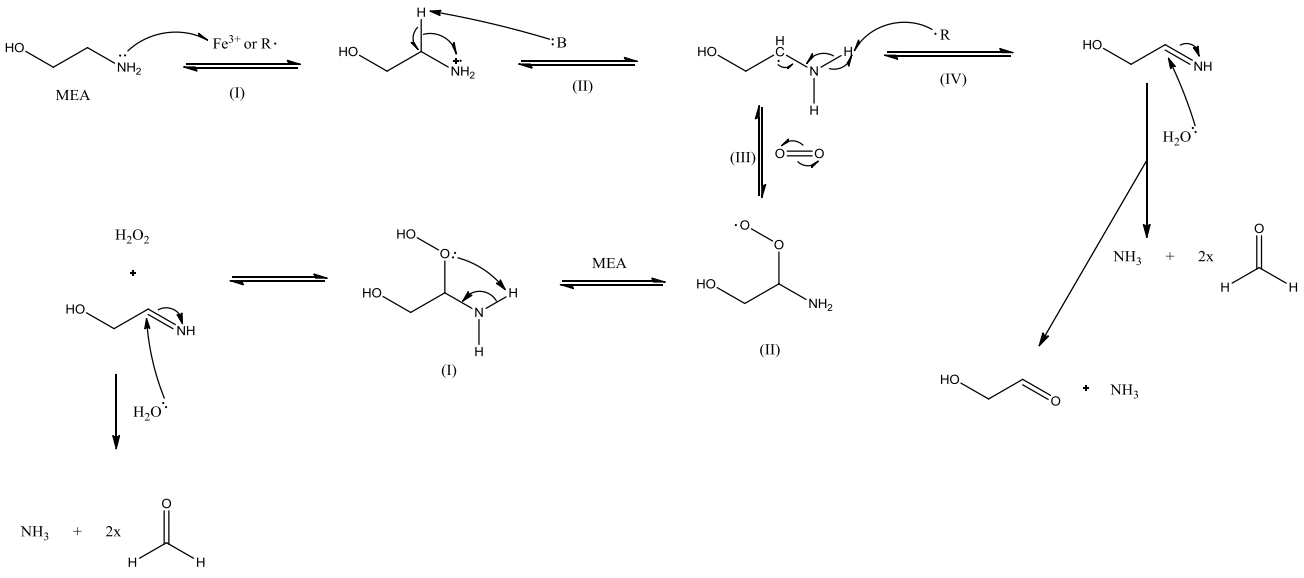

Figure 4: Electron abstraction mechanism according to Chi and Rochelle. [21]

Sexton described another plausible route for the electron abstraction mechanism, without an imine intermediate. This mechanism is given in Figure 5.

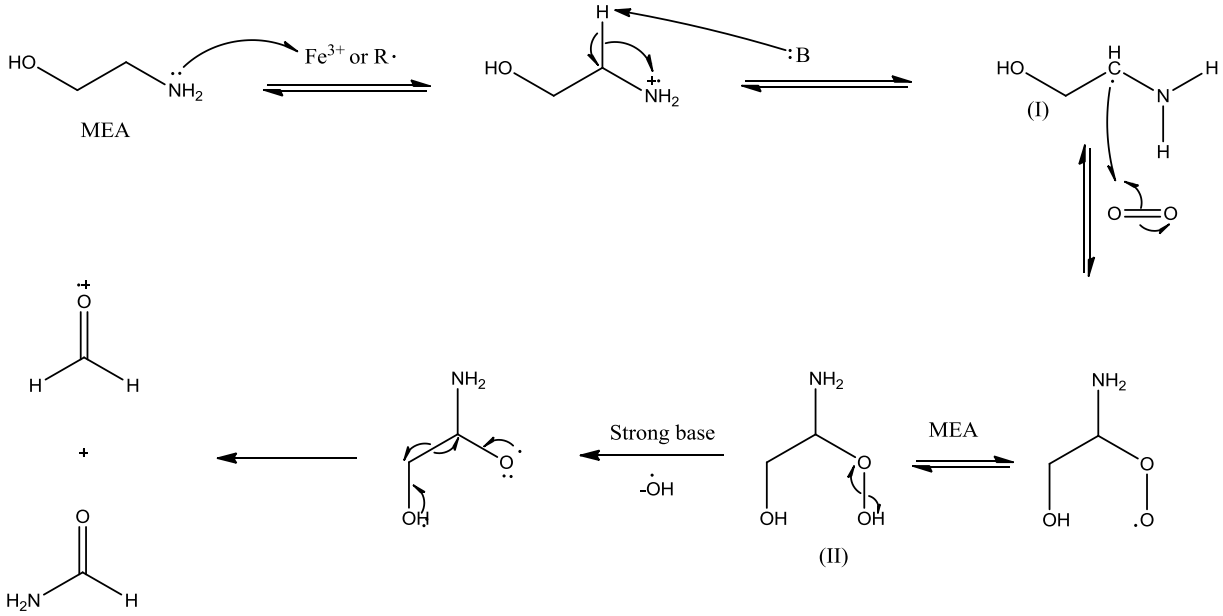

Figure 5: Electron abstraction mechanism described by Sexton. [20]

The difference from the mechanism proposed by Chi and Rochelle is the reaction of the the aminoperoxide (II). The carbon centered imine radical (I) can still lose a proton to form an imine as in Figure 4.

A study by Petryaev et al. [23] claim MEA to degrade via the hydrogen abstraction mechanism. In this study, alkanolamines were degraded using ionizing radiation to form initiating radicals for the reaction. The reaction was proposed to proceed via a five membered ring conformation, formed via the hydrogen bonds between the amine- and alcohol function of the molecule. A radical will abstract a hydrogen radical from the molecule, causing a radical chain reaction within the molecule, resulting in the cleavage of the C-N-bond. [22, 23]

Sexton [20] give the mechanism based on the work by Petryaev et al. [23] shown in Figure 6.

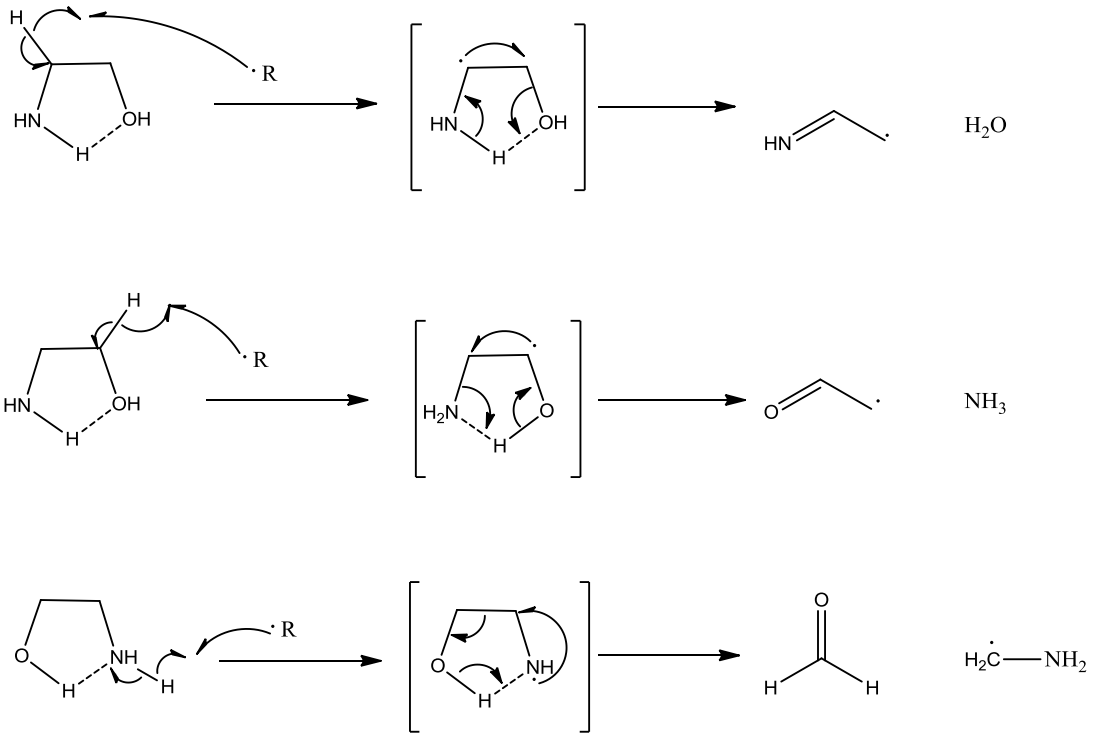

Figure 6: Hydrogen abstraction mechanism given by Sexton [20] based on the work by Petryaev et al. [23]

The radicals formed in these reactions can participate in further oxidation of the solvent by abstracting hydrogens. Imines can hydrolyze to aldehydes, which again can be oxidized to carboxylic acids.

1.2.2. Carbamate polymerization

The degradation in the stripper due to temperature and CO_2 is called carbamate polymerization. This is believed to be initiated by the formation of 2-oxazolidone (OZD), from the cyclization of MEA-carbamate. OZD (1) can react with MEA to give new polymerization products such as 1-(2-hydroxyethyl) imidazolidin-2-one (HEIA, 3), 2-((aminoethyl)aminoethanol (HEEDA, 2) and *N*-(2-aminoethyl)-*N'*-(2-hydroxyethyl) imidazolidinone (AEHEIA, 4). A proposed mechanism for the formation is given in Figure 7. [13, 20]

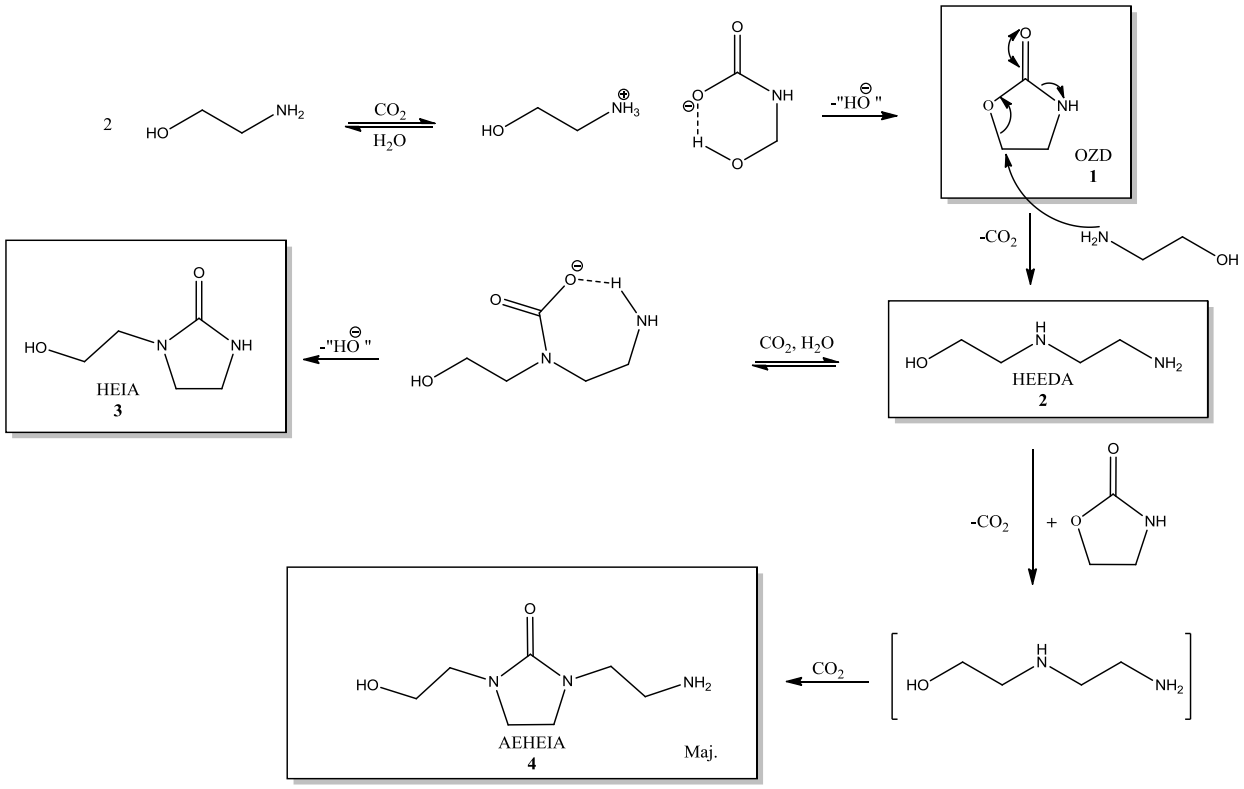

Figure 7: Proposed mechanism for the thermal degradation. [13]

1.2.3. Nitrosamines

Nitrosamines are a class of carcinogenic compounds with the general structure R_1R_2N-N=O. Sun et al. [24] studied the formation of nitrosamines from secondary amines. They found that the nitrosation using a weak nitrosing agent, such as nitrite (NO_2^-) or peroxynitrite ($ONOO^-$), could be catalyzed by carbonyl compounds such as aldehydes and CO_2. Figure 8 shows the mechanism for formation of N-nitrosodiethanolamine (NDELA) from the nitrosation of DEA with nitrite.

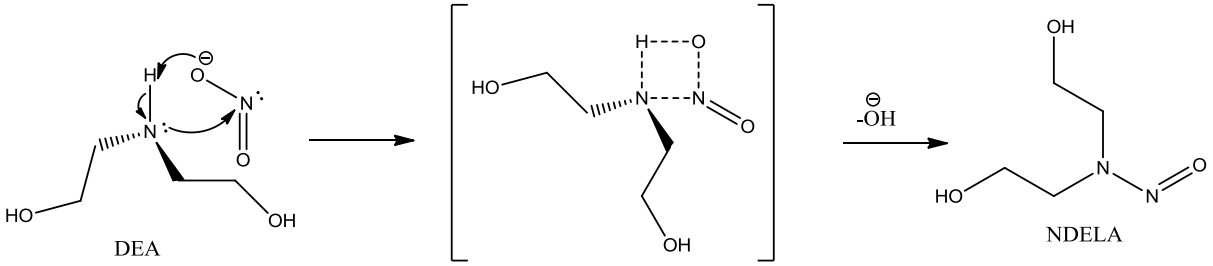

Figure 8: Formation of NDELA from nitrite and DEA.

Nitrite, together with nitrate, is a known oxidation product of ammonia [25, 26], and has earlier been reported as minor products by Voice [8] and Sexton et al. [27, 28]

1.2.4. Earlier studies

Blachly and Ravner [29, 30] conducted experiments by sparging a 4 M MEA solution with 1 mL air/mL solution at 55°C. Evolution of ammonia was measured by trapping in a 2% boric acid solution, peroxide concentrations by iodine-thiosulfate method and total nitrogen using Kjeldahl analysis. This study showed no degradation without CO_2 present in the gas phase.

Rooney [31] studied the degradation of 50% and 30% methyldiethanolamine (MDEA), 30% diehanolamine (DEA), 50% diglycolamine (DGA) and 20% MEA unloaded and loaded with 0,25 mol CO_2/mol amine, over a period of 28 days. These experiments were conducted at 82 °C (180 °F) with a gas flow rate of 5,5 mL/min of compressed air. This study identified acetate, formate, glycolate and oxalate as degradation products. The oxidation resistance was given as DEA>DGA>MEA>MDEA. The amount of anions was reported to be much less for loaded than unloaded solutions of DEA, DGA and MEA. An oxidation route from MEA to oxalic acid was also proposed.

Strazisar [10] analyzed degraded MEA samples from the reclaimer bottoms from the IMC Chemicals Factory in Trona, California. This study focused on identification of degradation compounds. This was done using GC-MS, gas chromatography-Fourier transform infrared (GC-FTIR) and gas chromatography-atomic emission detection (GC-AED). This study identified several new degradation compounds.

Chi and Rochelle [21] studied the oxidative degradation at 55°C using 5 L/min air or nitrogen sparged through a MEA solution using concentrations of 13-42 wt%. The rate of degradation was determined by measuring gas phase ammonia concentration by FTIR. Ferrous iron (Fe^{2+}) was found to have a catalytic effect, increasing the ammonia evolution by a factor of five with the addition of 1 mM iron in a solution loaded with 0,4 mol CO_2/mol MEA. This study saw no difference in adding ferrous- or ferric (Fe^{3+}) iron, as the ferrous would be expected to be oxidized by the oxygen present.

Bello and Idem [32] conducted experiments at 55-120°C, with MEA concentrations of 5 and 7 M with O_2 pressures of 250 and 350 kPa and CO_2-loading ranging from 0-0,44 mol CO_2/mol MEA. Results showed that an increase in temperature or O_2 pressure increased degradation in both loaded and unloaded systems. However, an increase in MEA concentration gave the opposite effect for all the systems.

Goff and Rochelle [22] studied the degradation of 7,0 m MEA at 55 °C, with loadings of 0,15 (lean loading) and 0,40 mol CO_2/mol MEA (rich loading). The gas used was air for the lean loading, and air with 2% CO_2 for the rich loading. The gas flow rates ranged up to 8 L/min. A FTIR was used for gas phase analysis, and ammonia evolution was used as a measure of MEA degradation. This study found that, with iron present, the solution with lean loading degraded more than the one with rich loading. They claimed the rate of ammonia evolution to be dependent on the mass transfer of O_2, and not degradation kinetics.

Sexton and Rochelle [27] studied the degradation of MEA in two experimental setups. One called the low-gas-flow apparatus, using 5 and 7 M MEA with a gas flow of 100 mL/min of a 98% O_2/2% CO_2 gas blend. The other setup, called the high-gas-flow apparatus, a 5 M MEA solution was degraded using a gas flow of 7,5 L/min with a gas consisting of 15% O_2/2% CO_2 (rest N_2). This apparatus was coupled with a FTIR analyzer continuously collecting gas-phase data. Degraded samples were analysed with ion chromatography (IC) and high-performance liquid chromatography (HPLC) with evaporative light scattering detector (ELSD). Formate, N-(2-hydroxyethyl) formamide (HEF), N-(2-hydroxyethyl) imidazole (HEI) and ammonia were found to be the major degradation compounds in this study. Formate, HEF and HEI were found to account for 92% of the degraded carbon in the low gas flow apparatus and 18-59% in the high-gas-flow apparatus. HEF, HEI and ammonia were found to account for 84% of the degradation in the low-gas-flow apparatus and 83-92% in the high gas flow apparatus.

Lepaumier et al. [13] studied oxidative and thermal degradation at 55 and 135 °C respectively. The experiments were conducted using 30 wt% MEA solutions, with loading 0,4 mol CO_2/mol MEA for the oxidative, and 0,5 mol CO_2/mol MEA for the thermal experiments. Quantification of the main degradation compounds were done by GC-MS and LC-MS. When they compared the products from lab experiments with Strazisar [10], they concluded pilot plant degradation to be dominated by products from the oxidative degradation. They also found the reactions between MEA and carboxylic acid degradation products to play a significant role in the degradation.

da Silva et al. [9] analyzed degraded MEA samples from three different pilot plants from Tiller, Esbjerg and Longannet. The samples were compared with lab scale experiments done at oxidative and thermal conditions. Deviations between pilot plant- and lab experiments were thought to be a result of the cycling of the solvent. A new degradation product, N-(2-hydroxyethyl) glycine (HeGly), was found in high concentrations in the pilot plant samples. This was thought as a precursor of another major degradation product 4-(2-hydroxyethyl) piperazin-2-one (HEPO).

1.3. Inhibitors for oxidative degradation

Inhibitors can work via different mechanisms to inhibit the oxidation. The main groups of inhibitors and how they work are presented in this part chapter. A review of earlier studies is also presented.

1.3.1. Radical scavengers

Chain breaking antioxidants, or radical scavengers, react with free radicals to delay or inhibit the initiation step or interrupt the propagation step of autoxidation. This is done by donating a hydrogen atom to the radicals to produce molecular products and low energy antioxidant radicals. The antioxidant radicals can also work in a chain termination step where they react with another radical to give molecular products. For

optimal effect, these inhibitors should be added before the autoxidation reaction begins, as this will quench the initiation step. [33]

Equations 3-8 show reactions between chain breaking antioxidants (AH) and peroxyl radicals (ROO·), alkyl radicals (R·) and alkoxy radicals (RO·). [33, 34]

$$ROO\cdot + AH \rightarrow ROOH + A\cdot \quad (3)$$

$$R\cdot + AH \rightarrow RH + A\cdot \quad (4)$$

$$ROO\cdot + A\cdot \rightarrow ROOA \quad (5)$$

$$RO\cdot + AH \rightarrow RH + A\cdot \quad (6)$$

$$RO\cdot + A\cdot \rightarrow ROA \quad (7)$$

$$A\cdot + A\cdot \rightarrow AA \quad (8)$$

The radical products of the chain breaking antioxidants are low energy molecules which, as long as they are present in low concentrations, should not initiate or participate in autoxidation reactions. If they are present in higher concentrations they can act as pro-oxidants. A such pro-oxidative effect was seen for hydroquinone in the experiments conducted by Goff and Rochelle [14]. At elevated temperatures, the chain breaking antioxidants can lose their efficiency due to homolytic decomposition of the peroxides formed in Equations 3 and 5, and because of reactions with oxygen as shown in Equation 9. [33, 35]

$$AH + O_2 \rightarrow radical\ products \quad (9)$$

Many of the chain breaking antioxidants are mono- or polyhydroxy phenols with various ring substitutions which can influence the reactivity. Molecules with electron donating groups in ortho or para position to the hydroxyl group will increase the antioxidant activity of the compound by inductive effect. [33]

1.3.2. Chelating agents

Since the oxidative degradation is catalyzed by dissolved metals, reducing their activity is a good way to reduce autoxidation of the amines. By adding a compound that tie up the metals, they are prevented from participating in the reactions.

A chelating agent is a molecule that contains two or more electron donating atoms that can form coordination bonds to a metal ion. The resulting complex is called a chelate. This chelate has properties markedly different from both the metal ion and the chelating agents. The chelating agents can therefore be used to control metals in a solution and preventing metal redox cycling. The pro-oxidant activity of the metal is thus reduced by increasing the energy of activation for metal initiated reactions. The amount of chelating groups on one molecule is called the denticity, likewise the number of groups that can coordinate to the metal is called the coordination number. [33, 36, 37]

The equilibrium between the chelating agent, the metal ion and the chelate is dependent on the number of chelating groups of the chelating agent. The equilibrium constants are often magnitudes greater for chelating agents than for complexing molecules containing only one donor atom. The greater stability of the chelate compared to the monodentate complexes is largely a result of an increase in the number of free molecules, usually the solvent, liberated as the chelate is formed. [36]

Molecules having only one donor atom, like water, are called monodentates and can form coordination complexes, but not chelates. The chelating agents can be bidentate, tridentate, tetradentate etc. according to whether they contain two, three, four or more chelating groups. N, O and S are the most common electron donating atoms, but P, Se and As can also form chelates. The most stable compounds form five- or six ringed complexes. Steric hindrance on the chelating compounds can also stabilize the complex from competing ligands. [36]

Metal ions are considered Lewis acids, and the chelating agents Lewis bases. This means that there are competing reactions with other acids and bases in the system, and that the equilibrium changes with the pH. Equations 10-12 show the pH dependency in the equilibrium between a protonated bidentate chelant, A^-, and a tetracoordinated metal ion, M^{2+}.

$$HA \rightleftharpoons H^+ + A^- \qquad K_a = \frac{[H^+][A^-]}{[HA]} \qquad (10)$$

$$M^{2+} + 2A^- \rightleftharpoons MA_2 \qquad K = \frac{[MA_2]}{[M^{2+}][A^-]^2} \qquad (11)$$

Giving the relation:

$$[M^{2+}] = [H^+]^2 \times \frac{[MA_2]}{[HA]^2} \times \frac{1}{K \times K_a^2} \qquad (12)$$

Equation 12 shows that a decrease in pH will cause an increase in the concentration of free metal ions in the solution. Some of the chelating agents have multiple acid dissociation stages and chelates can be formed from the different protonation stages, according to the pH in the solution. The activity is also dependent on the presence of other chelatable ions in the solution. [33, 36, 38]

1.3.3. Oxygen scavengers

Since oxygen is essential to the degradation in the absorber, removing dissolved oxygen is one way to inhibit the degradation. Oxygen scavengers inhibit degradation by reacting with the dissolved oxygen before it can react with the amine. Since the oxygen scavengers are used in the reactions, continuous addition is needed to withhold concentrations. Some of the oxygen scavengers give water soluble oxidation products, which will have to be removed from the solution. [39]

Oxygen scavengers are widely used in steam plants to prevent corrosion. Some of the oxygen scavengers used in these facilities show metal passivating properties. This means that they can reduce metals. [39] In amine systems, this means that the oxygen scavengers can reduce, for example, ferric- to ferrous iron, making the ferric unable to participate in reactions. This gives the inhibitors a combined effect.

1.3.4. Synergy of inhibitors

Synergism is the cooperative effect where an antioxidant together with another antioxidant exhibits a larger inhibitory effect than the sum of the activities of the compounds. This can be through either a catalytic effect, where one of the inhibitors increases the rate of the other, or that the two through different mechanisms increase the total inhibitory effect. [33, 35]

In lipid oxidation in food chemistry, significant synergism is usually observed when a chain breaking antioxidant is used together with a chelating agent or oxygen scavenger. By adding these together both the initiation and the propagation steps are suppressed, and the total effect is increased. It is also possible to use several chain breaking antioxidants in the same system and get a synergistic effect. Since the compounds have different bond dissociation energies, they have different reaction rates with the radicals. This makes it possible for the most reactive of the antioxidants to react with the radicals, while the other is used in a regeneration step of the first inhibitor. [35]

In boiler systems, hydroquinone, a chain breaking antioxidant, can be added together with sodium sulfite, an oxygen scavenger, or diethyl hydroxylamine (DEHA), a radical and oxygen scavenger, to increase the reaction rate with dissolved oxygen. In degradation experiments, by Supap et al., sodium sulfite and potassium sodium tartrate, a chelating agent, were added together to give a combined effect. [15, 39, 40]

1.3.5. Earlier studies

Blachly and Ravner [29, 30] studied the degradation of MEA for submarine CO_2-scrubbers. Experiments were conducted at 55, 98, 138 and 149 °C, using a 4 M MEA solution and a gas consisting of air and 1% CO_2. Of several screened inhibitors, the monosodium salt of N,N-diethanol glycine (VFS) and ethylene diamine tetraacetic acid (EDTA) at 1,5 wt% were found to be the most effective. At 98 °C, in a MEA solution containing metal salts, VFS and EDTA were found to give a synergist effect. With higher temperatures, the inhibitors did not have any effect.

Goff and Rochelle [14, 22] examined the effect of a number of additives on oxidative degradation of MEA in the presence of dissolved copper and iron. Experiments were done using 7,0 m MEA, loaded with 0,4 mol CO_2/mol MEA, 55 °C and the stirring speed of 1450 rpm. Gas used was air with 2 % CO_2 at a flow rate of 8 L/min. Gas phase ammonia analysis by FTIR was used to monitor degradation. An undisclosed compound, inhibitor A, together with sodium sulfite and formaldehyde were found to effectively inhibit degradation at concentrations below 100 mM. EDTA was found to be an effective chelating agent, but unstable. Sodium phosphate was a weak chelating agent. Heat stable

salts were tested for oxygen salting out effect, with the most effective, potassium formate, decreasing degradation with 15 %. Hydroquinone, ascorbic acid, manganese sulfate and potassium permanganate all increased degradation.

Sexton and Rochelle [28] degraded MEA solutions using a 98 % O_2/2 % CO_2 gas at a flow rate of 100 mL/min. Parallel experiments were run using 15 % O_2/2 % CO_2 at a flow rate of 7,5 L/min. The effect of metals as catalysts were assessed, and the oxidative degradation potential was found to be as follows: Cu^{2+}>Cr^{3+}/Ni^{2+}>Fe^{2+}>V^{5+}. In this study, undisclosed inhibitor A and B together with EDTA were all found to be effective degradation inhibitors. Sodium sulfite, formaldehyde and formate were all ineffective as degradation inhibitors.

Supap and Idem [15, 41] investigated O_2 and SO_2 induced degradation of amines in sour gas capture. 3-7 M MEA solutions, loaded with 0-0,52 mol CO_2/mol MEA were used in the experiments at 120 °C (393 K) with a stirring speed of 500 rpm. O_2 and SO_2 concentrations used were 6-100 % and 0-196 ppm respectively (N_2 balance). Sample analysis was conducted on a HPLC with a refractive index detector (RID). Successful inhibitors from this study were sodium sulfite, potassium sodium tartrate, EDTA and hydroxylamine. The optimum concentrations were found to be 0,05, 0,01, 0,0025, and 0,025M respectively. A mix of sodium sulfite and potassium sodium tartrate (0,05 M:0,015 M) was found to be the most efficient. Figure 9 displays the average degradation of a 5 M MEA solution loaded with 0,33 mol CO_2/mol MEA, using 6 % oxygen, 196 ppm SO_2 at 120 °C, with inhibitors added.

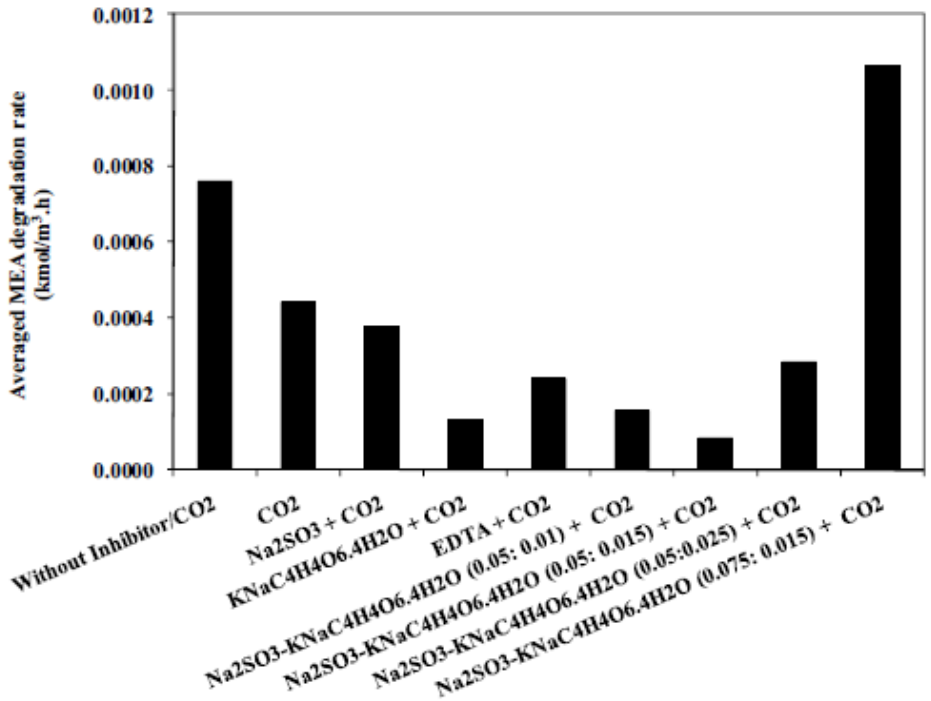

Figure 9: Effect of inhibitors in the presence of CO2 (5 kmol/m³, 6 % O2, 196 ppm SO2, 0.33 CO2 loading, 393 K). [15]

2. Experimental

This part gives an overview of the analytical methods and experimental setups and procedures used to obtain the results in this thesis.

2.1. Analytical methods

Both chromatographic analyses and titration methods were used to analyze the samples from the experiments. The different methods are presented in this chapter.

2.1.1. Chromatographic methods

Different chromatographic methods were used in order to identify and quantify degradation compounds and inhibitors in the experiments. For the experiments regarding oxidative degradation, IC-EC and LC-MS/MS were used to quantify degradation compounds. LC-MS/MS was also used for determining MEA concentrations in selected samples from the thermal degradation experiments. The standards for the analyses are given in Appendix A – Chemicals, while the degradation compounds with structure and analytical method is given in Appendix K: Degradation products.

2.1.1.1. LC-MS/MS

The *Liquid Chromatography* analyses of the degraded samples were carried out on a LC-MS/MS system, 6460 Triple Quadrupole Mass Spectrometer coupled with 1290 Infinity LC Chromatograph and Infinity Autosampler 1200 Series G4226A from the supplier Agilent Technologies. The molecules were converted to ions by an electrospray ionization source (ESI). The analytical column was an Ascentis® Express RP-Amide HPLC Column (4.6 mm*150mm, 2.7 µm, Cat#:53931-U, Supelco Analytical, Bellefonte, USA). The eluent was 25 mM formic acid in water, with a 0.6 ml/min flow rate. For more details around the method used see [9]. Analyses were performed by Kai Vernstad, SINTEF biotechnology.

2.1.1.2. IC-EC

The *Anion Chromatography* analyses were carried out on a Dionex ICS-5000 system equipped with an Autosampler (AS-50), Gradient pump (GP50), Column Oven (TCC-3000), CD conductivity detector, CRD200 carbonate removal device, eluent generator system and a ASR300 suppressor. The column used was an Ion Pac AS11-HC column (2mm*250mm) with an Ion Pac AG11-HC guard column (2mm*50mm). The mobile phase used was potassium hydroxide solution diluted in deionized water (18,2 MΩ) obtained from ICW-3000 water purification system. The system has an eluent generator that was used in a gradient method for separation of the analytes. The samples and standards were prepared using deionized water (18,2 MΩ). The samples from experiments were diluted 1/500 for analyses, except for the experiment using 6% O_2 where the samples were diluted 1/50 due to low degradation. Quantification was done using external standards.

An assessment on the standard deviations for procedures on the IC-EC was performed. These are described in 3.2.5., results are given in part chapter 3.2.3 in Results and discussion.

2.1.1.3. ICP-MS

Inductively coupled plasma mass spectroscopy (ICP-MS) was conducted on the samples for quantification of metals. The metals assessed were iron, chromium and nickel. System used was an Element 2 from Thermo Fisher (Bremen, Germany). Analyses were performed by Per Ole M. Gundersen, St. Olav hospital.

2.1.2. Titration methods

Two different titration methods were used to measure the total alkalinity and CO_2 content in the samples. Assessments on the uncertainties for these methods were performed, and are described in 3.2.5.

2.1.2.1. Total alkalinity titration method

Total alkalinity titration was used to measure the loss of alkalinity in the samples from the experiments. Approximately 0,3 grams of sample was weighed out and diluted in water (50 mL), this was titrated with sulfuric acid (0,2 N) on a Mettler Toledo G20 Compact titrator equipped with a Mettler Toledo Rondolino carousel and a Mettler Toledo DGi115-SC pH probe.

2.1.2.2. CO_2 titration method

To determine the CO_2-concentration in the samples, approximately 0,5 grams of sample was weighed out to a solution consisting of barium chloride (0,1 N, 25 mL) and sodium hydroxide (0,1 N, 50 mL). To precipitate the barium carbonate, the solution was boiled for approximately three minutes. The solution was filtrated, and hydrochloric acid (0,1 N, 40 mL) was weighed in and added to the precipitate. The excess hydrochloric acid was titrated with sodium hydroxide (0,1 N) on a Metrohm 809 Titrando, with a Metrohm 814 Sample processer, a Metrohm 800 Dosino dosing unit and a Metrohm 6.0262.100 pH probe. A blank sample was used to determine the CO_2 concentration in the solutions used for analysis.

2.2. Experimental setups

2.2.1. Inhibitor screening apparatus

The apparatus used for the inhibitor screening experiments was a Heidolph Starfish Multi-Experiment work station with 5 parallels. The magnetic stirrer used was a MR Hei-End, temperature sensor PT1000, with gas coolers used for hindering evaporative losses (400 mm coolers with spiral vapor tubing). The reactors used were three-necked 250 mL round bottom flasks, with connections to a cooler, gas sparger (8*250mm tube with a 25 mm diameter plate of porosity 4), via a porous sinter, and a septum, which allowed for taking samples with a syringe without opening the system. The system was delivered

by Chiron AS. Figure 10 shows a drawing of a reactor on the inhibitor screening apparatus.

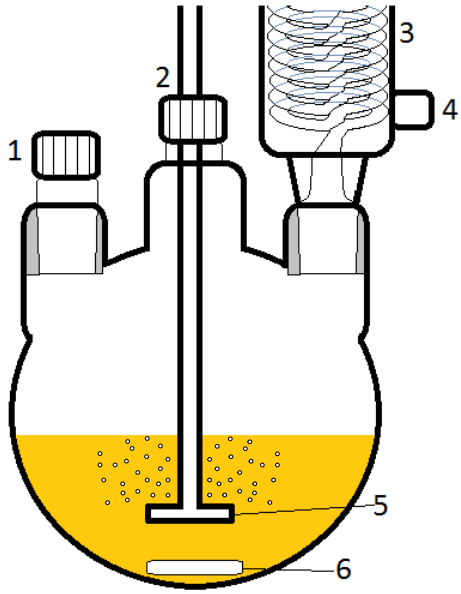

1. Septum for sample taking
2. Gas inlet
3. Spiral gas cooler
4. Water inlet gas cooler
5. Porous sinter for gas bubbling
6. Magnetic stirrer

Figure 10: Scheme of a reactor in the inhibitor screening apparatus.

Hamilton 5 mL glass syringes, 1005TLL with 150 mm stainless steel needles, provided by VWR, were used in the sampling procedure.

The gas used in the initial experiment was a premixed gas consisting of 2,03% CO_2, 5,94% O_2 ("6 %")and 92,03% N_2, delivered by Yara Praxair. The gas flow was controlled by gas flow meters calibrated with N_2 prior to the experiments.

2.2.2. Rebuilt inhibitor screening apparatus

After the first experiment, a rebuild of the apparatus was conducted. The single gas flask with a premixed gas was switched with two gas flasks respectively containing O_2 (5.0 purity, Yara Praxair) and CO_2 (5.0 purity, Yara Praxair) to obtain a mixed gas of 98 % O_2 and 2 % CO_2. Gas lines from the flasks were connected to mass flow meters controlled by a mass flow controller (MFC) to obtain the preferred gas composition. The MFC's were calibrated using N_2 gas, and corrected for the gas used using a table from the manufacturer. A purge valve was also installed to prevent overpressure in the gas lines. The mass flow meters and the MFC were manufactured by Bronkhorst High Tech and delivered by Flow-Teknikk AS, specifications are given in Table 1.

Table 1: Specifications mass flow meters and –controller.

Equipment	Specification
Mass flow meter O_2	F-201C-FAC-22-Z, 200 mLn/min CO_2
Mass flow meter CO_2	F-201CV-050-RAD22-V, 20 mLn/min CO_2
Mass flow controller	E-5714-AAA

The other part of the rebuild was that gas washing flasks were connected to the out streams. The flasks were filled with sulfuric acid to trap ammonia developed in the degradation. Pictures of the rebuilt inhibitor screening apparatus are shown in Figure 11, while a flowchart of the set-up is shown in Figure 12.

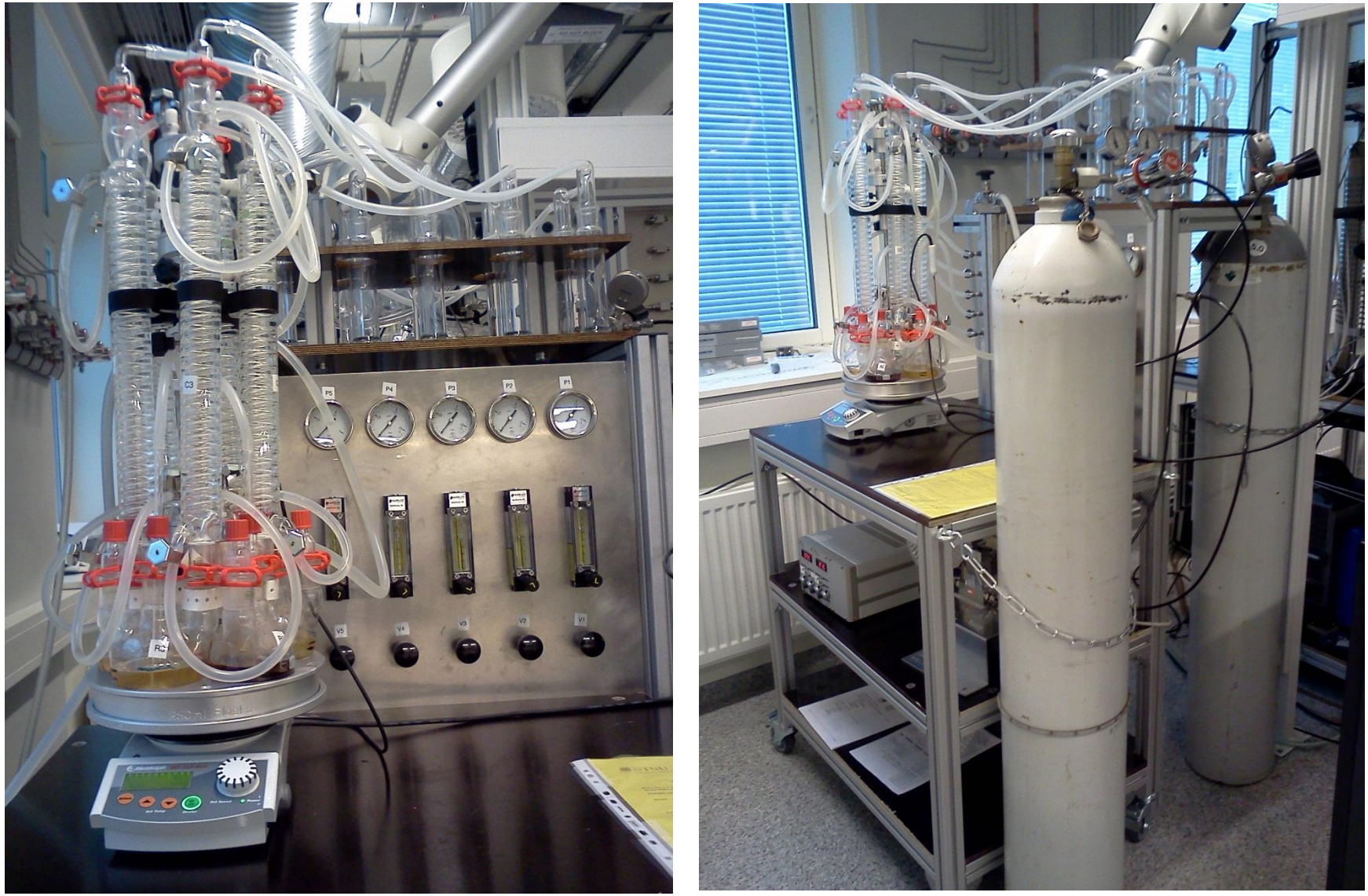

Figure 11: Pictures of the rebuilt inhibitor screening apparatus.

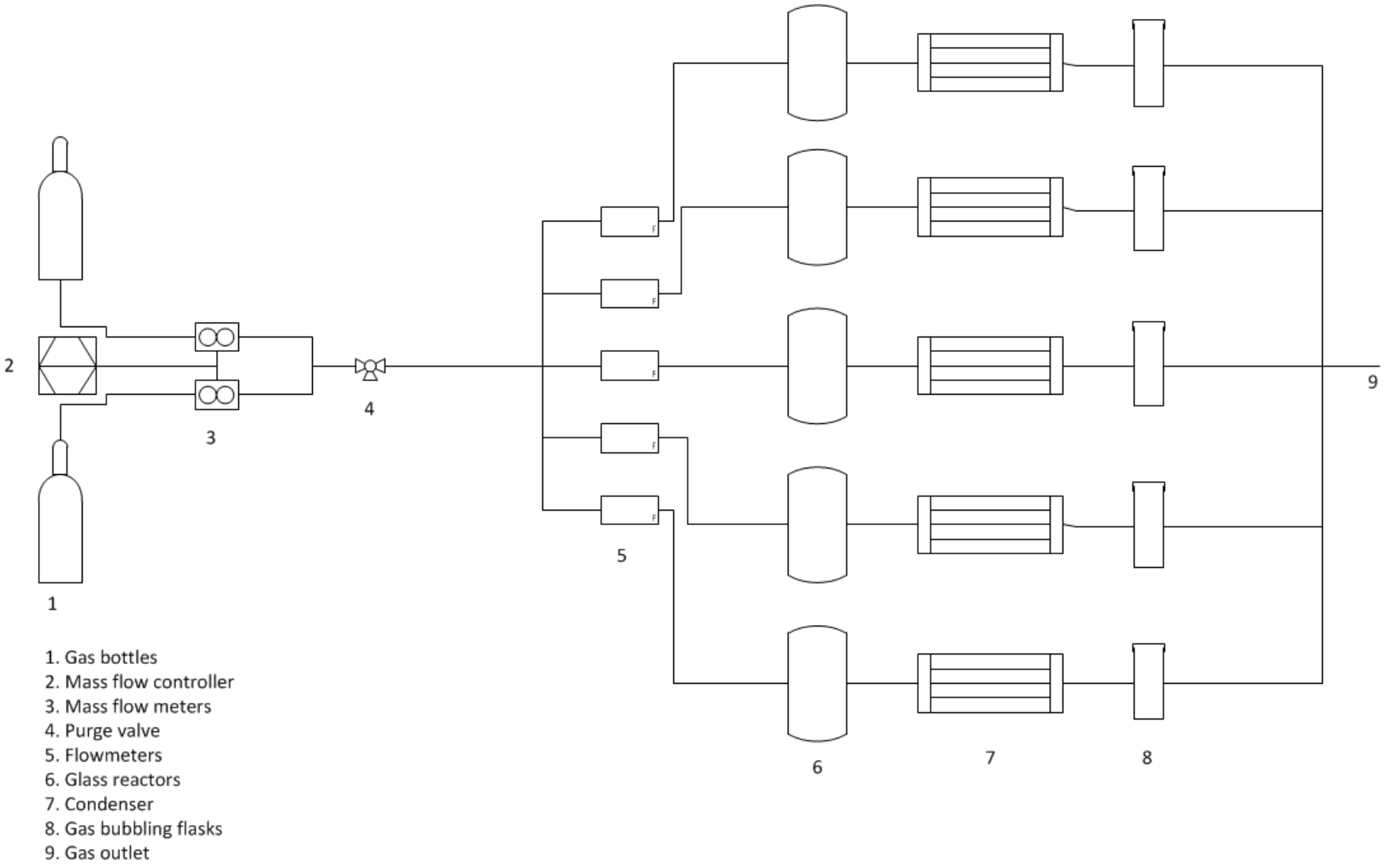

Figure 12: Flowchart of the rebuilt screening apparatus.

2.2.3. Circulative closed loop apparatus

The circulative closed loop apparatus is a closed setup of an absorber used for oxidative degradation experiments. Gas and liquid are circulated in the system, with countercurrent contact via a Sulzer DX stainless steel packing with diameter 80 mm and total height of 275 mm. The column was heated and insulated to keep the temperature stable. The temperature in the liquid phase was measured by a probe placed in the liquid sump, while a Servomex 5200 multipurpose and a Rosemount Binos 100 measured the gas phase concentrations of O_2 and CO_2 respectively. These were connected to a computer with continuous logging. Samples were taken via the liquid pump.

Standard operational parameters used in experiments are given in Table 2.

Table 2: Operational parameters for circulative closed loop apparatus.

Parameter	Value
Gas flow rate [L/min]	24,6
Liquid flow rate [L/min]	0,91
Temperature [°C]	50-55

Figure 13 shows a picture of the circulative closed loop apparatus.

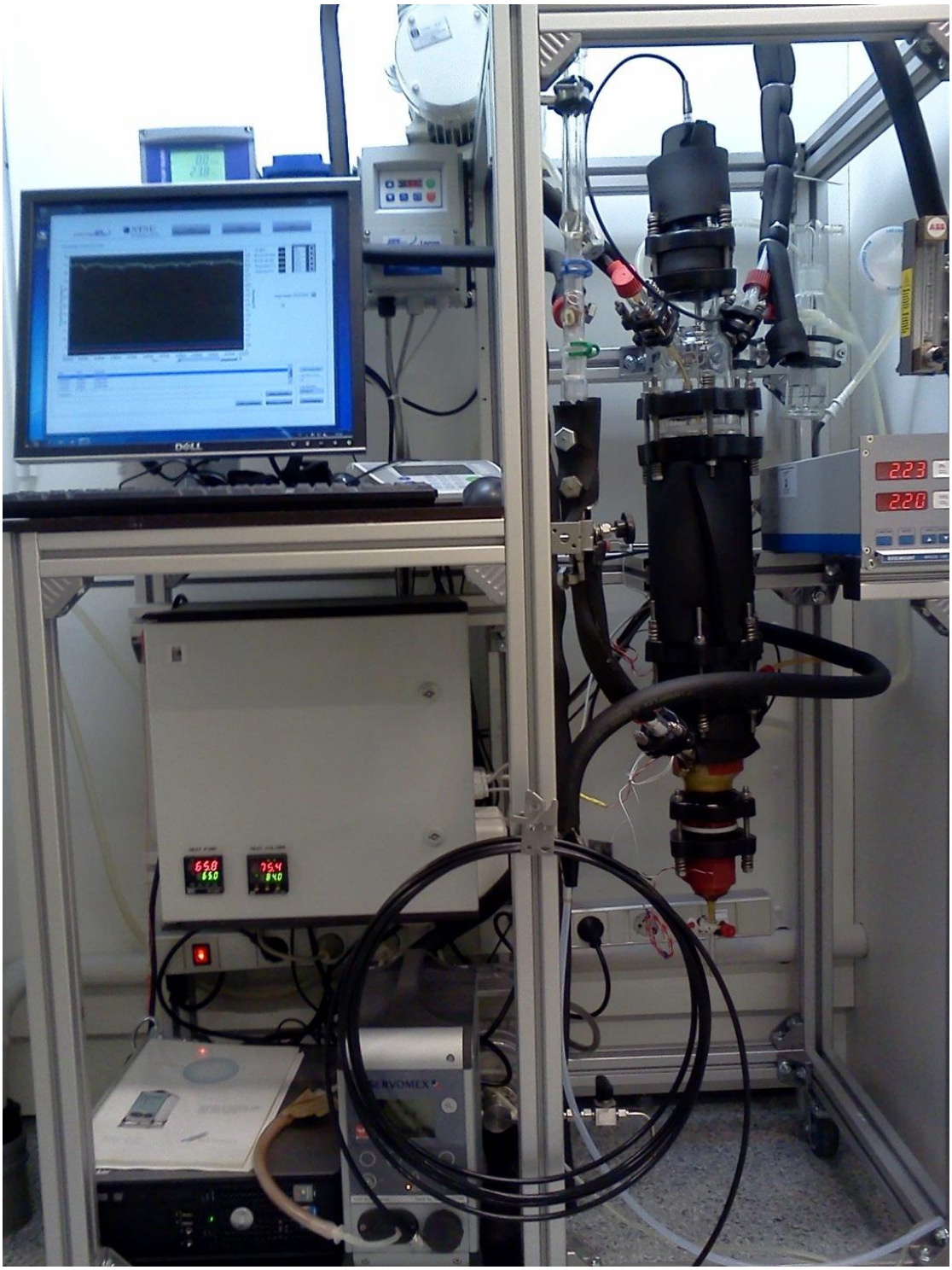

Figure 13: Circulative closed loop apparatus.

2.2.4. Thermal degradation

The experiments at thermal conditions were conducted in stainless steel cylinders with Swagelok fittings. Figure 14 shows a picture of a cylinder used in experiments.

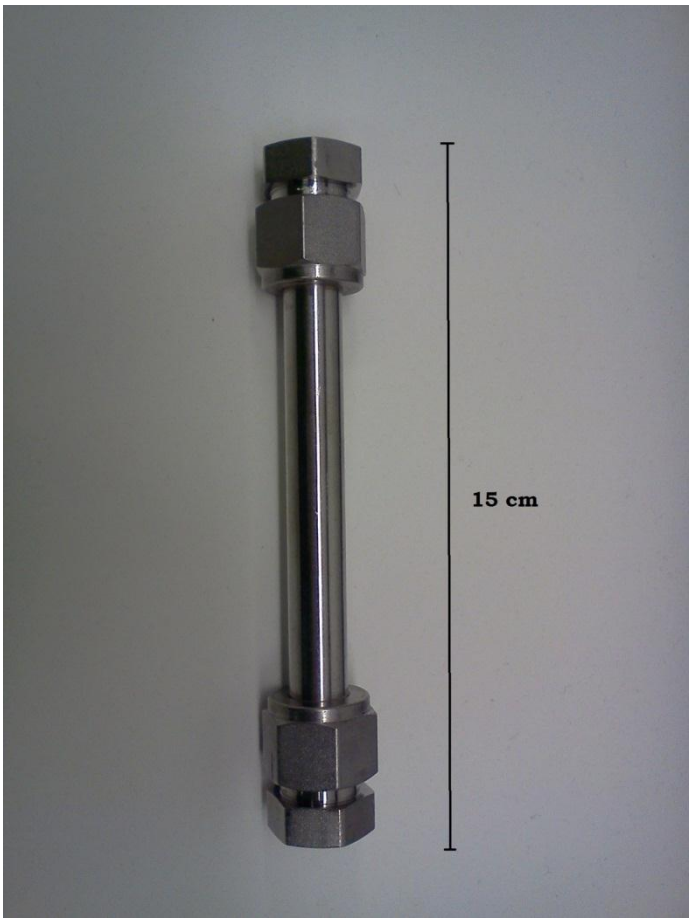

Figure 14: Stainless steel cylinder used for thermal experiments.

2.3. Experimental procedures

All chemicals were bought in analytical grade if available. More information about the chemicals used is given in Appendix A – Chemicals. All solutions were made gravimetrically using deionized water. CO_2 loading was done by sparging CO_2 gas through the amine solution. For the oxidative degradation experiments, all the solutions and samples were weighed to check the water loss. The inhibitors tested in this thesis are presented in Table 3 together with the concentrations used in experiments. The calculated concentrations for the experiments are given in the results.

Table 3: Presentation of inhibitors tested in this thesis.

Inhibitor	Final products [39]	Theroretical concentration	Inhibitor function	Reference
Potassium sodium tartrate	-	0,01 M	Chelating agent	[15, 36]
HEDP (etidronic ecid)	-	0,20%	Chelating agent	[36, 42]
Sodium triphosphate	-	0,01M	Chelating agent	[36]
Citric acid	-	0,50%	Chelating agent	[36, 43]
Hydroquinone	HCO_3^-,H_2O	0,011 M	Oxygen/radical scavenger	[14, 39]
Methallyl alcohol	-	0,05 M	Oxygen scavenger	
Sodium sulfite	SO_4^{2-}	0,05 M	Oxygen scavenger	[15, 22, 39, 40]
Hydrazine	N_2, H_2O	0,05 M	Oxygen scavenger, metal passivator	[39, 40, 44]
Carbohydrazide	N_2, H_2O, CO_2	0,05 M	Oxygen scavenger, metal passivator	[39, 40, 44]
Erythorbic acid	$C_6H_6O_6$, H_2O	0,05 M	Oxygen scavenger, metal passivator	[39, 40, 44]
MEKO (methylethyl ketoxime)	C_4H_8O, N_2O, H_2O	0,05 M	Oxygen/radical scavenger, metal passivator	[39, 40, 44, 45]
DEHA (diethyl hydroxylamine)	CH_3COOH, N_2, H_2O	0,05 M	Oxygen/radical scavenger, metal passivator	[39, 40, 45, 46]

2.3.1. Inhibitor screening experiments

A 30 wt% MEA solution was prepared using deionized water, and loaded with 0,4 mol CO_2/mol MEA. Ferrous sulfate ($FeSO_4$, 400 µM), Nickel(II) sulfate ($NiSO_4$, 50 µM), chromium(III) sulfate ($Cr_2SO_4)_3$, 100 µM), and sodium sulfate (Na_2SO_4) were added as aqueous solutions. For the experiments containing inhibitors, aqueous inhibitor solutions were added to the MEA solution before filling the reactors. Approximately 150 mL was filled in each reactor. The temperature was set to 55 °C and a gas mixture of 98 % O_2/2 % CO_2 was bubbled through the solutions at a rate of 10 mL/min. Stirring was performed with a magnetic stirring bar at 500 rpm. Samples were taken after 0, 1, 4,

9 and 13 days and analyzed using total alkalinity titration, IC-EC, LC-MS, ICP-MS in addition to CO_2-titration on the initial and end samples.

The first experiment used 6 % O_2 and 2 % CO_2 (N_2 balance). The other experimental parameters were the same as the other experiments on the setup, but with samples after 0, 1, 4, 8, 13, 21 and 25 days.

Gas bubbling flasks containing H_2SO_4 (1 M, 150 mL) were connected to the outgoing gas lines to capture ammonia. Samples from these were taken after 2, 6, 10 and 13 days. Ammonia analyses were however not done in time for this thesis.

2.3.2. Circulative closed loop experiment

A 30 wt% MEA solution was prepared using deionized water, and loaded with 0,4 mol CO_2/mol MEA. Hydrazine was added and the solution was pumped into the apparatus. The temperature was adjusted to 50-55 °C, gas- and liquid pumps were turned on according to Table 2, and temperature- and gas phase logging were started. Samples were taken after 0, 1, 2, 7, 11, 15, 19 and 21 days and analyzed with total alkalinity titration, IC-EC, LC-MS, ICP-MS in addition to CO_2-titration on the initial and end samples.

2.3.3. Thermal experiment

A 30 wt% MEA solution was prepared using deionized water. The solution was degassed with nitrogen for 15 minutes to remove air contamination, and loaded with CO_2 to 0,5 mol CO_2/mol MEA. Aqueous solutions of the inhibitors were added to the loaded MEA solution allocated on different containers. An initial sample was taken from all the solutions before 7 mL of each solution were introduced to stainless steel cylinders, five parallels for each inhibitor. The chelating agents were also added to 3 mL glass tubes and placed inside stainless steel cylinders. The transfer of the solutions was done in a gloves box under N_2-gas to ensure air free conditions. The cylinders were placed in an oven that held 135 °C. One cylinder was taken out every week for a total of five weeks. The cylinders were weighed prior to and after the experiment to check for leakages. All samples were analyzed using total alkalinity titration, CO_2-titration was conducted on the start and end samples to check the CO_2-loading. Three samples were chosen for LC-MS analysis to determine the MEA concentration for comparison with earlier results and with the total alkalinity titration.

2.3.4. Density

Density measurements were performed to convert analytical data from µg/mL to mg/kg. These were conducted by weighing known volumes of oxidative degraded solutions from the experiments. The densities were corrected by weighing deionized water by the same procedure and correcting the values according to literature values. Ten parallels were done for each sample.

2.3.5. Uncertainty assessments

Four different tests were conducted on the IC-EC to check the standard deviations for the analyses. 1/500 was the standard dilution used for most of the samples, and was therefore natural to use this dilution in the tests. The method used was the same as in the experiments. These tests are described below, while the results are displayed in Section 3.2.3.

In the first test (Test 1), the purpose was to see how the dilution of the sample affected the final concentration. This was done by diluting a sample in dilutions 1/100, 1/200, 1/300, 1/400, 1/500, 1/600 and 1/700. The second test (Test 2) was developed to see if the results were consistent when several analyses were run from the same vial. A sample was diluted 1/500 and run seven times on the IC-EC. The third test (Test 3) was almost like the second test, but with several vials; a degraded solvent was diluted 1/500 and distributed on ten vials. The fourth test (Test 4) was a test of the analytical balance by diluting the same sample ten times in parallel to give ten vials diluted 1/500.

To determine the standard deviation for the total alkalinity titration method, eight parallels of a degraded amine solution were run on the same sample in accordance to the procedure described in 2.1.2.1.

Eight samples of a degraded amine solution were run in accordance to the CO_2-titration procedure described in 2.1.2.2 to check the standard deviations.

The calculations in this procedure assume that 0,1 M HCl and 0,1 M NaOH have the same density and are done by Equation 13.

$$C_{CO_2} = \frac{1}{20} * (m_{HCl} - V_{NaOH} - (m_{HCl}^{Blank} - V_{NaOH}^{Blank})) \quad (13)$$

3. Results and discussion

In the first experiment, using 6 % O_2/2 % CO_2, the system gave on average 4,66 % degradation over a period of 25 days. At this low degradation, seeing the effect of inhibitors would be hard, and the uncertainties large. Therefore, it was determined that the gas composition should be changed to 98 % O_2/2 % CO_2 to increase the degradation. Alternate ways to increase the degradation were reviewed, but increasing the oxygen content was seen to be the best way. The alternate ways to increase degradation assessed were increasing temperature or -metal concentrations. A metal mix was added to get more realistic conditions since the experiments are conducted in glass reactors.

In the first part of this chapter, the results from a simplistic density measurement and an assessment on the uncertainties in experiments and analytical methods are presented. This gives a better ground for evaluating the results from the inhibitor experiments.

Standard deviation calculations were done using Equation 14, where S is the standard deviation, x_i is the value for sample i, $\bar{x}$ is the mean value for the selection and n is the number of values in the selection.

$$S = \sqrt{\frac{\sum_{i=1}^{n}(x_i - \bar{x})^2}{n}} \qquad (14)$$

Next, an assessment on the influence of metals and oxygen content on the degradation and distribution of degradation compounds will be presented. Then the inhibitors will be evaluated, both how good they inhibit degradation and how they impact the formation of different degradation compounds. The oxidative and thermal stability of the chelating agents is discussed, before a summarizing discussion of the chapter.

The experiments run with metal mix and a gas blend of 98 % O_2/2 % CO_2 are regarded the base case experiments. Because of the large deviations between the reactors in the base case experiments, the experiments containing inhibitors are compared with the respective reactors before they are compared with each other. The concentrations of the inhibitors used were based on the concentrations used in literature. The previously not tested inhibitors were chosen to have the same concentration as an inhibitor of similar function referred to in literature. The oxygen- and radical scavengers are assessed together as many of these have a combined effect.

Since the data from chromatographic analysis methods are given in ppm, no decimals are given in the results part due to the uncertainties, both from analyses and from the conversion.

The inhibitor screening apparatus was untested before this thesis, therefore the consistency of the experiments on the set-up cannot be guaranteed.

For the IC-EC analyses a detection limit is given. This limit is calculated according to the lowest concentration of the standard and the dilution of the specific sample. For simplicity, the mean detection limits are displayed in the charts and tables.

3.1. Density

The density of water at 25 °C and atmospheric pressure was given by Kell [47] to be 0.9970752 kg/m^3. This value was used to correct the water density to obtain the calculated densities shown in Table 4. Standard deviations were calculated according to Equation 14.

Table 4: Density measurements of degraded samples with standard deviations.

Amine loss [%]	Measured density [g/mL]	Calculated density [g/mL]	Standard deviation [g/mL]
0,00	1,084	1,085	0,000
4,31	1,104	1,105	0,002
5,70	1,097	1,097	0,002
21,68	1,108	1,108	0,002
25,33	1,114	1,115	0,001
37,63	1,130	1,131	0,002

Figure 15 shows a plot for the calculated density versus the amine loss in the samples.

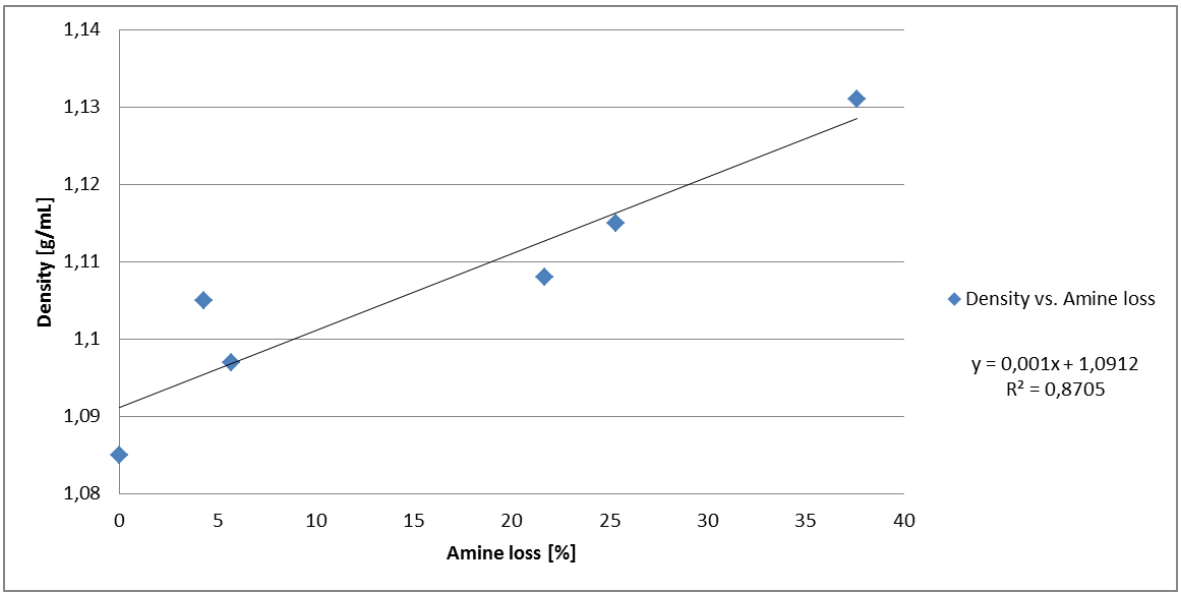

Figure 15: Plot of calculated density versus amine loss for the samples.

The formula given in Figure 15, y=0,001x+1,0912 [g/mL], is used to convert the LC-MS- and ICP-MS data for comparison purposes. The conversion is done in a linear manner, where the density is calculated as a function of the percentage amine loss, x. This implies larger uncertainties, but makes it easier to discuss the data. In the future, analyses should be done on the same basis to avoid these problems and reduce uncertainties.

3.2. Uncertainties in analyses and experiments

The results from the standard deviation calculations for the titration methods and the IC-EC method are given in this subchapter. The standard deviations were calculated using Equation 14.

3.2.1. Total alkalinity titration

The data from the test of the total alkalinity titration method is given in Table 5

Table 5: Experimental data for determination of standard deviation of amine analysis.

Parallel	Concentration [mol/kg]
1	3,61
2	3,61
3	3,61
4	3,60
5	3,61
6	3,60
7	3,60
8	3,59

These data gave a mean concentration of 3,60 mol/kg amine, with a standard deviation of 0,01 mol/kg. This correspond to a deviation of 0,23%.

When using this method, it is important to remember that it measures the alkalinity of the solution and not the MEA concentration. This is especially important for the experiments performed at thermal conditions, where some of the main degradation products are amines. For the oxidative degradation experiments, this method is used as a measure of the amine loss, since low concentrations of alkaline degradation compounds are expected.

3.2.2. CO_2-titration method

The data from the test of the CO_2-titration method is given in Table 6.

Table 6: Experimental data for determination of standard deviation of CO_2-analysis.

Parallel	Concentration CO_2 [mol/kg]
1	1,71
2	1,72
3	1,70
4	1,73
5	1,71
6	1,72
7	1,72
8	1,72

These data gave a mean concentration of 1,72 mol/L CO_2, with a standard deviation of 0,01 mol/L. This corresponds to a deviation of 0,44%.

3.2.3. Assesment of IC-EC analytical method

The concentration of oxalate in the sample used was below the detection limit, therefore the standard deviation for this anion is not assessed for the IC-EC. The tables present the average concentrations of the anions together with the standard deviation in mg/kg and per cent of the mean values.

The standard deviations for Test 1 are presented in Table 7.

Table 7: Results from Test 1, checking the effect of different dilutions.

	Formate	Nitrite	Nitrate	Sulfate
Average concentration [mg/kg]	612	765	459	1456
Standard deviation [mg/kg]	19	73	31	79
Standard deviation [%]	3,2	9,5	6,7	5,5

The standard deviations from this test are the largest from all the tests performed on the IC-EC. Figure 16 show a plot of dilution versus the calculated anion concentrations.

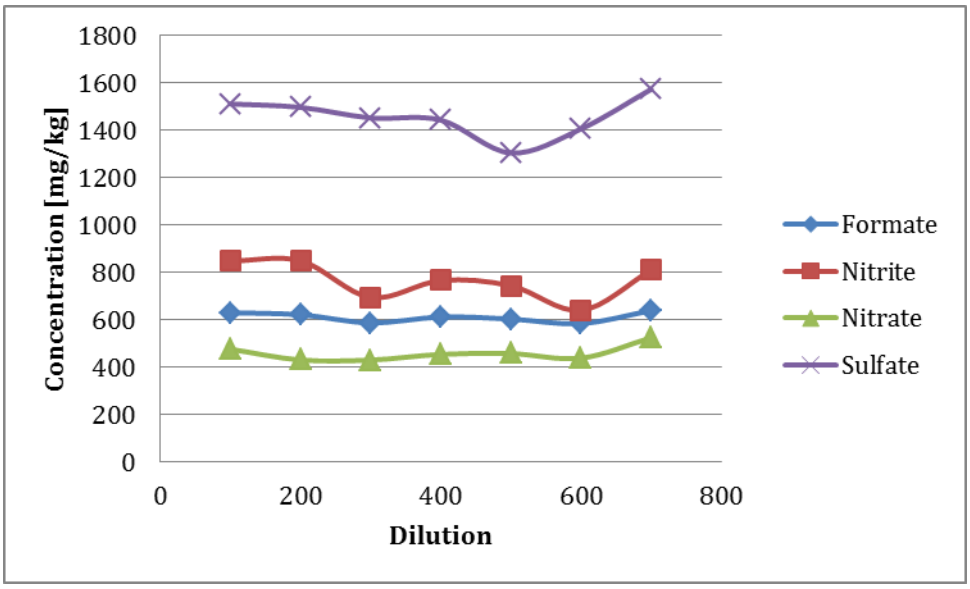

Figure 16: Effect of dilution on the calculated concentrations in a degraded amine solution.

In this plot it can be seen that the variation in concentrations of the anions does not seem to follow any specific trends according to the dilution.

In Test 2, where seven analyses were run on the same vial, the smallest standard deviations were found. This was also the expected result. Table 8 shows the values obtained from Test 2.

Table 8: Results from Test 2, running seven analyses on the same vial.

	Formate	Nitrite	Nitrate	Sulfate
Average concentration [mg/kg]	636	680	456	1456
Standard deviation [mg/kg]	11	20	6	8
Standard deviation [%]	1,7	2,9	1,3	0,6

The exact same solution used in Test 2, was used in Test 3, shown in Table 9. The only difference between these two tests was the use of one vial in Test 2 compared to ten vials in Test 3.

Table 9: Results from Test 3, with ten vials containing the same solution.

	Formate	Nitrite	Nitrate	Sulfate
Average concentration [mg/kg]	613	721	467	1471
Standard deviation [mg/kg]	12	21	18	16
Standard deviation [%]	2,0	3,0	3,8	1,1

The results indicate that there are bigger deviations when using several vials. There are no apparent reasons for why the amount of vials should affect the results. The tops of the vials were pre-slit, so the material should not interfere with the injector needle. Contamination from the vials is also unlikely, as these are single use only.

Test 4 is the most representative test according to the analyses in this thesis. Ten samples were diluted and analyzed in the same manner as the samples from experiments. Table 10 gives the average concentrations and standard deviations for the anions in this test.

Table 10: Results from Test 4, with ten samples diluted separately.

	Formate	Nitrite	Nitrate	Sulfate
Average concentration [mg/kg]	597	720	446	1446
Standard deviation [mg/kg]	34	50	15	70
Standard deviation [%]	5,7	6,9	3,4	4,8

Test 4 shows the standard deviations which are expected to be applicable to the analyses used in this assignment. The deviations between this test and Test 3 would be related to the dilution process. Since the dilution is done on weight basis, the uncertainty is in the analytical balance. The analytical balance used in these dilutions has three digits on a gram scale, by using a more precise balance, the uncertainties would be reduced.

The variations between the different anions can be related to the individual peak properties. Figure 17 shows a chromatogram from this test.

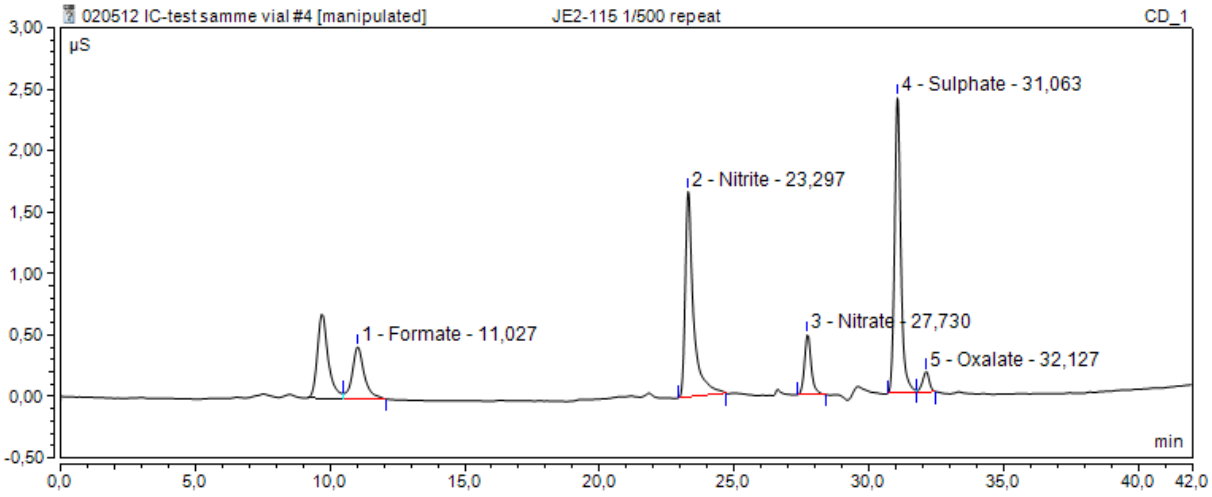

Figure 17: Chromatogram from the IC-EC tests, showing peak properties.

Here it can be seen that neither the formate peak nor the sulfate and oxalate peaks have baseline separation. This overlap will cause an uncertainty in the measured areas of the peaks, and thus the calculated concentrations. The peak with retention time of approximately ten minutes is assumed to be the single condensation product of MEA and oxalic acid as discussed by da Silva [9]. No standard was available for quantification of this compound. The nitrite peak has quite a long tail which makes it hard to determine the borders of the peak for the integration of the chromatogram. Since the tail sometimes overlaps with smaller peaks, this gives cause for some uncertainties for this peak. The nitrate has baseline separation and no tail, but the uncertainties related to this anion are in the same range as for the others. This indicates that the uncertainties found in these tests are not only related to the integration of the peaks, which is done manually.

3.2.4. Reproducibility

In this part chapter the reproducibility for the reactors are assessed. Two experiments were run where the same solution was loaded in all the reactors. The gas contained 6% oxygen for the first run, and 98% oxygen for the second run. Other conditions were equal, as explained in experimental part 2.3.1.

The degradation using 6% oxygen in the gas was very low. With a mean value of 4,66% amine loss after 25 days, the system had to be modified to give more degradation. The low rate of degradation means that the uncertainties in the analyses are larger relative to the experiments with higher degradation. For the experiment using 98% oxygen, major leaks were found in the system. The concentrations were corrected for the water loss using the sulfate concentration from the IC-EC analysis. This gives an extra uncertainty due to the uncertainty from the IC-EC analysis. Since the water loss was quite substantial, the concentration of the degradation compounds increased as well. This can give basis to a higher amount of reactions in the reactors, giving more degradation.

Table 11 gives the amine loss and standard deviations for experiments at 98% and 6% O_2 after 13 days.

Table 11: Amine loss for reactors at 6% and 98% oxygen.

Reactor	Amine loss 6 % O_2 [%]	Amine loss 98 % O_2 [%]	98 %/6 %
R1	2,92	21,68	7,40
R2	2,66	37,63	14,10
R3	3,04	17,20	5,70
R4	3,11	14,06	4,50
R5	3,32	25,33	7,60
Mean	3,01	23,18	7,90
Standard deviation	0,22	8,18	3,34
Standard deviation [%]	7,2	35,3	42,4

The large deviations between the reactors support the decision to compare the inhibitor screening experiments with the base case for the given reactor. With a standard deviation of 35,3% for the average base case, comparing the inhibitor screening experiments directly with each other would be wrong. The factors between the 98 % and 6 % varies a lot, which support the need for more experiments to determine a good baseline for comparison.

The large differences between the degradation in the separate reactors give ground to a discussion to whether the results are comparable. If the oxidative degradation is controlled by the oxygen mass transfer, as claimed by Goff [22], the relative concentrations of the some inhibitors would be affected by this. The concentration of an oxygen scavenger will be dependent on the amount of dissolved oxygen present, and therefore it will disappear faster in R2 compared to R4. By observation, it seems like the gas spargers in the reactors giving more degradation (in base case) also give a finer dispersion of the gas compared with the reactors with lower degradation. It should be considered to replace these spargers to get more equal conditions in the reactors for easier comparison.

An additional parallel was conducted on reactor R4 without metals by Solrun J. Vevelstad. The standard deviation calculated for the two experiments is shown in Table 12.

Table 12: Standard deviation calculation for the two parallels run on reactor R4.

Run	Amine loss [%]
1	9,10
2	7,05
Mean	8,08
Standard deviation	1,03
Standard deviation [%]	12,7

Although this standard deviation is based on two experiments, the value is quite large. It has to be taken into account that the first of the experiments had a substantial water loss, concentrating the solution which may have increased the degradation. Regardless, this shows the need for running more baseline experiments, testing the reproducibility of the reactors.

Sexton [27] analyzed the degradation compounds in an experiment using a 98% O_2/2% CO_2 gas blend at a gas flow of 100 mL/min. The experiments were conducted using 5 M MEA, loaded with 0,4 mol CO_2/ mol MEA, with 1,0 mM iron, at 55 °C, and ran for 20,8 days (500 hours). The product rate formation is given in Table 13, and compared to the mean formation rates for the base case experiments. These are calculated using a linear approach. In the experiments, the oxalate concentration was below the detection limit for three of five experiments. The values given are for the two where the oxalate was above the detection limit.

Table 13: Comparison of degradation product formation rates between Sexton low gas flow apparatus [27] and base case experiments.

Experiment	HEF [mM/h]	HEI [mM/h]	Formate [mM/h]	Nitrate [mM/h]	Oxalate [mM/h]	Nitrite [mM/h]	Amine loss [mM/h]
Mean 98% O_2	0,33	0,26	0,07	0,03	0,01	0,11	3,6
Sexton 2011	0,77	0,66	0,29	0,09	0,02	0,21	3,8

It seems like although the amine loss is approximately the same, the formation rate of the degradation compounds in the experiments done by Sexton are higher. The three main differences between the experiments are the flowrates (100 mL/min vs. 10 mL/min), iron concentrations (1,0 mM vs. 0,4 mM) and time used for the experiment. The amine concentration was also slightly higher in Sextons experiment. It may be that the harsher conditions in Sextons experiment account for a higher degree of oxidation of the degradation products, while the rate of amine loss is the same. For example, if the oxidation of formaldehyde is favored compared to the oxidation of MEA, a larger concentration of formate will be detected, while the amine loss is the same. The length of the experiment will also affect the results, since the degradation not is linear.

3.3. Effect of metals

Since one of the reactors on the inhibitor screening apparatus was run both with and without metals added, it is natural to look at the differences between these two experiments. Table 14 gives the LC-MS and Table 15 gives the IC-EC data for the end samples in reactor R4 run with and without metals added at the same conditions.

Table 14: LC-MS data for end samples with- and without metals added.

Sample	OZD [mg/kg]	BHEOX [mg/kg]	HEA [mg/kg]	HeGly [mg/kg]	HEPO [mg/kg]	HEF [mg/kg]	HEI [mg/kg]
Without metals	886	1090	56	170	42	3927	696
With metals	1243	1758	163	150	55	5682	5087
Ratio	1,40	1,61	2,90	0,88	1,30	1,45	7,31

Table 15: IC-EC data for end samples with- and without metals added.

Sample	Formate [mg/kg]	Nitrate [mg/kg]	Oxalate [mg/kg]	Nitrite [mg/kg]
Without metals	291	70	0	231
With metals	418	336	0	482
Ratio	1,44	4,83	-	2,09

The total degradation in the experiment without metals was 9,10% and 14,06% in the experiment with metals added. The ratios are calculated by dividing the concentrations with metals on the concentrations without metals. Ratio for the degradation is 1,55.

The two most significant differences between these experiments are regarding HeGly and HEI. The mechanism for the formation of HEI is not known, but there are several patents based on synthesizing it from glyoxal, MEA, ammonia and formaldehyde, with water as a solvent at low temperatures. [48-50] From the literature, this reaction does not appear to need metal catalysis; it is therefore natural to assume that the effect of metals is due to the formation of its precursors. Ammonia and formaldehyde are primary degradation products and are not assumed to be the limiting factor for this reaction. Glyoxal has not been reported as a degradation product, but is a two carbon oxidation product of MEA, so its presence is not unlikely.

The mechanism for formation of HeGly is not known, but it seems to be dependent on metal concentrations, since the concentration is higher in the sample without metals added. da Silva [9] claim HeGly to be the precursor of another degradation compound, HEPO. It may be that it is the formation of HEPO that is affected by metals, and not the formation of HeGly. The condensation product of HeGly and MEA, N-(2-hydroxyethyl)-2-(2-hydroxyethylamino) acetamide (HEHEAA), is believed to be an intermediate in the formation of HEPO. A quantification of HEHEAA or more experiments around this reaction could clear up how the metals affect the formation of HeGly and HEPO.

2-hydroxyethyl acetamide (HEA), nitrite and nitrate also seem to increase more than the overall degradation by the addition of metals. This implies a catalytic effect in the formation of these species. HEA is assumed to be the condensation product between acetic acid and MEA. [13] Such condensation reactions are often metal catalyzed, but since acetate is not detectable in the samples it is hard to say how the formation of HEA is affected by metals. Transition metals have proved effective in the wet oxidation of ammonia to nitrous oxides [25, 26]; this is likely to be the background of the increased concentrations of nitrite and nitrate. If the addition of metals both increase ammonia evolution and –oxidation, an increase in nitrite and nitrate would be expected.

According to Lepaumier and da Silva [9, 13], OZD is the precursor in the carbamate polymerization at thermal conditions. They do not see an effect of metals in the thermal degradation, something that would be expected if the precursor was affected by metals. Since the concentration of OZD increase with the addition of metals, there is a possibility that the MEA-carbamate cyclization is metal catalyzed. It is possible that this effect is not seen at higher temperatures because metal catalysis is unnecessary at those conditions. Another possibility is that there is another mechanism for the formation of OZD at absorber conditions. This is discussed further in Section 3.4.

3.4. Effect of oxygen content

As discussed in 3.2.4, the low degree of degradation in the experiment run with 6% O_2 give larger uncertainties. Some of the values are very close to the detection limits, which are given together with the raw data in Appendix B: LC-MS raw data and Appendix I: IC-EC raw data. Table 16 and Table 17 give the average concentrations of degradation products and ratios between them from LC-MS and IC-EC analyses respectively, after 13 days.

Table 16: Average concentrations of degradation compounds from 98% O_2 and 6% O_2, from LC-MS analysis.

	OZD [mg/kg]	BHEOX [mg/kg]	HEA [mg/kg]	HeGly [mg/kg]	HEPO [mg/kg]	HEF [mg/kg]	HEI [mg/kg]
6 % O_2	87	268	74	283	21	2165	2978
98 % O_2	1559	2043	226	132	69	6845	6552
Ratio	17,92	7,62	3,05	0,47	3,29	3,16	2,20

Table 17: Average concentrations of degradation compounds from 98% O_2 and 6% O_2, from IC-EC analysis.

	Formate [mg/kg]	Nitrate [mg/kg]	Oxalate [mg/kg]	Nitrite [mg/kg]
6 % O_2	144	57	24	67
98 % O_2	876	569	153	1453
Ratio	6,08	9,98	6,38	21,69

Formate, oxalate and BHEOX increase approximately with the same factor as the overall degradation. The formation of HEA, HEPO, HEF and HEI is not increased as much as the overall degradation. In the formation of HEF, it is likely that the reaction between formate and MEA is limiting, since the formate concentration follows the overall degradation. Similar reasons may be limiting HEA, but acetate is not detectable. HEI is assumed to have several precursors, of which only MEA concentration is known. If glyoxal is the limiting factor, as discussed in 3.3., it may be the formation of this that is limiting HEI formation. The total mechanism for the formation of HEPO is not known, but da Silva [9] suggest a mechanism with HeGly as a precursor. Since the HeGly concentrations are lower at 98% O_2 compared with the 6% O_2, the HEPO concentration would not be expected to increase.

Nitrite and nitrate also increase more than the average degradation. This might be a result of the oxygen dependency of the oxidation of ammonia, or the formation of ammonia, as discussed in Section 3.3.. Ammonia analyses were however not performed in time for this thesis.

Both OZD and HeGly seem to be affected by oxygen concentration. OZD has been reported as a product in both thermal and oxidative degradation. According to da Silva [9], the formation of OZD at absorber conditions follow the same mechanism as at thermal conditions; by MEA-carbamate ring closure. This mechanism should not be affected by the amount of oxygen present. As clearly seen in Table 16, the formation of OZD is markedly (factor of eighteen) larger at the experiments conducted at 98% O_2 compared to 6% O_2. To explain the increased formation of OZD at increased oxygen concentrations, a proposition for a new mechanism for the formation of OZD at absorber conditions is given in Figure 18.

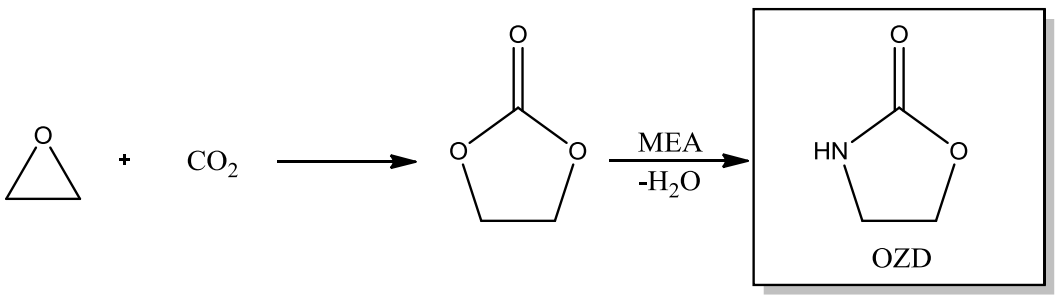

Figure 18: Proposed mechanism for the formation of OZD at absorber conditions.

This mechanism is based on the work of Patil et al. [51] where cyclic carbonates, formed by reactions between an epoxide and CO_2, react with alkanolamines to give 2-oxazolidinones in good yields using a phosphonium based catalyst. Ethylene oxide has been believed to be the product of the deamination of MEA, and is a reported product in the degradation of methyl diethanolamine (MDEA). [52, 53] If ethylene oxide is a degradation product affected by the oxygen concentration, by for example a radical initiated deamination, this could be a plausible route for formation of OZD at absorber

conditions. An effect of metals was also detected in Section 3.3., which means this reaction may be metal catalyzed.

da Silva [9] reported HeGly to be the most abundant degradation compound in Esbjerg pilot plant samples, and second most abundant in samples from the Tiller pilot plant. The Esbjerg pilot plant used pulverized coal, which means 6-7% oxygen in the flue gas. The oxygen content in the flue gas used in the Tiller pilot plant was was 7% oxygen (Personal communication Andreas Grimstvedt). In the experiments in this thesis, it is seen that the formation of HeGly is favored at lower oxygen concentrations. The concentrations of HeGly are on average two times higher at 6% O_2 compared to 98% O_2, even though the degradation is only one eighth. This supports the claim that HeGly is favored at lower oxygen concentrations. The mechanism of HeGly is unknown, but the results suggest that the precursor of this compound is an intermediate in the oxidation of MEA. In the oxidation route from MEA to oxalic acid described by Rooney [31], some of the intermediates have structures which makes them possible precursors for HeGly. None of these are quantified in the experiments, but the final oxidation product, oxalic acid, is. Oxalic acid is generally found in small amounts, but is just above detection limit in reactor R4 for the experiment with 6% O_2 in a concentration of 24 mg/kg. The same reactor ran with 98% O_2 gave in comparison a concentration of 203 mg/kg, this is a factor of about eight. The double condensation product of MEA and oxalic acid, N,N'-bis(2-hydroxyethyl) oxalamide (BHEOX) [9], is also present at in average eight times higher concentrations in the same samples. Since the concentration of these higher oxidation products is larger at higher oxygen concentrations, HeGly may be favored at lower oxygen concentrations due to a higher availability of its precursors.

An oxidation of HeGly would most likely yield MEA and glyoxylic acid, as glycine and sarcosine give similar products in aerobic, enzymatic oxidation. [54] Glyoxylic acid is one of the precursors of oxalic acid in the oxidation route proposed by Rooney. [31] Thus, the reason that higher concentrations of HeGly are present at low oxygen concentration may be due to its destruction at higher oxygen concentrations.

Since HeGly is such an important degradation product in pilot samples, further work should be put into determining the mechanism for its formation. This work should focus on precursors favored at less oxidizing conditions, in reactions that do not require metal catalysis. The stability and reactions of HeGly should also be studied to see how it fits into the full picture of amine degradation.

3.5. Inhibitors

The results of the experiments screening inhibitors for antioxidative effect are presented first in this chapter. Next, it is discussed whether the inhibitors have an effect on the carbamate polymerization. Lastly are the results from the tests of the stability of the chelating agents presented.

3.5.1. Screening experiments

The effect of the inhibitors was determined by amine loss, found using total alkalinity titration. The amine losses were compared with the respective reactors for the base case to calculate the percentage inhibition. This, together with the calculated concentrations of the inhibitors is shown in Table 18.

Table 18: Inhibitory effect and concentrations used of the inhibitors for screening experiments.

Inhibitor	Calculated concentration [wt%]	Calculated concentration [mol/kg]	Reduction in degradation [%]	Class
Potassium sodium tartrate	0,25	0,009	23,59	Chelating agents
Sodium triphosphate	0,37	0,01	64,42	
Citric acid	0,46	0,024	32,05	
HEDP	0,18	0,008	67,81	
Hydroquinone	0,12	0,011	-17,19	Oxygen/radical scavengers
Erythorbic acid	0,89	0,051	57,42	
Carbohydrazide	0,45	0,05	59,69	
Methallyl alcohol	0,35	0,049	-21,36	
Sodium sulfite	0,59	0,047	50,34	
DEHA	0,4	0,044	37,60	
MEKO	0,41	0,047	55,67	
Sodium triphosphate	0,36	0,01	61,90	Synergy
Carbohydrazide	0,43	0,048		
Citric acid	0,48	0,025	51,04	
Carbohydrazide	0,43	0,048		
HEDP	0,2	0,009	58,57	
Carbohydrazide	0,45	0,05		

From Table 18 it can be seen that most of the inhibitors did exhibit antioxidative effect, except for two; hydroquinone and methallyl alcohol which increased the rate of degradation.

3.5.1.1. Unsuccessful inhibitors

Hydroquinone seems to increase the overall oxidation of the solution. It gives a decrease in HeGly concentration, which supports HeGly formation to be favored in a less oxidizing environment. See Appendix B: LC-MS raw data.

Hydroquinone is an oxygen- and radical scavenger used to scavenge oxygen in boiler systems. [39] The radicals formed in the oxidation of hydroquinone may have been unstable, and participated in oxidation of the amine. [14] This can be a result of too high concentrations being added [33], or that the intermediate is too unstable to work in a system like this. If further work should be done using this chemical, lower concentration should be used.

Methallyl alcohol is a water soluble alkene which has not previously been used as an antioxidant. This compound was screened for inhibitory effect due to the transition metal catalyzed reaction between alkenes and oxygen to form epoxides. [55, 56] The experimental results indicate that this was not the case. There is a possibility that the alkene reacted with the amine in a metal catalyzed amination of the alkene, but the increase in typical MEA oxidative degradation compounds suggest that it increased oxidation. [57]

Table 19 shows the LC-MS data for the end samples with the calculated ratio between them while Table 20 shows the concentrations of the anionic species from these two experiments.

Table 19: End sample concentrations of compounds quantified by LC-MS for methallyl alcohol- and base case experiments.

	OZD	BHEOX	HEA	HeGly	HEPO	HEF	HEI
Methallyl alcohol [mg/kg]	1735,9	2712,8	206,9	101,8	46,6	7818,1	6322,5
Base case [mg/kg]	1242,8	1758,5	163,4	150	54,9	5682,3	5086,9
Ratio	1,40	1,54	1,27	0,68	0,85	1,38	1,24

Table 20: End sample concentrations of anionic species quantified on IC-EC for methallyl alcohol- and base case experiments.

	Formate	Nitrate	Oxalate	Nitrite
Methallyl alcohol [mg/kg]	627	398	0	674
Base case [mg/kg]	418	336	0	482
Ratio	1,50	1,19	-	1,40

The ratio between the degradation with methallyl alcohol and the base case is 1,21. The concentrations of the products favored at higher oxygen concentrations, such as formate, BHEOX and OZD, have slightly higher relative values in samples from the experiment with methallyl alcohol added compared with the base case. The concentration of HeGly, favored at low oxygen concentrations, is lower. This indicate that the alkene increase the solubility of oxygen in the solution to increase the oxidation rate. HEPO, which increased with higher oxygen concentration shown in Table 16, do however decrease in the experiment with methallyl alcohol added. HEPO is a compound present at low concentrations, so the uncertainties in its values are large.

3.5.1.2. Oxygen/radical scavengers

Out of seven oxygen/radical scavengers screened for antioxidative effect in amine systems, five gave an inhibitory effect. The percentage of inhibitory effect ranges from 37,60-59,69 % inhibition, with carbohydrazide as the best and DEHA as the least good. It has to be included that only one concentration has been tested for each of the inhibitors.

The ratios between degradation compounds for the respective base case experiments and the experiments with oxygen scavengers added are shown in Table 21 and Table 22. Table 22 also shows the relative degradation in the samples.

Table 21: Ratios of LC-MS degradation products in base case experiments compared with experiments containing oxygen scavengers.

	OZD	BHEOX	HEA	HeGly	HEPO	HEF	HEI
DEHA	1,57	1,18	0,13	1,46	2,02	1,49	1,70
Erythorbic acid	2,74	1,42	1,71	0,88	2,60	1,86	1,57
Sodium sulfite	1,56	2,67	2,53	1,16	1,78	2,40	1,90
Carbohydrazide	1,30	2,05	1,53	1,65	2,18	1,53	1,51
MEKO	1,67	1,62	0,92	1,00	1,18	1,94	2,68

Table 22: Ratios of IC-EC degradation products in base case experiments compared with experiments containing oxygen scavengers, as well as degradation ratios.

	Formate	Nitrate	Oxalate	Nitrite	Degradation
DEHA	2,15	1,42	-	2,21	1,60
Erythorbic acid	1,96	1,71	0,45	11,80	2,35
Sodium sulfite	2,42	2,26	-	-	2,01
Carbohydrazide	2,48	2,05	-	7,60	2,48
MEKO	2,91	1,55	-	3,39	2,26

In these tables, high numbers compared to the degradation mean that the amount of the degradation product is reduced. For oxalate and nitrite, the empty fields mean that the concentration was below the detection limit for the sample containing inhibitor. The base case experiment conducted on the same reactor as carbohydrazide did not show any oxalate in the end sample.

The only degradation product reduced more than the overall degradation for all the inhibitors is nitrite. The reduction of nitrite may be due to a decrease in the oxidation of ammonia and in an overall reduction in ammonia formation. Nitrate seems to be more favored than nitrite with oxygen scavengers added. In the comparison between 6 % and 98 % O_2 in the gas (Section 3.4), it is also seen that nitrite increased more when the oxygen was increased. Thus it seems like oxygen scavengers can be efficient in reducing nitrite formation. HeGly is reduced less than the overall degradation for all these inhibitors. This can be related to this compound being favored at less oxidizing conditions, as discussed in Section 3.4. For the other degradation compounds, no apparent trend is present.

None of the other compounds follow a specific trend. The scavengers can favor different reactions and reactants in the solutions, which affect the product composition. DEHA and MEKO are reported to be both radical and oxygen scavengers. [44, 46] It is seen from Table 21 and Table 22 that these favor the same degradation products, except for

HEPO. This indicates that they work by the same mechanisms, although MEKO is more efficient.

It also has to be considered that the stoichiometries in the reactions with oxygen are not the same for all the inhibitors. The most efficient oxygen scavenger, carbohydrazide, react 1:2 with oxygen, compared to erythorbic acid, the second most efficient which react 2:1 with oxygen.[39] These are added in approximately the same molar amounts and inhibit degradation to approximately the same degree (59,69 vs. 57,42 % inhibition). This implies that it is not the amount of the inhibitors that gives the difference in inhibitory effect. It suggests that it is the kinetics of the oxygen scavenging reactions that is determining for the effect in these experiments. The scavengers should anyway be tested in different concentrations before any conclusions can be drawn.

Since the scavengers are to be added continuously, it is important that their products do not affect the process. In Table 3 the products from the oxidation of the scavengers are reported. For DEHA, acetic acid is a reported oxidation product, which is likely to be the reason for the increase in the concentration of HEA seen in Table 21. It would be preferred for an inhibitor that its oxidation products do not accumulate or react with the other species in the solution.

3.5.1.3. Chelating agents

All of the chelating agents gave inhibitory effect, with HEDP as the most efficient, inhibiting 67,81 % of the degradation. Potassium sodium tartrate was the least efficient, reducing the degradation with 23,59 %. It has to be mentioned that citric acid was added in a different concentrations from the others, the concentrations are given in Table 18.

Table 23 and Table 24 show the relative concentrations in the base case experiments compared to the concentrations in the samples containing chelating agents. The relative degradation is also shown in Table 24.

Table 23: Ratios of LC-MS degradation products in base case experiments compared with experiments containing chelating agents.

	OZD	BHEOX	HEA	HeGly	HEPO	HEF	HEI
Potassium sodium tartrate	0,98	0,92	0,75	0,93	0,77	0,90	0,86
Citric acid	1,05	1,54	0,87	0,94	1,49	1,54	2,05
HEDP	2,96	2,40	1,73	1,13	4,47	1,37	34,37
Sodium triphosphate	2,29	2,00	2,73	0,77	2,56	2,31	2,63

Table 24: Ratios of IC-EC degradation compounds in base case experiments compared with experiments containing chelating agents, as well as the degradation ratios.

	Formate	Nitrate	Oxalate	Nitrite	Degradation
Potassium sodium tartrate	0,97	0,74	-	1,32	1,31
Citric acid	2,06	2,14	-	3,10	1,47
HEDP	1,39	-	-	-	3,10
Sodium triphosphate	2,96	-	-	11,46	2,81

HeGly, OZD and HEA are all reduced less than the overall degradation in the experiments with chelating agents added. This is also seen for HeGly in the chapter discussing the effect of metals (Section 3.3.).

For the experiment with HEDP added, the nitrite and nitrate concentrations were reduced to below the detection limit. The amount of HEI was also strongly reduced. This reduction in HEI can be related to the metal dependency of this compound discussed in Section 3.3.

Sodium triphosphate did also reduce the nitrite and nitrate formations markedly more than the change in degradation. The rest of the degradation compounds do not deviate very much from the total degradation.

It may be that a salting out effect, decreasing the solubility of oxygen, is present by the addition of the chelating agents. This effect has earlier been observed from other ionic species in experiments by Goff. [14]

A common effect found in the chelating agents, was that they seemed to keep the metal concentrations constant throughout the experiments. For the other experiments, the iron and chromium concentrations decreased continuously, probably due to precipitation of iron oxides/hydroxides. The nickel concentrations were relatively stable throughout the experiments. There was also observed a presence of a rust-colored layer on the spargers in the base case experiment, which assumedly were precipitated metal salts. This layer was not present in the experiments containing chelating agents. Erythorbic acid, which was added as an oxygen scavenger did also keep the iron concentrations constant, which indicates that this compound also have metal chelating properties.

Figure 19 shows a plot of the metal concentrations in the samples containing citric acid and the base case from the same reactor.

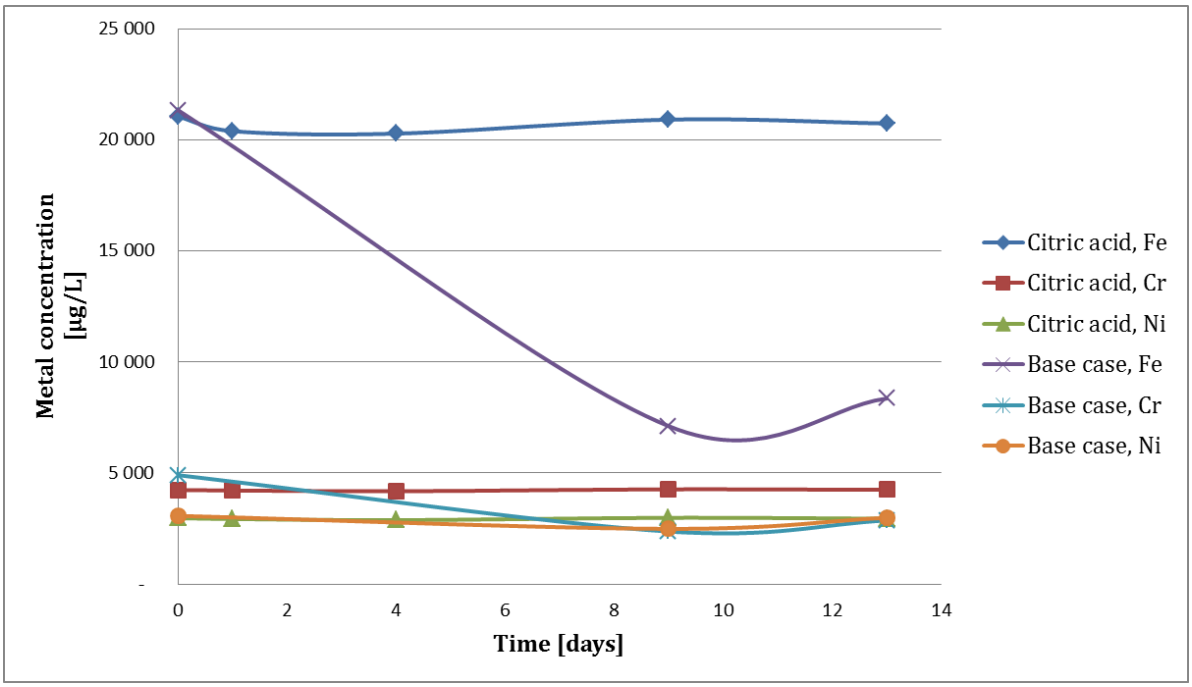

Figure 19: Plot of metal concentrations in experiments with- and without citric acid added.

The chelating agents seem to hold the metals in solution. It is important to see how this affects the corrosion if the inhibitors are to be used in industrial applications.

Since one metal ion can coordinate to several chelating groups, calculations were made to check that the concentrations of inhibitors were sufficient to chelate the metal present in the solutions. The highest possible coordination number for transition metals is nine [58]. This coordination number is therefore used for the metal ions present here, as a "worst case scenario". For potassium sodium tartrate, sodium triphosphate, citric acid and HEDP, the denticity (amount of chelating groups) are set to 4, 5, 4 and 7 respectively. By calculating the total coordination numbers and total denticity in the start samples, the results in Table 25 were obtained.

Table 25: Total coordination numbers and –denticity in samples containing chelating agents.

Inhibitor	Total coordination numbers [mol/kg]	Total denticity [mol/kg]
K Na tartrate	0,0042	0,0359
Na triphosphate	0,0051	0,0507
Citric acid	0,0042	0,0957
HEDP	0,0041	0,0570

The unit is given based on the calculations. From this table, it is clear that there is an excess of chelating agents. The concentrations should in other words not be the reason for the differences between the chelating agents.

3.5.1.4. Synergy experiments

No synergy effect was seen for the experiments with two different inhibitors added. In Table 18, the inhibitory effect was not larger than the best inhibitor alone in any of the experiments. The reason for this is suspected to be the metal passivating properties of carbohydrazide interfering with the chelation of the metal ions. The relative concentrations of the degradation compounds seem to follow the same trends as for the chelating agents added.

For further experiments containing a chelating agent and oxygen scavenger, the oxygen scavenger should be chosen to not have metal passivating properties. Other types of inhibitors should also be tested for synergy effects.

3.5.2. Effect of inhibitors on distribution of degradation compounds

Table 26 gives the rating of the products in the different experiments containing inhibitors.

Table 26: Effects of inhibitors on degradation product composition.

Inhibitor							Class
Potassium sodium tartrate	HEF	>HEI	>BHEOX	>OZD	>Nitrite	>Formate	Chelating agents
Sodium triphosphate	HEF	>HEI	>BHEOX	>OZD	>Nitrite	>Nitrate	
Citric acid	HEF	>HEI	>OZD	>BHEOX	>Nitrite	>Formate	
HEDP	HEF	>BHEOX	>Nitrite	>Formate	>OZD	>Nitrate	
Hydroquinone	HEF	>HEI	>BHEOX	>OZD	>Nitrite	>Formate	
Erythorbic acid	HEI	>HEF	>BHEOX	>OZD	>Formate	>Nitrate	
Carbohydrazide	HEF	>HEI	>OZD	>BHEOX	>Formate	>Nitrite	Oxygen and radical scavengers
Methallyl alcohol	HEF	>HEI	>BHEOX	>OZD	>Nitrite	>Formate	
Sodium sulfite	HEI	>HEF	>OZD	>BHEOX	>Formate	>Nitrate	
DEHA	HEF	>HEI	>BHEOX	>OZD	>HEA	>Nitrite	
MEKO	HEF	>HEI	>BHEOX	>OZD	>Nitrite	>Nitrate	
Sodium triphosphate Carbohydrazide	HEI	>HEF	>OZD	>BHEOX	>Formate	>Nitrite	Synergy
Citric acid Carbohydrazide	HEF	>BHEOX	>HEI	>OZD	>Nitrite	>Nitrate	
HEDP Carbohydrazide	HEF	>BHEOX	>OZD	>Nitrite	>Formate	>HEI	

HEF and HEI seem to be the most abundant degradation products for most of the samples. HEI concentrations are reduced in some of the experiments with chelating agents added, which can be related to the metal dependence of this compound, as discussed in 3.5.1.3.

An interesting observation is seen in the synergy experiment using citric acid and carbohydrazide. The formation of HEI has been reduced more than in the separate experiments, and BHEOX is the second most abundant degradation product. This is not seen for e. g. sodium triphosphate and carbohydrazide. This implies a synergy effect

between citric acid and carbohydrazide not present in the other synergy experiments. It may be that citric acid chelate ferrous iron better than ferric, and that the carbohydrazide reduce the ferric to ferrous. The overall degradation is still larger than with only carbohydrazide added, so the net effect does not imply synergy.

HEDP also reduce HEI formation marketly, but to a bigger extent in the experiment without carbohydrazide. This has been discussed earlier, and is believed to be due to the strong chelation of metal ions, which have a distinctive effect on HEI formation.

Formate is not among the six largest degradation compounds for the experiments containing MEKO and citric acid/carbohydrazide. The reason seems to be that nitrite is favored compared to formate in these samples, and not that the formation of formate is inhibited.

Table 27 gives the relative concentrations of the degradation compounds compared to their respective reactors. The relative amine losses are also given. These values are calculated by dividing the concentration in the base case experiments on the concentrations in the experiments containing inhibitors.

Table 27: Relative concentration of degradation products compared to the respective reactors.

Inhibitor	OZD	BHEOX	HEA	HeGly	HEPO	HEF	HEI	Formate	Nitrate	Oxalate	Nitrite	Relative amine loss
Potassium sodium tartrate	0,99	0,92	0,75	0,93	0,77	0,90	0,87	0,97	0,74	-	1,32	1,32
Sodium triphosphate	2,32	2,03	2,77	0,78	2,60	2,34	2,67	2,96	-	-	11,46	2,78
Citric acid	1,06	1,55	0,87	0,95	1,49	1,55	2,06	2,06	2,14	-	3,10	1,47
HEDP	2,98	2,42	1,75	1,14	4,50	1,38	34,67	1,39	-	-	-	3,13
Hydroquinone	0,82	0,64	0,98	1,79	3,76	0,76	0,71	0,67	0,85	0,55	1,01	0,85
Erythorbic acid	2,79	1,44	1,74	0,90	2,65	1,90	1,60	1,96	1,71	0,45	11,80	2,33
Carbohydrazide	1,31	2,07	1,55	1,66	2,20	1,54	1,53	2,48	2,05	-	7,60	2,50
Methallyl alcohol	0,71	0,65	0,79	1,47	1,17	0,80	0,80	0,67	0,84	-	0,71	0,83
Sodium sulfite	1,59	2,72	2,57	1,18	1,81	2,44	1,93	2,42	2,26	-	-	2,00
DEHA	1,58	1,18	0,13	1,47	2,04	1,50	1,71	2,15	1,42	-	2,21	1,61
MEKO	1,69	1,64	0,94	1,01	1,20	1,97	2,71	2,91	1,55	-	3,39	2,27
Sodium triphosphate Carbohydrazide	1,97	3,01	2,79	0,85	1,94	1,78	1,65	2,11	2,50	-	3,48	2,63
Citric acid Carbohydrazide	1,40	1,08	0,59	1,16	1,90	1,54	3,45	2,06	1,63	-	1,54	2,04
HEDP Carbohydrazide	2,03	1,44	1,24	0,98	-	2,10	36,27	2,99	3,46	-	2,32	2,44

The values given in Table 27 show some interesting points. Potassium sodium tartrate gives higher concentrations of all degradation products except for nitrite. The total degradation is still lower than in the base case. This can mean that the antioxidative effect lies in the first step of the oxidation of MEA, or a reduction in the formation of compounds not analyzed for here.

HeGly concentration is relatively higher compared with the change in degradation for the experiments with inhibitors exhibiting metal chelating properties. It is lower for HEDP, but it is the compound with the least reduction. This can be the same effect seen in the experiments without metals added, in Section 3.3.

Erythorbic acid gave a slight increase in HeGly concentration, which both can be due to its chelating and oxygen scavenging properties. The oxalate concentration in the end sample for this inhibitor was quite high compared to the base case. In Appendix B: LC-MS raw data, where the LC-MS data is given, it can be seen that the BHEOX concentration in this sample also is acting weird. It starts with a value of 5406 µg/mL and ends up at 2130 µg/mL. Erythorbic acid was tested on the LC-MS to see if it could be mistaken for BHEOX, as they have the same molecular weight. The results from this test did not indicate that erythorbic acid should be able to be mistaken for BHEOX. There is a possibility that the inhibitor has reacted with MEA to form BHEOX, but this will need further investigation.

Goff [14] found that 65,5 mM ascorbic acid added to 7,0 m MEA increased the ammonia evolution by a factor of more than 2,5. Erythorbic acid is a stereoisomer of ascorbic acid and would be assumed to react by the same mechanisms. The concentration used in the experiment with erythorbic acid was 51 mmol/kg, and gave 57,4% inhibition. These differences in activity show how important it is to test inhibitors in different concentrations and systems.

In the end sample from the MEKO experiment, HEA is the only degradation compound present in higher quantities than in the base case. Based on the structure of the inhibitor, it is not plausible that it degrades to a precursor of HEA. It is more likely that it affect the degradation mechanism to give more acetaldehyde in the initial step.

NDELA was found in two of the experiments, in the base case for reactor R2, and for the experiment with hydroquinone added. Both these reactors had high degradation and -concentrations of nitrite. In the base case for reactor R5, the nitrite concentration was higher than in the hydroquinone experiment. The actual concentrations in the base case experiments were actually higher than the numbers given, as the leaks in these experiments concentrated the solutions. This indicates that hydroquinone can increase NDELA formation. The raw data for the IC-EC analyses are given in Appendix I: IC-EC . Table 28 shows the amine loss, nitrite- and NDELA concentrations for the two experiments where NDELA was detected.

Table 28: Amine loss, nitrite- and NDELA concentrations for base case R2 and hydroquinone experiment.

Experiment	Amine loss	Nitrite concentration [mg/kg]	NDELA concentration [ng/mL]
Base case R2	37,63	2146	955
Hydroquinone	29,68	1664	607

3.5.3. Circulative experiment with hydrazine

Hydrazine was screened for inhibitory effect in a closed system because of its hazardous properties. The background for screening hydrazine was for mechanistic purposes, rather than as an actual alternative for industrial use.

Data for MEA without additives run on the same apparatus were obtained from unpublished work by Solrun J. Vevelstad. Figure 20 shows a plot for the amine loss with- and without hydrazine added.

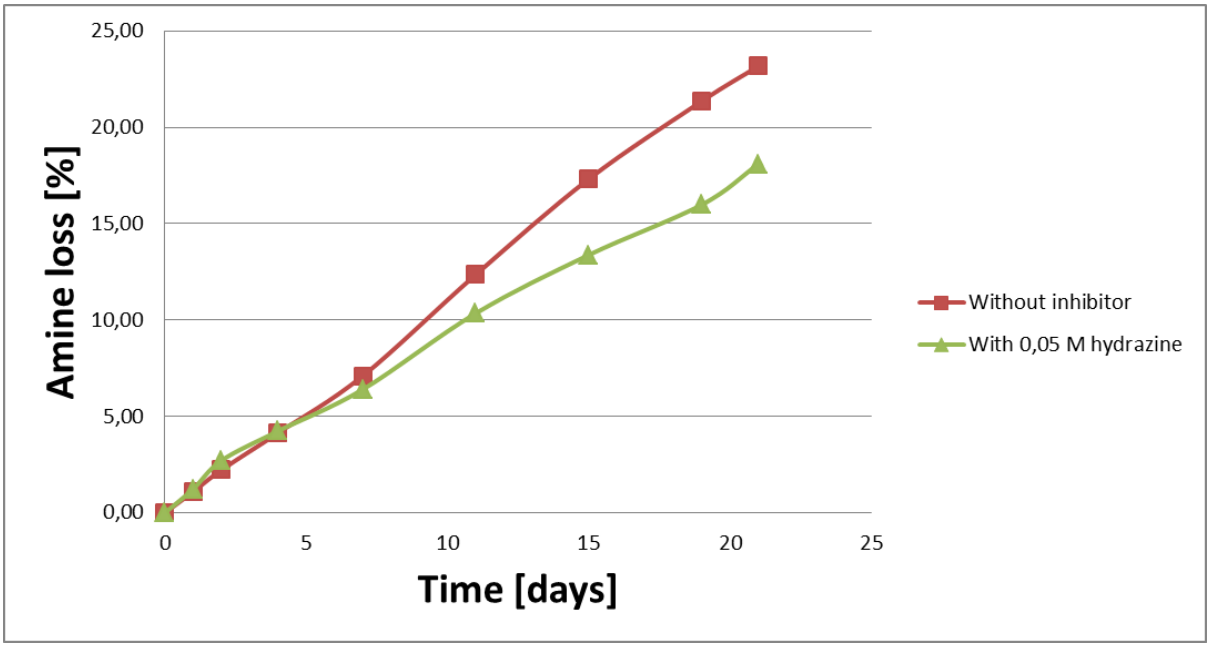

Figure 20: Comparison of MEA with- and without hydrazine added, run on the closed circulative apparatus.

It is seen from this plot that hydrazine, at the given concentration, do not inhibit degradation very well. The difference in amine loss between the two cases is 21,93%.

Table 29 shows how the ranking of the largest degradation compounds change between the two experiments.

Table 29: Ranking of the largest degradation products for experiments with- and without hydrazine added.

MEA + 0,005M hydrazine	HEI	>HEF	>BHEOX	>OZD	>HeGly	>HEA
MEA	HEI	>HEF	>HeGly	>BHEOX	>OZD	>HEA

HeGly seems to be favored in the experiment without hydrazine added. This is not the expected result, as an oxygen scavenger would decrease the overall oxidation and thus favor HeGly, as discussed in Section 3.5.1.2.

It is hard to compare the results from this experiment with the results from inhibitor screening apparatus, since the experimental conditions are so different. By running some of the other inhibitors on the circulative closed loop apparatus, comparable data would be obtained.

3.5.4. Thermal experiments

Experiments at thermal conditions were performed to see whether the inhibitors were stable at higher temperatures, resembling stripper conditions. Since the samples were available, it was natural to see if the inhibitors affected the carbamate polymerization degradation that occurs at these conditions. Inhibitors were added to a 30 wt% MEA solution loaded with 0,5 mol CO_2/mol MEA, degassed with N_2. Figure 21 show the results from the total alkalinity titration conducted on the samples.

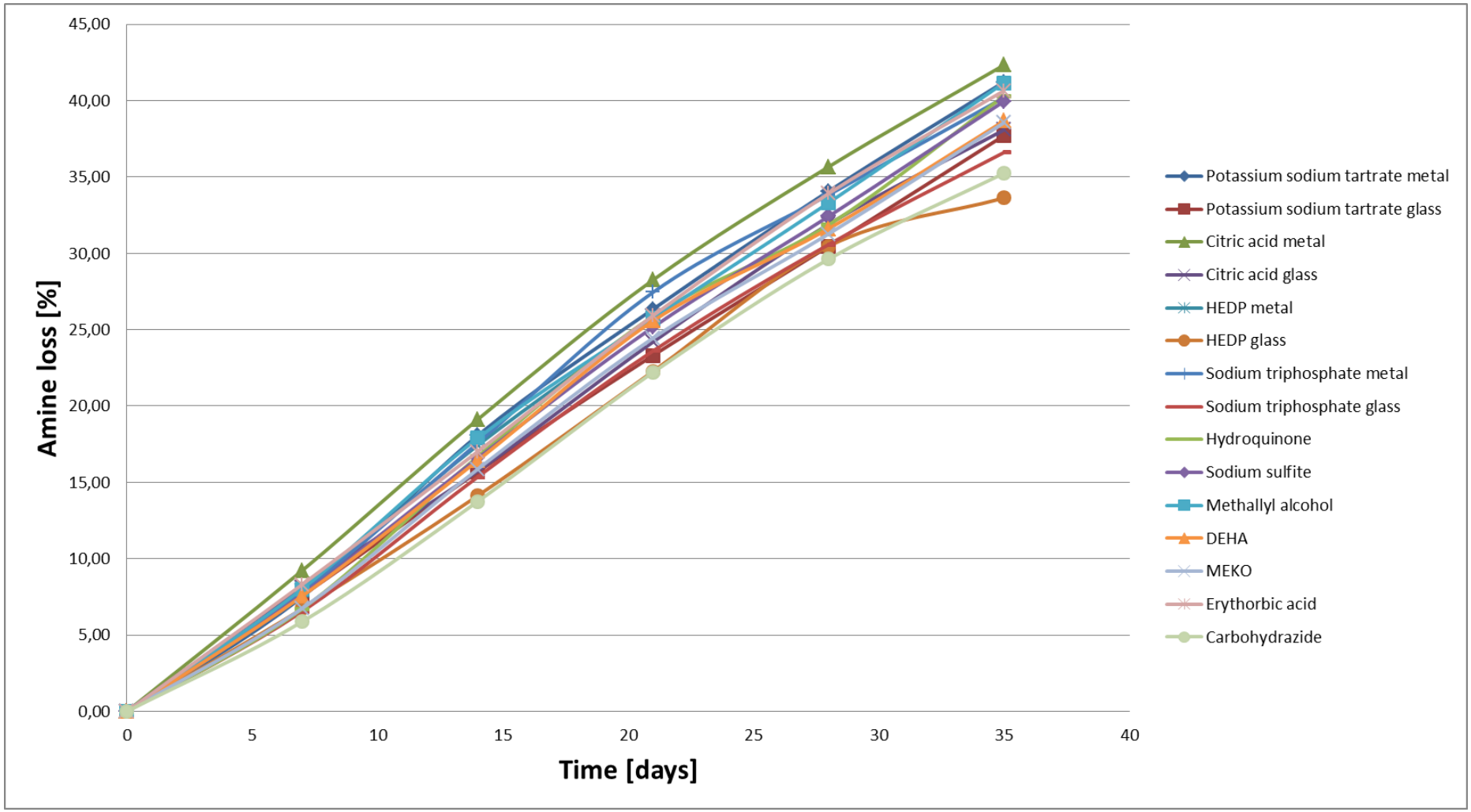

Figure 21: Amine loss in thermal degradation experiments with inhibitors added (30 wt% MEA, α=0,5, 135 °C).

From Figure 21, it can be seen that the total loss in alkalinity varies from 33-43%. All the samples follow a somewhat straight line, and the inhibitors do not appear to affect the carbamate polymerization to any extent. For hydroquinone, the starting concentration was set to 4,25 mol /kg MEA as the initial sample was lost.

AEHEIA and HEEDA (shown in Figure 7) is reported by Lepaumier [13] and da Silva [9] to be major products from experiments conducted at similar conditions as here. These have primary and secondary amine functions that will respond to the total alkalinity titration. Therefore LC-MS analysis was conducted on selected samples from the experiment to compare with values similar experiments without inhibitor by Eide-Haugmo [16]. This is shown in Figure 22.

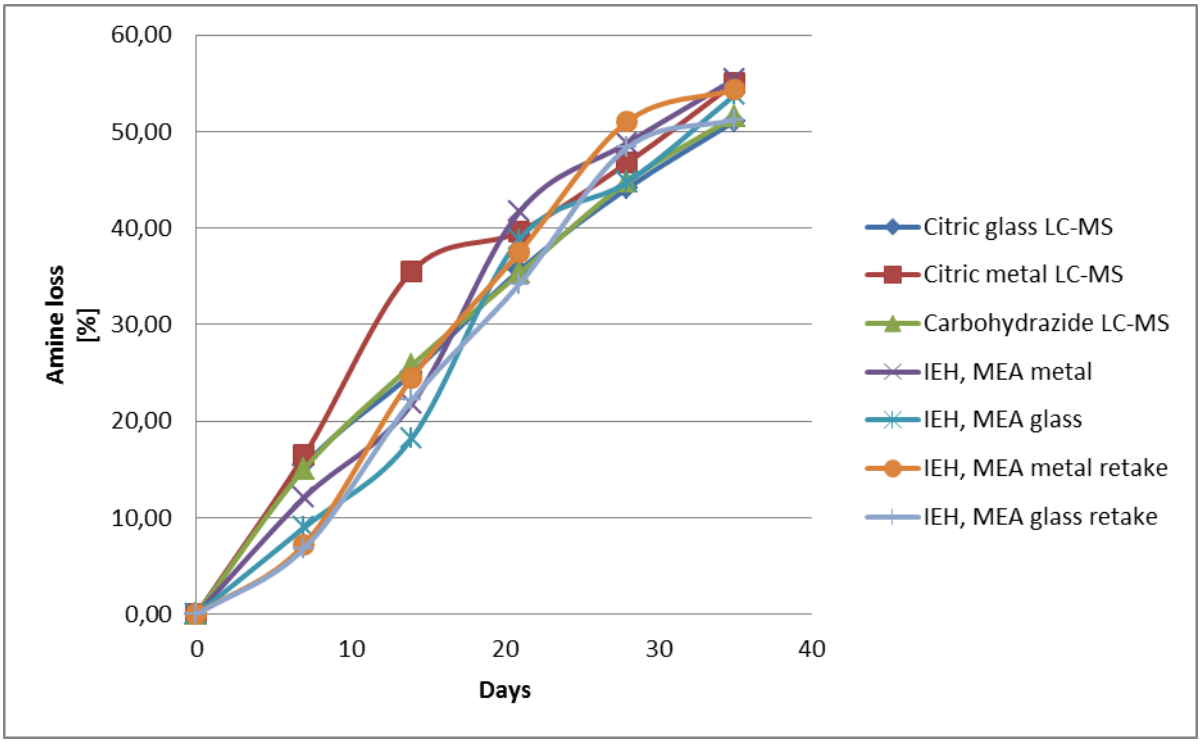

Figure 22: LC-MS analysis on selected samples in comparison with data from Eide-Haugmo [16].

There are differences between the end points for these analyses, but the deviations are not very big. It may be that the addition of inhibitors has affected the distribution of the degradation compounds. To determine if this is the case, the samples have to be analyzed by GC-MS to see if there are variations in the amounts of degradation products. It would however not be expected that the inhibitors would affect the carbamate polymerization. A more plausible explanation is that the concentrations of MEA and CO_2 are not the same in all parallels, since the inhibitors were added as aqueous solutions of different concentrations. The more concentrated solutions would have a higher degradation, giving a spread. The effect of metals is also low, which is in accordance with literature. [9]

3.5.5. Stability of chelating agents

By determining the concentrations of the chelating agents throughout the experiments conducted at thermal and oxidative conditions, the stability could be assessed. Initially, the plan was to determine the thermal stability of all the inhibitors, but analytical methods were not available for other than the anionic compounds. The oxygen/radical scavengers would be analyzed on LC-MS or GC-MS if methods and/or apparatuses were available.

The concentrations of the chelating agents were determined using the IC-EC. By using the samples from the oxidative inhibitor screening- and thermal experiments, the stability could be determined. It was necessary to adjust the pH in the standards for HEDP to make the external standard curve. A pH-adjustment of the citric acid gave less accurate concentrations. The method for HEDP would need some work, since the calculated concentrations deviate from the concentrations found on the IC-EC. In this assignment however, the most important was to see if the concentrations changed throughout the experiments. The calculated concentrations and concentrations from analyses are given in Appendix J: Calculated concentrations of inhibitors and Appendix I: IC-EC raw data respectively.

Figure 23 shows the measured concentrations of the chelating agents from the oxidative screening apparatus.

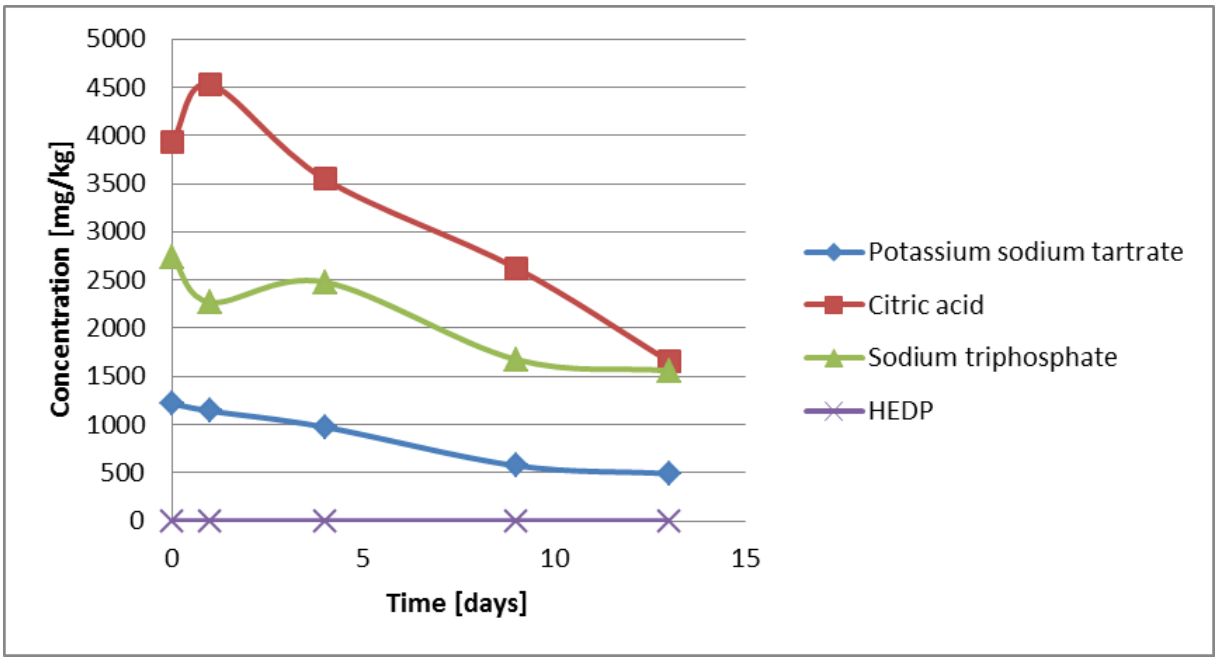

Figure 23: Plot of chelating inhibitor concentrations at oxidative conditions.

Figure 24 show a plot of the concentrations of the chelating agents from the experiment at thermal conditions.

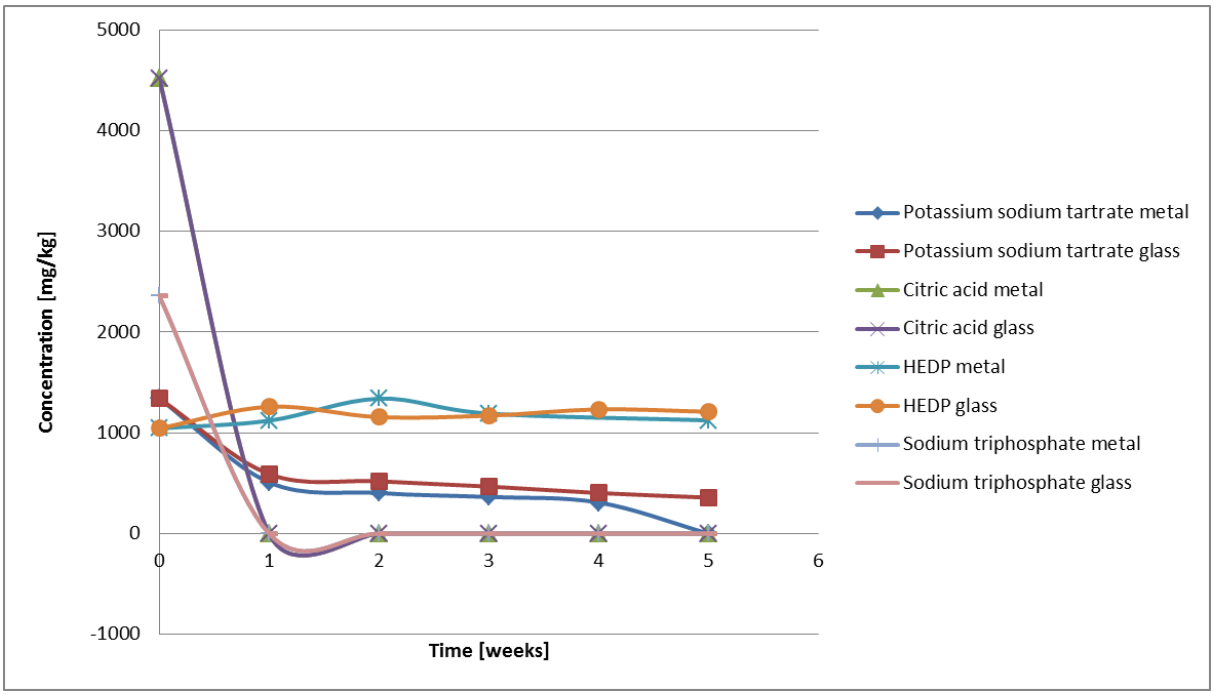

Figure 24: Plot of chelating inhibitor concentrations at thermal conditions.

HEDP was not detectable on the IC-EC in the samples from the inhibitor screening experiments. Since this compound was stable at 135 °C for five weeks, and gave the least degradation from all the inhibitor screening experiments, the probability that it has been degraded in the solution is low. A more plausible explanation is that the HEDP is bonded so strongly to the metal ions in the solution that it is not ionized in the IC-EC and thus not detectable. In the IC-EC analysis done on HEDP in the thermal experiments, seen in Figure 24, only minor variations are present, showing no sign of degradation.

The other inhibitors do not seem to be stable at neither absorber nor stripper conditions. In the experiments conducted using the inhibitor screening apparatus, the degradation of the inhibitors would be most likely to go by either an oxidation or a hydrolysis. At stripper conditions, either a thermal decomposition or a hydrolysis would be most likely. For the experiments containing citric acid and sodium triphosphate, the anion chromatography of the thermal experiments showed a new peak at a new retention time for the samples where the inhibitor disappeared. Sodium triphosphate has been reported to readily hydrolyze to ortho- and pyrophosphate at 70 and 100°C. [59] Potassium sodium tartrate is not stable at either of the conditions it was exposed for.

The figures on the next page show chromatograms from the IC-EC in the quantification of the chelating agents. Figure 25 shows an overlaid chromatogram for the samples containing citric acid from the inhibitor screening apparatus.

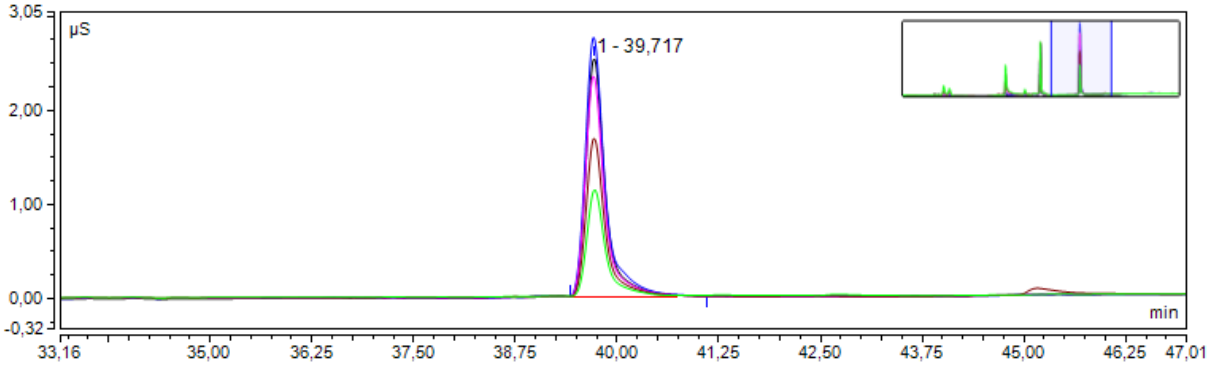

Figure 25: Overlaid IC-EC chromatogram of citric acid from the oxidative inhibitor screening experiment.

By this figure it is clearly seen that the concentration of citric acid continuously decrease throughout the experiment. Figure 26 shows an overlaid chromatogram for the thermal experiment with sodium triphosphate, for the initial sample and after one week.

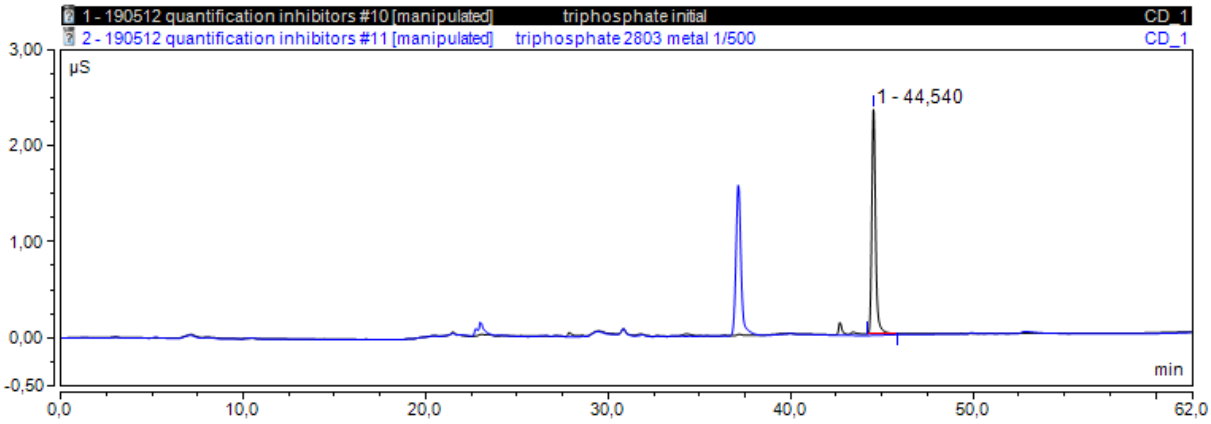

Figure 26: Overlaid IC-EC chromatograms for the initial sample and after one week for sodium triphosphate for the thermal experiment.

Here it is clearly seen how the initial peak for the triphosphate anion disappear completely after one week, and a new peak appears at a new retention time.

Figure 27 shows an overlaid chromatogram of HEDP from the thermal experiment, showing its stability.

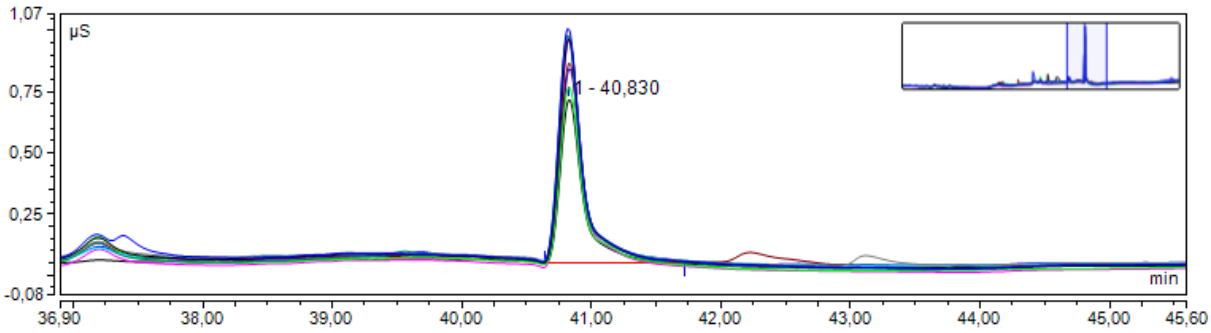

Figure 27: Overlaid IC-EC chromatogram for HEDP from the thermal experiment.

The variations in HEDP signals in the chromatograms shown in Figure 27 are not due to degradation, but a result of the variations in the dilution step. The concentrations from the analyses given in Appendix I: IC-EC raw data can confirm that.

4. Conclusions

The densities of the samples from the different experiments do vary quite a bit. In the future, all the analyses should be conducted on the same basis, to avoid unnecessary uncertainties in the results.

The largest uncertainty is due to the reproducibility of the reactors, especially since some of these experiments had substantial water loss. Concentration of solutions due to evaporative losses of water may increase the overall degradation, causing large uncertainties in the base case experiments.

The titration methods show low uncertainties in the results. Having standard deviations of 0,23% and 0,44%, these methods are considered quite good.

For the IC-EC method, the largest deviations were found when different dilutions were used. The second largest source of deviations in this test was in the dilution step, due to uncertainties in the weighing. When determining concentrations of anionic inhibitors the pH should be adjusted to ensure that the inhibitors have the same protonation stage in the standards as in the samples.

The degradation increases with the addition of metals. The amount of the different degradation compounds is also affected by the metal concentration. This is best seen for HEI, but also HEA and nitrate concentrations are increased more than the overall degradation when metals are added. This is a result of metal catalyzed reactions to get either the precursor or the given degradation product, or a combination of the two. HeGly is favored at low metal concentration, which indicates that the precursor of this compound is an intermediate in the oxidation route.

The effect of oxygen content in the gas on both degradation and relative concentrations of the degradation compounds is clearly seen. HeGly is favored at lower oxygen concentrations, which support that its precursor is a partial oxidation product. The amount of nitrate and nitrite increase more than the overall degradation, which can be a result of an increase in both evolution and oxidation of ammonia. The amount of OZD also increases more than the overall degradation, which causes ground for a new mechanism for its formation at absorber conditions. HEA, HEPO, HEF and HEI do not show the same increase as the overall degradation.

HEDP is the most efficient of the inhibitors tested in this thesis. It is also the only of the chelating agents that appears to be stable at both absorber and stripper conditions. Sodium triphosphate proved to be a good inhibitor, but is not stable in this process. A salting out effect of O_2 may be present for the chelating agents, giving a combined effect of inhibition. It has been raised concern about whether the chelating agents are corrosive.

The best oxygen scavengers were found to be carbohydrazide, erythorbic acid and MEKO. Whether these are stable at thermal conditions is unknown, since no suitable

analytical method was available at the time. The stability of the oxygen scavengers at stripper conditions should also be determined when an analytical method is available. It is important to consider the oxidation products of the scavengers, and how these affect the process through formation of dissolved solids and potential hazardous volatile products. Hydrazine was not effective in the concentration used in the experiment in this thesis.

In the experiments where carbohydrazide was added together with HEDP, citric acid and sodium triphosphate, respectively, no synergy effect was seen. All of these mixes gave more degradation than the best inhibitor added in the experiment. This may have been a result of the reducing properties of carbohydrazide interfering with the chelation.

None of the inhibitors had any specific effect on the thermal degradation. This was as expected, since the inhibitors were not believed to interfere with the carbamate polymerization mechanism. The total alkalinity titration did not give a good picture of the overall degradation, since two of the main thermal degradation compounds have amine functionality.

5. Further work

For further work on the inhibitor screening apparatus, more experiments with base case conditions should be conducted to check the reproducibility. It should also be considered to replace the spargers, to give more similar distribution of the gas in the separate reactors. This will require new inhibitor experiments.

The effect of different oxygen concentrations should be studied further. By using a lower oxygen concentration, the relative amount of primary degradation products would be higher, which could help to determine the primary mechanism. The mechanism for formation of HeGly should be investigated further, focusing on precursors favored at less oxidizing conditions, in reactions that do not require metal catalysis. The stability and further reactions of HeGly should also be investigated to determine the connection to HEPO. Work should be done to determine if glyoxal is present in the solutions to validate if this is the limiting precursor for formation of HEI.

The inhibitors should be tested in different concentrations to determine efficiency, keeping in mind the reaction stoichiometry of the inhibitors. The thermal stability of the oxygen/radical scavengers should be examined when an analytical method is available. To see if a salting out effect is present in the experiments containing chelating agents, degradation experiments using high purity MEA with chelating agents added can be conducted. If a chelating agent is to be used in industrial applications, it is important that corrosivity tests are performed, to see if they increase the corrosiveness of the solution. If radical/oxygen scavengers are considered to be used, it is important to see which oxidation products they yield, and how these can affect the process.

More work should be done in the quantification of HEDP, since the IC-EC method used in this thesis does not seem to give a concentration in accordance with the calculated value.

For further work regarding synergy experiments, an oxygen scavenger without metal passivating properties, such as sodium sulfite, should be used instead of carbohydrazide when combining with a chelating agent. Catalyzed oxygen scavengers, as used in boiler systems, should also be investigated.

References

1. Change, I.P.O.C., *Climate change 2007: The physical science basis.* Agenda, 2007. **6**: p. 07.
2. Ramaswamy, V., et al., *Radiative forcing of climate change*, 2001, Pacific Northwest National Laboratory (PNNL), Richland, WA (US).
3. Lu, J., G.A. Vecchi, and T. Reichler, *Expansion of the Hadley cell under global warming.* Geophys. Res. Lett, 2007. **34**(1.06805).
4. Stangeland, A. *CO2 Capture*. 2007 [cited 2012 03.05.12]; Available from: http://www.bellona.org/factsheets/1191913555.13.
5. Thomas, D.C., *Carbon Dioxide Capture for Storage in Deep Geologic Formations-Results from the CO2 Capture Project*. Vol. 1. 2005: Elsevier Science Ltd.
6. Bedell, S.A., *Oxidative degradation mechanisms for amines in flue gas capture.* Energy Procedia, 2009. **1**(1): p. 771-778.
7. Kohl, A.L. and R. Nielsen, *Gas Purification*, 1997, Gulf publisher company. p. 1414.
8. Voice, A.K. and G.T. Rochelle, *Oxidation of amines at absorber conditions for CO2 capture from flue gas.* Energy Procedia, 2011. **4**(0): p. 171-178.
9. da Silva, E.F., et al., *Understanding MEA degradation in post-combustion CO_2 capture.* Industrial & Engineering Chemistry Research, 2012. **In review**.
10. Strazisar, B.R., R.R. Anderson, and C.M. White, *Degradation Pathways for Monoethanolamine in a CO_2 Capture Facility.* Energy & fuels, 2003. **17**: p. 1034-1039.
11. Aouini, I., et al., *Study of carbon dioxide capture from industrial incinerator flue gas on a laboratory scale pilot.* Energy Procedia, 2011. **4**: p. 1729-1736.
12. Rao, A.B. and E.S. Rubin, *A Technical, Economic, and Environmental Assessment of Amine-Based CO2 Capture Technology for Power Plant Greenhouse Gas Control.* Environmental Science & Technology, 2002. **36**(20): p. 4467-4475.
13. Lepaumier, H., et al., *Comparison of MEA degradation in pilot-scale with lab-scale experiments.* Energy Procedia, 2011. **4**(0): p. 1652-1659.
14. Goff, G.S. and G.T. Rochelle, *Oxidation Inhibitors for Copper and Iron Catalyzed Degradation of Monoethanolamine in CO2 Capture Processes.* Industrial and engineering chemistry research, 2006. **45**: p. 2513-2521.
15. Supap, T., et al., *Investigation of degradation inhibitors on CO2 capture process.* Energy Procedia, 2011. **4**(0): p. 583-590.
16. Eide-Haugmo, I., *Environmental impacts and aspects of absorbents used for CO_2 capture*, in *Department of Chemical Engineering*2011, Norwegian University of Science and Technology: Trondheim.
17. Tobiesen, F.A. and H.F. Svendsen, *Study of a Modified Amine-Based Regeneration Unit.* Industrial & Engineering Chemistry Research, 2006. **45**(8): p. 2489-2496.
18. Bedell, S.A., *Amine autoxidation in flue gas CO2 capture—Mechanistic lessons learned from other gas treating processes.* International Journal of Greenhouse Gas Control, 2011. **5**(1): p. 1-6.
19. Sexton, A.J. and G.T. Rochelle, *Catalysts and inhibitors for MEA oxidation.* Energy Procedia, 2009. **1**(1): p. 1179-1185.
20. Sexton, A.J., *Andrew Sexton Dissertation.* 2008.
21. Chi, S. and G.T. Rochelle, *Oxidative Degradation of Monoethanolamine.* Industrial and engineering chemistry research, 2002. **41**: p. 4178-4186.
22. Goff, G.S. and G.T. Rochelle, *Monoethanolamine Degradation: O2 Mass Transfer Effects under CO2 Capture Conditions.* Industrial and engineering chemistry research, 2004. **43**: p. 6400-6408.
23. Petryaev, E., A. Pavlov, and O. Shadyro, *Homolytic deamination of amino alcohols.* Zh. Org. Khim, 1984. **20**(1): p. 29-34.
24. Sun, Z., Y.D. Liu, and R.G. Zhong, *Carbon Dioxide in the Nitrosation of Amine: Catalyst or Inhibitor?* The Journal of Physical Chemistry A, 2011. **115**(26): p. 7753-7764.

25. Hung, C.-M., J.-C. Lou, and C.-H. Lin, *Catalytic Wet Oxidation of Ammonia Solution: Activity of the Copper--Lanthanum--Cerium Composite Catalyst.* Journal of Environmental Engineering, 2004. **130**(2): p. 193-200.
26. Imamura, S., A. Doi, and S. Ishida, *Wet oxidation of ammonia catalyzed by cerium-based composite oxides.* Industrial & Engineering Chemistry Product Research and Development, 1985. **24**(1): p. 75-80.
27. Sexton, A.J. and G.T. Rochelle, *Reaction Products from the Oxidative Degradation of Monoethanolamine.* Industrial & Engineering Chemistry Research, 2011. **50**(2): p. 667-673.
28. Sexton, A.J. and G.T. Rochelle, *Catalysts and inhibitors for oxidative degradation of monoethanolamine.* International Journal of Greenhouse Gas Control, 2009. **3**(6): p. 704-711.
29. Blachly, C. and H. Ravner, *The stabilization of monoethanolamine solutions for submarine carbon dioxide scrubbers*, 1964, DTIC Document.
30. Blachly, C.H. and H. Ravner, *Stabilization of Monoethanolamine Solutions in Carbon Dioxide Scrubbers.* Journal of Chemical & Engineering Data, 1966. **11**(3): p. 401-403.
31. Rooney, P.C., T.R. Bacon, and M.S. DuPart, *Oxygen's role in alkanolamine degradation.* Hydrocarbon processing, 1998(July): p. 109-113.
32. Bello, A. and R.O. Idem, *Pathways for the Formation of Products of the Oxidative Degradation of CO2-Loaded Concentrated Aqueous Monoethanolamine Solutions during CO2 Absorption from Flue Gases.* Industrial & Engineering Chemistry Research, 2005. **44**(4): p. 945-969.
33. Wanasundara, P. and F. Shahidi, *Antioxidants: Science, technology, and applications.* Bailey's Industrial Oil and Fat Products, 2005.
34. E. Denisov, I.A., *Oxidation and Antioxidants in Organic Chemistry and Biology*, 2005, Taylor & Francis: Boca Raton, FL.
35. Frankel, E., *Lipid oxidation.* Progress in Lipid Research, 1980. **19**: p. 1-22.
36. Kirk, R.E., et al., *Encyclopedia of chemical technology*. Vol. 8. 1965: Wiley-Interscience.
37. Graf, E. and J.W. Eaton, *Antioxidant functions of phytic acid.* Free Radical Biology and Medicine, 1990. **8**(1): p. 61-69.
38. Lamson, M.L., J.L. Fox, and W.I. Higuchi, *Calcium and 1-hydroxyethylidene-1,1-bisphosphonic acid: polynuclear complex formation in the physiological range of pH.* International Journal of Pharmaceutics, 1984. **21**(2): p. 143-154.
39. Jaffer, A.E., J.D. Ensslen, and D.E. Fulmer, *Recent Developments in Organic Oxygen Scavenger Technology.* CORROSION 2006, 2006.
40. Arkema. *Oxygen scavengers*. 2001 [cited 2012 21.03]; Selection guide for oxygen scavengers]. Available from: http://www.arkema-inc.com/literature/pdf/346.pdf.
41. Idem, R., et al., *Method for inhibiting amine degradation during CO2 capture from flue gas stream*, 2009, The University of Regina, Can. . p. 41pp.
42. Rochelle, G., *CO_2 Capture by Aqueous Absorption Summary of First Quarterly Progress Reports 2011*, G. Rochelle, Editor 2011, The University of Texas at Austin.
43. Hraš, A.R., et al., *Comparison of antioxidative and synergistic effects of rosemary extract with α-tocopherol, ascorbyl palmitate and citric acid in sunflower oil.* Food Chemistry, 2000. **71**(2): p. 229-233.
44. Rondum, K.D., G.A. DeVicaris, and D.E. Emerich, *Method for inhibiting foulant formation in organic streams using erythorbic acid or oximes*, 1993, Google Patents.
45. Veldman, R., *Alkanolamine Solution Corrosion Mechanisms and Inhibition From Heat Stable Salts and CO2.* CORROSION 2000, 2000.
46. Abuin, E., et al., *On the reactivity of diethyl hydroxyl amine toward free radicals.* International Journal of Chemical Kinetics, 1978. **10**(7): p. 677-686.
47. Kell, G.S., *Density, thermal expansivity, and compressibility of liquid water from 0.deg. to 150.deg.. Correlations and tables for atmospheric pressure and saturation reviewed and expressed on 1968 temperature scale.* Journal of Chemical & Engineering Data, 1975. **20**(1): p. 97-105.

48. Katsuura, A. and N. Washio, *Preparation of imidazoles from imines and iminoacetaldehydes*, 2005, Nippon Synthetic Chemical Industry Co., Ltd., Japan . p. 6 pp.
49. Kawasaki, N., et al., *Preparation of 1-substituted imidazoles*, 1991, Mitsui Toatsu Chemicals, Inc., Japan . p. 7 pp.
50. Arduengo, A.J., et al., *Process for manufacture of imidazoles*, 2001, US 5077414 (Dec, 1991) Arduengo 548/335.1: US.
51. Patil, Y.P., et al., *Synthesis of 2-oxazolidinones/2-imidazolidinones from CO2, different epoxides and amino alcohols/alkylene diamines using Br−Ph3+P-PEG600-P+Ph3Br− as homogenous recyclable catalyst.* Journal of Molecular Catalysis A: Chemical, 2008. **289**(1–2): p. 14-21.
52. Talzi, V.P., *NMR Determination of the Total Composition of Commercial Absorbents Based on Monoethanolamine.* Russian Journal of Applied Chemistry, 2004. **77**(3): p. 430-434.
53. Chakma, A. and A. Meisen, *Identification of methyl diethanolamine degradation products by gas chromatography and gas chromatography-mass spectrometry.* Journal of Chromatography A, 1988. **457**(0): p. 287-297.
54. Ratner, S., V. Nocito, and D. Green, *Glycine oxidase.* Journal of Biological Chemistry, 1944. **152**(1): p. 119-133.
55. Ruiz, R., et al., *Iron(III) oxamato-catalyzed epoxidation of alkenes by dioxygen and pivalaldehyde.* Chem. Commun. (Cambridge), 1997(Copyright (C) 2011 American Chemical Society (ACS). All Rights Reserved.): p. 2283-2284.
56. Shryne, T.M. and L. Kim, *Epoxidation of olefins*, 1977, Shell Oil Co., USA . p. 5 pp.
57. Roundhill, D.M., *Transition metal and enzyme catalyzed reactions involving reactions with ammonia and amines.* Chemical Reviews, 1992. **92**(1): p. 1-27.
58. Crabtree, R.H., *The organometallic chemistry of the transition metals*2009: John Wiley & Sons Inc.
59. Bell, R.N., *Hydrolysis of dehydrated Sodium Phosphates.* Industrial & Engineering Chemistry, 1947. **39**(2): p. 136-140.

Appendices

Appendix A – Chemicals

Appendix B: LC-MS raw data

Appendix C: LC-MS NDELA raw data

Appendix D: ICP-MS raw data

Appendix E: Total alkalinity and CO_2-titration inhibitor screening apparatus

Appendix F: Total alkalinity- and CO_2-titration circulative experiment

Appendix G: Total alkalinity- and CO_2-titration thermal experiments

Appendix H: LC-MS MEA thermal experiments

Appendix I: IC-EC

Appendix J: Calculated concentrations of inhibitors

Appendix K: Degradation products

Appendix A – Chemicals

Table 30: Overview of the chemicals used in this thesis.

Chemical name	CAS nr.	Quality	Supplier	Cat. Nr.	Lot nr.
Sulfuric acid	7664-93-9	95-97%	Sigma-Aldrich	84720	-
Ferrous sulfate heptahydrate	7782-63-0	>99,5%	Merck	7475628	-
2-aminoethanol	141-43-5	≥99,0%	Sigma-Aldrich	398136	BCBF8098V
2-methyl-2-propen-1-ol	513-42-8	98 %	Sigma-Aldrich	112046	BCBB2690V
Sodium triphosphate pentabasic	7758-29-4	≥98%	Sigma-Aldrich	72061	BCBF7795V
Potassium sodium tartrate tetrahydrate	6381-59-5	99 %	Sigma-Aldrich	217-255	MKBF8214V
Hydroquinone	123-31-9	≥99%	Fluka	53960	BCBF2364V
Etidronic acid monohydrate	25211-86-3	≥95%	Aldrich	54342	BCBC7777V
Citric acid	77-92-9	99 %	Sigma-Aldrich	C0759	120M0061V
Formic acid	64-18-6	98 %	Fluka	6440	1434094
Oxalic acid	144-62-7	≥99,0%	Sigma-Aldrich	75688	BCBD6467V
Sodium nitrate	7757-79-1	≥99+%	Sigma-Aldrich	221295	06228CJ
Sodium nitrite	7632-00-0	≥97,0%	Sigma-Aldrich	237213	1451880
Sodium hydroxide	1310-73-2	50% in water	J. T. Baker	-	1029301033
Sodium sulfate	7757-82-6	≥99,0%	Sigma-Aldrich	23,859-7	MKAA4008F9

Appendix B: LC-MS raw data

Table 31: LC-MS degradation mix, raw data inhibitor screening experiment 1.

Reactor	Additive	Day	Journal ID	OZD	BHEOX	HEA	HeGly	HEPO	HEF	HEI	Unit
R1	Metal mix, 6%	0	P12626	< 10	56,1	< 10	< 10	< 10	459,2	188,7	µg/mL
R1	Metal mix, 6%	1	P12627	< 10	100,1	20,2	12,4	< 10	722,7	348,7	µg/mL
R1	Metal mix, 6%	4	P12628	< 10	122,6	16,0	30,2	< 10	976,2	659,4	µg/mL
R1	Metal mix, 6%	8	P12629	34,6	269,7	34,3	81,0	< 10	1578,9	1385,9	µg/mL
R1	Metal mix, 6%	13	P12630	65,4	395,1	60,3	134,7	< 10	2275,0	2231,3	µg/mL
R1	Metal mix, 6%	21	P12631	123,1	552,7	116,0	228,4	15,0	3178,7	3487,5	µg/mL
R1	Metal mix, 6%	24	P12632	213,9	657,1	148,2	301,2	18,0	3873,6	4441,2	µg/mL
R2	Metal mix, 6%	0	P12633	< 10	52,8	< 10	10,3	< 10	489,3	173,5	µg/mL
R2	Metal mix, 6%	1	P12634	< 10	77,0	< 10	30,5	< 10	623,0	397,8	µg/mL
R2	Metal mix, 6%	4	P12635	< 10	130,6	39,9	146,9	< 10	1236,7	1357,9	µg/mL
R2	Metal mix, 6%	8	P12636	25,5	170,2	68,8	322,6	19,3	1694,1	2952,3	µg/mL
R2	Metal mix, 6%	13	P12637	62,6	229,2	121,0	680,1	36,2	2155,7	4772,3	µg/mL
R2	Metal mix, 6%	21	P12638	77,9	331,5	239,6	962,9	54,1	3075,1	7110,5	µg/mL
R2	Metal mix, 6%	24	P12639	186,4	389,5	333,5	1293,5	76,9	3599,9	8836,8	µg/mL
R3	Metal mix, 6%	0	P12640	< 10	33,6	< 10	< 10	< 10	374,4	138,5	µg/mL
R3	Metal mix, 6%	1	P12641	< 10	85,9	15,2	22,1	10,1	595,5	271,2	µg/mL
R3	Metal mix, 6%	4	P12642	< 10	119,8	24,0	51,1	< 10	928,1	807,4	µg/mL
R3	Metal mix, 6%	8	P12643	45,2	253,8	57,6	109,8	10,4	1631,2	1705,3	µg/mL
R3	Metal mix, 6%	13	P12644	113,7	348,5	73,6	205,8	20,6	2639,6	2850,4	µg/mL
R3	Metal mix, 6%	21	P12645	150,7	496,1	130,9	325,8	21,0	3312,0	4469,1	µg/mL
R3	Metal mix, 6%	24	P12646	239,1	574,0	169,8	473,0	36,3	4027,6	5614,0	µg/mL
R4	Metal mix, 6%	0	P12647	< 10	51,9	< 10	12,0	< 10	452,0	153,4	µg/mL
R4	Metal mix, 6%	1	P12648	< 10	52,9	< 10	23,0	< 10	566,0	289,4	µg/mL
R4	Metal mix, 6%	4	P12649	21,5	91,4	15,5	68,8	10,1	942,1	901,8	µg/mL
R4	Metal mix, 6%	8	P12650	33,0	136,4	34,5	114,9	< 10	1458,2	1709,1	µg/mL
R4	Metal mix, 6%	13	P12651	116,1	212,2	60,2	218,8	14,5	2015,4	2802,6	µg/mL
R4	Metal mix, 6%	21	P12652	241,0	283,8	111,4	384,2	20,5	2748,0	4327,4	µg/mL
R4	Metal mix, 6%	24	P12653	432,4	336,6	144,6	449,9	31,4	3347,0	5276,5	µg/mL
R5	Metal mix, 6%	0	P12654	< 10	50,2	< 10	18,9	< 10	568,0	182,0	µg/mL
R5	Metal mix, 6%	1	P12655	< 10	62,8	< 10	14,7	< 10	586,3	302,6	µg/mL
R5	Metal mix, 6%	4	P12656	14,2	92,8	22,0	59,4	< 10	1021,1	863,7	µg/mL
R5	Metal mix, 6%	8	P12657	63,8	146,8	50,2	127,7	11,8	1642,6	1794,2	µg/mL
R5	Metal mix, 6%	13	P12658	115,7	281,7	92,1	311,2	21,9	2759,8	3635,3	µg/mL
R5	Metal mix, 6%	21	P12659	176,3	319,1	131,0	415,0	22,8	3199,9	4669,7	µg/mL
R5	Metal mix, 6%	24	P12660	528,9	378,2	178,8	503,2	32,6	3704,6	5526,2	µg/mL

Table 32: LC-MS degradation mix, raw data inhibitor screening experiment 2.

Reactor	Additive	Day	Journal ID	OZD	BHEOX	HEA	HeGly	HEPO	HEF	HEI	Unit
R1	Metal mix, 98%	0	P12735	54,4	26,4	< 10	< 10	< 10	361,9	77,3	µg/mL
R1	Metal mix, 98%	1	P12736	328,9	316,8	14,9	< 10	< 10	1587,6	809,8	µg/mL
R1	Metal mix, 98%	4	P12737	977,5	1125,2	31,8	35,4	15,1	3605,0	2092,0	µg/mL
R1	Metal mix, 98%	9	P12738	1571,2	2115,4	97,7	65,2	19,1	6146,9	4173,0	µg/mL
R1	Metal mix, 98%	13	P12739	1908,6	2735,6	132,3	83,5	29,8	7966,5	6154,7	µg/mL
R2	Metal mix, 98%	0	P12740	< 10	73,0	15,3	< 10	10,6	529,7	152,2	µg/mL
R2	Metal mix, 98%	1	P12741	654,9	669,7	47,6	41,3	11,2	5760,9	2162,4	µg/mL
R2	Metal mix, 98%	4	P12742	1647,5	2209,7	218,0	120,5	38,7	6941,8	6823,5	µg/mL
R2	Metal mix, 98%	9	P12743	2339,7	2989,7	570,3	270,9	121,7	11527,2	15488,0	µg/mL
R2	Metal mix, 98%	13	P12744	2853,1	3077,7	868,1	451,2	301,3	13865,4	17239,0	µg/mL
R3	Metal mix, 98%	0	P12745	< 10	56,3	< 10	< 10	< 10	384,1	101,9	µg/mL
R3	Metal mix, 98%	1	P12746	291,7	337,7	< 10	14,7	< 10	1716,4	985,2	µg/mL
R3	Metal mix, 98%	4	P12747	1171,6	1338,8	57,8	46,4	< 10	4171,3	2811,4	µg/mL
R3	Metal mix, 98%	9	P12748	1694,2	2252,3	126,1	79,2	34,8	6660,9	5547,9	µg/mL
R3	Metal mix, 98%	13	P12749	1932,7	2641,5	204,8	118,7	52,4	8310,1	7481,8	µg/mL
R4	None	0	P12750	< 10	18,2	< 10	< 10	< 10	217,6	26,1	µg/mL
R4	None	1	P12751	135,2	74,0	15,8	< 10	< 10	725,2	82,3	µg/mL
R4	None	4	P12752	309,9	412,8	26,2	45,7	< 10	2025,6	250,4	µg/mL
R4	None	9	P12753	723,7	821,2	35,3	126,4	15,3	3113,4	487,6	µg/mL
R4	None	13	P12754	975,0	1199,6	62,0	187,0	46,4	4320,8	765,5	µg/mL
R5	Metal mix, 98%	0	P12755	99,7	48,9	14,7	< 10	< 10	409,0	81,1	µg/mL
R5	Metal mix, 98%	1	P12756	537,2	395,5	24,3	13,7	< 10	1883,1	1068,3	µg/mL
R5	Metal mix, 98%	4	P12757	1290,2	1466,1	64,5	50,4	11,2	4438,4	3103,8	µg/mL
R5	Metal mix, 98%	9	P12758	2072,7	2485,7	139,6	91,4	30,0	7332,8	6146,0	µg/mL
R5	Metal mix, 98%	13	P12759	2397,5	3099,6	259,2	120,0	65,6	9835,2	8933,9	µg/mL

Table 33: LC-MS degradation mix, raw data inhibitor screening experiment 3.

Reactor	Additive	Day	Journal ID	OZD	BHEOX	HEA	HeGly	HEPO	HEF	HEI	Unit
R1	K Na tartrate	0	P12817	< 10	13,5	12,5	< 10	< 10	183,8	30,8	µg/mL
R1	K Na tartrate	1	P12818	233,5	294,0	23,6	< 10	< 10	1425,0	756,6	µg/mL
R1	K Na tartrate	4	P12819	1068,4	1256,3	61,7	45,2	< 10	4028,8	2384,7	µg/mL
R1	K Na tartrate	9	P12820	1665,6	2401,0	114,8	66,8	13,7	6934,3	5119,9	µg/mL
R1	K Na tartrate	13	P12821	1930,7	2975,8	175,4	89,6	38,6	8807,5	7113,0	µg/mL
R2	Na sulfite	0	P12822	< 10	12,0	14,3	< 10	< 10	70,0	< 10	µg/mL
R2	Na sulfite	1	P12823	194,2	330,1	37,8	34,6	< 10	1168,4	545,2	µg/mL
R2	Na sulfite	4	P12824	820,1	639,3	102,3	139,5	31,2	2691,8	2595,3	µg/mL
R2	Na sulfite	9	P12825	1191,9	958,3	248,4	288,5	109,2	4806,6	5907,8	µg/mL
R2	Na sulfite	13	P12826	1794,9	1132,6	337,6	382,8	166,5	5685,5	8938,8	µg/mL
R3	Citric acid	0	P12827	< 10	13,5	10,0	< 10	< 10	118,8	211,4	µg/mL
R3	Citric acid	1	P12828	177,5	169,4	27,5	17,3	< 10	932,7	337,4	µg/mL
R3	Citric acid	4	P12829	1018,8	688,3	57,6	63,8	< 10	2482,7	1086,7	µg/mL
R3	Citric acid	9	P12830	1438,4	1230,4	132,5	100,0	26,0	3931,1	2234,1	µg/mL
R3	Citric acid	13	P12831	1831,5	1707,9	234,6	125,0	35,1	5354,9	3630,4	µg/mL
R4	HEDP	0	P12832	< 10	16,7	21,8	< 10	< 10	152,1	< 10	µg/mL
R4	HEDP	1	P12833	< 10	68,9	41,9	35,4	< 10	598,4	< 10	µg/mL
R4	HEDP	4	P12834	< 10	241,4	43,1	36,7	< 10	2060,8	35,2	µg/mL
R4	HEDP	9	P12835	< 10	591,6	77,6	87,2	12,0	3385,2	99,1	µg/mL
R4	HEDP	13	P12836	460,3	804,2	103,3	146,0	13,5	4537,4	162,2	µg/mL
R5	Hydroquinone	0	P12837	< 10	32,5	23,2	< 10	< 10	348,6	256,3	µg/mL
R5	Hydroquinone	1	P12838	1043,7	1386,2	45,2	20,0	< 10	4364,3	3924,8	µg/mL
R5	Hydroquinone	4	P12839	2022,8	3829,3	111,3	43,5	< 10	8463,2	7379,6	µg/mL
R5	Hydroquinone	9	P12840	2584,3	4697,3	192,2	63,9	12,6	11369,2	10386,3	µg/mL
R5	Hydroquinone	13	P12841	2913,5	4822,7	265,1	67,2	17,4	13014,1	12548,5	µg/mL

Table 34: LC-MS degradation mix, raw data inhibitor screening experiment 4.

Reactor	Additive	Day	Journal ID	OZD	BHEOX	HEA	HeGly	HEPO	HEF	HEI	Unit
R1	DEHA	0	P12874	< 10	< 100	< 10	< 10	< 10	19,3	16,2	µg/mL
R1	DEHA	1	P12875	< 10	< 100	119,7	< 10	< 10	479,6	195,5	µg/mL
R1	DEHA	4	P12876	730,4	959,4	459,6	< 10	< 10	2372,3	963,6	µg/mL
R1	DEHA	10	P12877	1031,7	1958,1	813,8	46,7	12,4	4339,6	2601,5	µg/mL
R1	DEHA	13	P12878	1210,4	2310,6	1006,8	56,8	14,6	5316,0	3594,0	µg/mL
R2	Erythorbic acid	0	P12879	< 10	5405,9	15,0	< 10	< 10	16,6	< 10	µg/mL
R2	Erythorbic acid	1	P12880	90,8	5683,2	111,9	51,1	< 10	843,9	419,7	µg/mL
R2	Erythorbic acid	4	P12881	380,3	3426,7	191,8	207,6	12,7	2953,0	4080,3	µg/mL
R2	Erythorbic acid	10	P12882	692,8	2107,2	369,8	413,4	88,1	5848,5	8560,3	µg/mL
R2	Erythorbic acid	13	P12883	1021,7	2130,2	498,6	502,0	113,8	7309,3	10766,3	µg/mL
R3	Carbohydrazide	0	P12884	< 10	< 100	< 10	< 10	< 10	180,4	< 10	µg/mL
R3	Carbohydrazide	1	P12885	134,2	< 100	< 10	< 10	< 10	1023,0	< 10	µg/mL
R3	Carbohydrazide	4	P12886	734,1	227,6	20,6	12,1	< 10	2092,9	766,9	µg/mL
R3	Carbohydrazide	10	P12887	1324,5	965,3	88,2	54,2	17,2	4190,8	3513,6	µg/mL
R3	Carbohydrazide	13	P12888	1477,2	1278,3	132,5	71,4	23,8	5388,4	4893,0	µg/mL
R4	Methallyl alcohol	0	P12889	< 10	< 100	11,1	< 10	< 10	71,9	13,3	µg/mL
R4	Methallyl alcohol	1	P12890	54,5	108,0	14,4	< 10	< 10	850,3	514,6	µg/mL
R4	Methallyl alcohol	4	P12891	951,8	1536,2	53,5	44,5	< 10	3309,7	2253,4	µg/mL
R4	Methallyl alcohol	10	P12892	1748,1	2400,1	148,4	84,4	40,9	6303,7	5236,6	µg/mL
R4	Methallyl alcohol	13	P12893	1923,8	3006,5	229,3	112,8	51,6	7818,1	7007,0	µg/mL
R5	Na triphosphate	0	P12894	< 10	< 100	< 10	< 10	< 10	44,2	< 10	µg/mL
R5	Na triphosphate	1	P12895	38,1	< 100	< 10	16,0	< 10	631,3	340,8	µg/mL
R5	Na triphosphate	4	P12896	320,2	653,5	23,5	31,9	< 10	2008,5	1301,0	µg/mL
R5	Na triphosphate	10	P12897	863,8	1088,9	68,3	97,2	18,5	3597,0	2608,1	µg/mL
R5	Na triphosphate	13	P12898	1031,9	1525,2	93,4	153,6	25,2	4195,9	3344,2	µg/mL

Table 35: LC-MS degradation mix, raw data inhibitor screening experiment 5.

Reactor	Additive	Day	Journal ID	OZD	BHEOX	HEA	HeGly	HEPO	HEF	HEI	Unit
R1	Citric acid + carbohydrazide	0	P121035	< 10	< 100	< 10	< 10	< 10	62,1	< 10	µg/mL
R1	Citric acid + carbohydrazide	1	P121036	95,8	< 100	< 10	< 10	< 10	657,7	10,4	µg/mL
R1	Citric acid + carbohydrazide	4	P121037	428,8	452,5	33,5	14,3	< 10	1812,2	107,8	µg/mL
R1	Citric acid + carbohydrazide	9	P121038	1048,5	1483,1	134,4	47,9	< 10	3769,6	855,9	µg/mL
R1	Citric acid + carbohydrazide	13	P121039	1359,8	2532,7	224,1	71,9	15,7	5175,2	1784,4	µg/mL
R2	Na triphosphate + carbohydrazide	0	P121040	< 10	105,8	< 10	< 10	< 10	322,8	< 10	µg/mL
R2	Na triphosphate + carbohydrazide	1	P121041	569,4	204,1	28,0	11,8	11,6	1787,7	541,8	µg/mL
R2	Na triphosphate + carbohydrazide	4	P121042	1014,1	760,8	92,2	115,9	44,0	3848,0	4244,1	µg/mL
R2	Na triphosphate + carbohydrazide	9	P121043	1340,1	1077,5	205,2	347,6	110,7	6317,9	8140,0	µg/mL
R2	Na triphosphate + carbohydrazide	13	P121044	1446,7	1023,3	311,6	531,5	155,5	7799,3	10460,5	µg/mL
R3	HEDP + carbohydrazide	0	P121045	< 10	< 100	< 10	< 10	< 10	55,1	< 10	µg/mL
R3	HEDP + carbohydrazide	1	P121046	< 10	< 100	13,7	< 10	< 10	121,6	< 10	µg/mL
R3	HEDP + carbohydrazide	4	P121047	219,6	278,0	44,4	14,4	< 10	909,6	< 10	µg/mL
R3	HEDP + carbohydrazide	9	P121048	588,3	1051,7	99,6	70,2	< 10	2515,1	10,8	µg/mL
R3	HEDP + carbohydrazide	13	P121049	950,2	1829,4	164,8	121,4	< 10	3953,9	206,3	µg/mL
R4	Metal mix, 98%	0	P121050	< 10	< 100	< 10	< 10	< 10	119,2	13,3	µg/mL
R4	Metal mix, 98%	1	P121051	168,9	387,8	15,9	16,5	< 10	1105,9	664,8	µg/mL
R4	Metal mix, 98%	4	P121052	742,4	685,9	44,3	65,2	< 10	3034,9	2088,4	µg/mL
R4	Metal mix, 98%	9	P121053	1175,3	1417,2	113,8	124,8	28,4	5050,8	4113,8	µg/mL
R4	Metal mix, 98%	13	P121054	1373,6	1943,6	180,6	165,7	60,7	6280,4	5622,3	µg/mL
R5	MEKO	0	P121055	< 10	< 100	< 10	< 10	< 10	97,4	< 10	µg/mL
R5	MEKO	1	P121056	308,7	< 100	23,3	< 10	< 10	677,4	121,9	µg/mL
R5	MEKO	4	P121057	962,2	604,9	91,4	37,8	< 10	2340,0	608,1	µg/mL
R5	MEKO	9	P121058	1422,5	1366,5	204,3	84,8	34,0	3939,9	1959,0	µg/mL
R5	MEKO	13	P121059	1420,5	1893,8	276,7	119,1	54,8	5001,4	3296,7	µg/mL

Table 36: LC-MS degradation mix, raw data circulative experiment with hydrazine.

Reactor	Additive	Day	Journal ID	OZD	BHEOX	HEA	HeGly	HEPO	HEF	HEI	Unit
Circulative	Hydrazine	0	P121060	< 10	< 100	< 10	< 10	< 10	13,8	< 10	µg/mL
Circulative	Hydrazine	1	P121061	< 10	854,5	14,0	< 10	17,9	320,3	57,2	µg/mL
Circulative	Hydrazine	2	P121062	19,5	1688,2	37,4	19,3	26,6	654,7	318,5	µg/mL
Circulative	Hydrazine	4	P121063	264,7	2146,2	81,6	52,3	36,4	1525,3	1365,7	µg/mL
Circulative	Hydrazine	7	P121064	545,5	2569,2	159,1	185,5	56,0	2793,6	3336,8	µg/mL
Circulative	Hydrazine	11	P121065	833,5	2123,5	222,4	295,4	101,1	3954,9	5277,8	µg/mL
Circulative	Hydrazine	15	P121066	995,9	1885,0	316,0	407,6	155,8	4887,4	7071,9	µg/mL
Circulative	Hydrazine	19	P121067	1235,4	1468,5	404,0	492,3	205,8	5974,3	9367,4	µg/mL
Circulative	Hydrazine	21	P121068	1252,6	1260,2	441,2	510,7	225,3	6254,4	9866,0	µg/mL

Appendix C: LC-MS NDELA raw data

Table 37: LC-MS NDELA quantification inhibitor screening experiment 1.

Prøve ID	Journal ID	NDELA	Unit
R1 - Metal mix 6% - end sample	P12632	< 500	ng/ml
R2 - Metal mix 6% - end sample	P12639	< 500	ng/ml
R3 - Metal mix 6% - end sample	P12646	< 500	ng/ml
R4 - Metal mix 6% - end sample	P12653	< 500	ng/ml
R5 - Metal mix 6% - end sample	P12660	< 500	ng/ml

Table 38: LC-MS NDELA quantification inhibitor screening experiment 2.

Prøve ID	Journal ID	NDELA	Unit
R1 - Metal mix 98% - end sample	P12739	< 500	ng/ml
R2 - Metal mix 98% - end sample	P12744	955	ng/ml
R3 - Metal mix 98% - end sample	P12749	< 500	ng/ml
R4 - Metal mix 98% - end sample	P12754	< 500	ng/ml
R5 - Metal mix 98% - end sample	P12759	< 500	ng/ml

Table 39: LC-MS NDELA quantification inhibitor screening experiment 3.

Prøve ID	Journal ID	NDELA	Unit
R1 - K Na tartrate - end sample	P12821	< 500	ng/ml
R2 - Na sulfite - end sample	P12826	< 500	ng/ml
R3 - Citric acid - end sample	P12831	< 500	ng/ml
R4 - HEDP - end sample	P12836	< 500	ng/ml
R5 - Hydroquinone - end sample	P12841	607	ng/ml

Table 40: LC-MS NDELA quantification inhibitor screening experiment 4.

Prøve ID	Journal ID	NDELA	Unit
R1 - DEHA - end sample	P12878	< 100	ng/ml
R2 - Erythorbic acid - end sample	P12883	< 100	ng/ml
R3 - Carbohydrazide - end sample	P12888	< 100	ng/ml
R4 - Methallyl alcohol - end sample	P12893	< 100	ng/ml
R5 - Na triphosphate - end sample	P12898	< 100	ng/ml

Table 41: LC-MS NDELA quantification inhibitor screening experiment 5 and circulative with hydrazine.

Prøve ID	Journal ID	NDELA	Unit
R1 - citric acid + carbohydrazide - end sample	P121039	< 100	ng/ml
R1 - citric acid + carbohydrazide - end sample	P121044	< 100	ng/ml
R1 - citric acid + carbohydrazide - end sample	P121049	< 100	ng/ml
R1 - metal mix - end sample	P121054	< 100	ng/ml
R1 - MEKO - end sample	P121059	< 100	ng/ml
Circulative - hydrazine - end sample	P121067	144	ng/ml

Table 42:ICP-MS raw data inhibitor screening experiment 1.

				Fe		Cr		Ni		Al	
Reactor	Additive	Day	Journal ID	[µg/L]	RSD%	[µg/L]	RSD%	[µg/L]	RSD%	[µg/L]	RSD%
R1	Metal mix, 6%	0	P12626	11 046	0,8	2 779	1,9	2 844	2,7	< loq	-
R1	Metal mix, 6%	8	P12629	5 769	5,9	2 380	7,3	2 916	2,4	< loq	-
R1	Metal mix, 6%	25	P12632	6 129	1,6	2 630	0,9	3 038	1,5	< loq	-
R2	Metal mix, 6%	0	P12633	18 079	1,2	4 048	4,1	3 056	4,9	< loq	-
R2	Metal mix, 6%	8	P12636	3 997	0,1	2 461	1,4	3 066	3	< loq	-
R2	Metal mix, 6%	25	P12639	4 123	2,3	2 657	1,2	3 200	2,1	< loq	-
R3	Metal mix, 6%	0	P12640	13 651	2,4	3 197	2,6	2 984	2,7	< loq	-
R3	Metal mix, 6%	8	P12643	6 081	0,9	2 589	1,5	3 024	2	< loq	-
R3	Metal mix, 6%	25	P12646	5 978	1,5	2 764	2,8	3 163	2,4	< loq	-
R4	Metal mix, 6%	0	P12647	12 475	2,3	2 912	2,5	2 794	4,7	< loq	-
R4	Metal mix, 6%	8	P12650	4 928	1,2	2 423	0,6	2 936	3,6	< loq	-
R4	Metal mix, 6%	25	P12653	4 948	0,8	2 491	1,9	2 973	0,1	< loq	-
R5	Metal mix, 6%	0	P12654	17 412	1,8	3 875	3,2	3 016	1,8	< loq	-
R5	Metal mix, 6%	8	P12657	6 279	0,3	2 578	0,9	2 987	0,9	< loq	-
R5	Metal mix, 6%	25	P12660	5 365	3,1	2 599	6,7	3 040	3,6	< loq	-

Table 43: ICP-MS raw data inhibitor screening experiment 2.

				Fe		Cr		Ni		Al	
Reactor	Additive	Day	Journal ID	[µg/L]	RSD%	[µg/L]	RSD%	[µg/L]	RSD%	[µg/L]	RSD%
R1	Metal mix, 98%	0	P12735	20 363	3,7	4 835	4,2	2 982	2,6	< loq	-
R1	Metal mix, 98%	9	P12738	6 158	1	1 967	0,9	2 101	0,7	< loq	-
R1	Metal mix, 98%	13	P12739	10 033	1,6	3 252	0,5	3 311	2,8	< loq	-
R2	Metal mix, 98%	0	P12740	20 418	3	4 630	5,6	2 980	3,5	< loq	-
R2	Metal mix, 98%	9	P12743	8 531	1,4	3 511	5,1	4 065	2	< loq	-
R2	Metal mix, 98%	13	P12744	9 566	0,7	4 037	1,4	4 604	1,2	< loq	-
R3	Metal mix, 98%	0	P12745	21 339	5,1	4 907	4,7	3 075	4	< loq	-
R3	Metal mix, 98%	9	P12748	7 116	1,8	2 371	3,3	2 491	0,9	< loq	-
R3	Metal mix, 98%	13	P12749	8 360	3	2 870	1,2	2 991	2,4	< loq	-
R4	None	0	P12750	140	2,2	5,82	6,6	5,44	8,5	< loq	-
R4	None	9	P12753	122	1,7	7,06	0,9	1,94	16,6	< loq	-
R4	None	13	P12754	104	1	7,00	1,6	2,35	20,4	< loq	-
R5	Metal mix, 98%	0	P12755	24 463	2,2	5 580	3	3 149	0,6	< loq	-
R5	Metal mix, 98%	9	P12758	8 854	2,7	3 022	0,3	3 169	1,4	< loq	-
R5	Metal mix, 98%	13	P12759	10 186	4,3	3 484	5,7	3 590	3,7	< loq	-

Table 44: ICP-MS raw data inhibitor screening experiment 3.

				Fe		Cr		Ni		Al	
Reactor	Additive	Day	Journal ID	[µg/L]	RSD%	[µg/L]	RSD%	[µg/L]	RSD%	[µg/L]	RSD%
R1	K Na tartrate	0	P12817	20 751	2,1	4 367	6	2 986	2,2	253	4,1
R1	K Na tartrate	1	P12818	17 767	2,9	3 699	4,1	2 634	3,3	< loq	-
R1	K Na tartrate	4	P12819	20 604	1,8	4 332	0,5	2 990	2,3	< loq	-
R1	K Na tartrate	9	P12820	20 290	2,7	4 160	6,8	3 032	1,5	< loq	-
R1	K Na tartrate	13	P12821	20 421	1,5	4 341	0,5	3 044	0,9	< loq	-
R2	Na sulfite	0	P12822	8 651	2,7	1 816	1,4	2 785	5,9	< loq	-
R2	Na sulfite	1	P12823	12 923	3	3 004	1,3	2 988	1,7	< loq	-
R2	Na sulfite	4	P12824	17 601	3,8	3 864	4,5	2 913	1	< loq	-
R2	Na sulfite	9	P12825	11 058	4,9	2 872	2,9	2 855	3,2	< loq	-
R2	Na sulfite	13	P12826	13 294	6	3 266	5,4	2 947	2,3	< loq	-
R3	Citric acid	0	P12827	21 057	2,5	4 234	1,9	2 973	3,6	695	2,8
R3	Citric acid	1	P12828	20 395	3,6	4 219	2,7	2 935	1,8	454	2,5
R3	Citric acid	4	P12829	20 280	1,1	4 185	0,9	2 884	0,5	218	3,7
R3	Citric acid	9	P12830	20 911	0,1	4 269	0,5	2 987	2,1	< loq	-
R3	Citric acid	13	P12831	20 737	1,6	4 249	2,2	2 948	1,5	< loq	-
R4	HEDP	0	P12832	20 706	1,3	4 221	1,9	2 944	2,1	2 404	1,3
R4	HEDP	1	P12833	21 409	2,2	4 176	1,5	2 957	1,8	2 163	1,5
R4	HEDP	4	P12834	20 775	0,1	4 190	0,6	2 962	1,3	1 996	0,9
R4	HEDP	9	P12835	20 658	2,4	4 210	4	2 965	3,6	2 076	5,2
R4	HEDP	13	P12836	20 050	0,9	4 103	1,5	2 872	1,2	2 361	1,8
R5	Hydroquinone	0	P12837	20 752	1,8	4 380	2,5	3 043	1,7	< loq	-
R5	Hydroquinone	1	P12838	15 106	2	3 177	3,9	2 940	1,2	< loq	-
R5	Hydroquinone	4	P12839	11 826	1,6	2 803	4,3	2 910	1	< loq	-
R5	Hydroquinone	9	P12840	11 154	3,1	2 806	4	2 875	1,5	< loq	-
R5	Hydroquinone	13	P12841	11 114	1,2	2 878	2,9	2 929	1,7	< loq	-

Table 45: ICP-MS raw data inhibitor screening experiment 4.

				Fe		Cr		Ni		Al	
Reactor	Additive	Day	Journal ID	[µg/L]	RSD%	[µg/L]	RSD%	[µg/L]	RSD%	[µg/L]	RSD%
R1	DEHA	0	P12874	10 476	0,8	2 465	0,6	2 823	1,7	< loq	-
R1	DEHA	1	P12875	21 111	4,5	3 998	5,6	2 982	0,5	< loq	-
R1	DEHA	4	P12876	10 339	2,4	2 562	1,7	2 910	2,2	< loq	-
R1	DEHA	10	P12877	10 038	1,6	2 582	4,1	2 980	2,5	< loq	-
R1	DEHA	13	P12878	10 418	2,5	2 675	2,1	2 853	4,1	< loq	-
R2	Erythrobic acid	0	P12879	23 531	1,9	4 309	2,9	2 781	2,1	1 346	4,4
R2	Erythrobic acid	1	P12880	22 815	3,3	4 325	1,4	2 858	3,5	227	1,7
R2	Erythrobic acid	4	P12881	22 533	2,3	4 222	3,8	2 795	2	< loq	-
R2	Erythrobic acid	10	P12882	22 427	3,5	4 361	5,9	2 788	3,8	< loq	-
R2	Erythrobic acid	13	P12883	22 283	4,2	4 265	5,6	2 797	1,4	< loq	-
R3	Carbohydrazide	0	P12884	29 618	1,3	5 607	3,9	2 959	1,7	< loq	-
R3	Carbohydrazide	1	P12885	17 399	2,5	3 528	2,2	2 950	3,1	< loq	-
R3	Carbohydrazide	4	P12886	8 669	0,8	2 377	1,4	2 806	1	< loq	-
R3	Carbohydrazide	10	P12887	8 286	0,5	2 450	1,6	2 809	0,7	< loq	-
R3	Carbohydrazide	13	P12888	7 319	1,9	2 341	2,5	2 829	2,9	< loq	-
R4	Methallyl alcohol	0	P12889	23 113	0,6	4 300	1,2	2 910	0,5	< loq	-
R4	Methallyl alcohol	1	P12890	21 711	4,4	4 103	5,8	2 906	3,6	< loq	-
R4	Methallyl alcohol	4	P12891	20 425	2,3	3 873	3,7	2 976	0,1	< loq	-
R4	Methallyl alcohol	10	P12892	14 214	1,6	3 075	6	2 859	3,3	< loq	-
R4	Methallyl alcohol	13	P12893	13 204	5,5	3 004	12,2	2 809	3,6	< loq	-
R5	Na triphosphate	0	P12894	25 824	1,8	5 110	1,7	3 009	1,4	< loq	-
R5	Na triphosphate	1	P12895	23 497	0,8	4 331	2,7	2 959	2,2	< loq	-
R5	Na triphosphate	4	P12896	23 519	2,2	4 434	2,9	2 967	2,8	< loq	-
R5	Na triphosphate	10	P12897	23 380	3,5	4 356	3,9	2 957	2,4	< loq	-
R5	Na triphosphate	13	P12898	23 773	3	4 445	4	2 985	2,1	< loq	-

Appendix E: Total alkalinity and CO_2-titration inhibitor screening apparatus

Table 46: Titration data inhibitor screening experiment 1.

Reactor	Additive	Day	ID	Amine concentration [mol/kg]	CO2-concentration [mol/kg]
R1	Metal mix, 6%	0	P12626	4,40	1,73
R1	Metal mix, 6%	1	P12627	4,33	
R1	Metal mix, 6%	4	P12628	4,29	
R1	Metal mix, 6%	8	P12629	4,26	
R1	Metal mix, 6%	13	P12630	4,27	
R1	Metal mix, 6%	21	P12631	4,25	
R1	Metal mix, 6%	25	P12632	4,24	2,00
R2	Metal mix, 6%	0	P12633	4,45	1,77
R2	Metal mix, 6%	1	P12634	4,44	
R2	Metal mix, 6%	4	P12635	4,43	
R2	Metal mix, 6%	8	P12636	4,41	
R2	Metal mix, 6%	13	P12637	4,34	
R2	Metal mix, 6%	21	P12638	4,25	
R2	Metal mix, 6%	25	P12639	4,20	1,83
R3	Metal mix, 6%	0	P12640	4,51	1,80
R3	Metal mix, 6%	1	P12641	4,42	
R3	Metal mix, 6%	4	P12642	4,41	
R3	Metal mix, 6%	8	P12643	4,38	
R3	Metal mix, 6%	13	P12644	4,37	
R3	Metal mix, 6%	21	P12645	4,31	
R3	Metal mix, 6%	25	P12646	4,29	2,00
R4	Metal mix, 6%	0	P12647	4,39	1,69
R4	Metal mix, 6%	1	P12648	4,40	
R4	Metal mix, 6%	4	P12649	4,34	
R4	Metal mix, 6%	8	P12650	4,28	
R4	Metal mix, 6%	13	P12651	4,25	
R4	Metal mix, 6%	21	P12652	4,22	
R4	Metal mix, 6%	25	P12653	4,18	1,88
R5	Metal mix, 6%	0	P12654	4,49	1,75
R5	Metal mix, 6%	1	P12655	4,45	
R5	Metal mix, 6%	4	P12656	4,37	
R5	Metal mix, 6%	8	P12657	4,34	
R5	Metal mix, 6%	13	P12658	4,34	
R5	Metal mix, 6%	21	P12659	4,31	
R5	Metal mix, 6%	25	P12660	4,30	1,91

Table 47: Titration data inhibitor screening experiment 2.

Reactor	Additive	Day	ID	Amine concentration [mol/kg]	CO2-concentration [mol/kg]
R1	Metal mix, 98%	0	P12735	4,34	1,75
R1	Metal mix, 98%	1	P12736	4,26	
R1	Metal mix, 98%	4	P12737	4,01	
R1	Metal mix, 98%	9	P12738	4,03	
R1	Metal mix, 98%	13	P12739	4,07	1,91
R2	Metal mix, 98%	0	P12740	4,35	1,75
R2	Metal mix, 98%	1	P12741	4,30	
R2	Metal mix, 98%	4	P12742	4,27	
R2	Metal mix, 98%	9	P12743	4,23	
R2	Metal mix, 98%	13	P12744	4,32	1,82
R3	Metal mix, 98%	0	P12745	4,36	1,75
R3	Metal mix, 98%	1	P12746	4,22	
R3	Metal mix, 98%	4	P12747	3,98	
R3	Metal mix, 98%	9	P12748	3,75	
R3	Metal mix, 98%	13	P12749	3,56	1,64
R4	None	0	P12750	4,43	1,78
R4	None	1	P12751	4,39	
R4	None	4	P12752	4,38	
R4	None	9	P12753	4,58	
R4	None	13	P12754	4,81	2,21
R5	Metal mix, 98%	0	P12755	4,47	1,78
R5	Metal mix, 98%	1	P12756	4,33	
R5	Metal mix, 98%	4	P12757	4,08	
R5	Metal mix, 98%	9	P12758	3,90	
R5	Metal mix, 98%	13	P12759	4,08	1,88

Table 48: Titration data inhibitor screening experiment 3.

Reactor	Additive	Day	ID	Amine concentration [mol/kg]	CO2- concentration [mol/kg]
R1	K Na tartrate	0	P12817	4,35	1,75
R1	K Na tartrate	1	P12818	4,27	
R1	K Na tartrate	4	P12819	4,07	
R1	K Na tartrate	9	P12820	3,79	
R1	K Na tartrate	13	P12821	3,63	1,73
R2	Na sulfite	0	P12822	4,34	1,74
R2	Na sulfite	1	P12823	4,19	
R2	Na sulfite	4	P12824	4,02	
R2	Na sulfite	9	P12825	3,75	
R2	Na sulfite	13	P12826	3,53	1,54
R3	Citric acid	0	P12827	4,23	1,71
R3	Citric acid	1	P12828	4,17	
R3	Citric acid	4	P12829	4,06	
R3	Citric acid	9	P12830	3,85	
R3	Citric acid	13	P12831	3,73	1,75
R4	HEDP	0	P12832	4,19	1,68
R4	HEDP	1	P12833	4,18	
R4	HEDP	4	P12834	4,26	
R4	HEDP	9	P12835	4,06	
R4	HEDP	13	P12836	4,00	1,89
R5	Hydroquinone	0	P12837	4,33	1,72
R5	Hydroquinone	1	P12838	4,03	
R5	Hydroquinone	4	P12839	3,66	
R5	Hydroquinone	9	P12840	3,23	
R5	Hydroquinone	13	P12841	3,04	1,40

Table 49: Titration data inhibitor screening experiment 4.

Reactor	Additive	Day	ID	Amine concentration [mol/kg]	CO2- concentration [mol/kg]
R1	DEHA	0	P12874	4,44	1,78
R1	DEHA	1	P12875	4,33	
R1	DEHA	4	P12876	4,10	
R1	DEHA	10	P12877	3,91	
R1	DEHA	13	P12878	3,84	1,85
R2	Erythorbic acid	0	P12879	4,16	1,74
R2	Erythorbic acid	1	P12880	4,07	
R2	Erythorbic acid	4	P12881	3,90	
R2	Erythorbic acid	10	P12882	3,65	
R2	Erythorbic acid	13	P12883	3,50	1,52
R3	Carbohydrazide	0	P12884	4,40	1,79
R3	Carbohydrazide	1	P12885	4,40	
R3	Carbohydrazide	4	P12886	4,32	
R3	Carbohydrazide	10	P12887	4,14	
R3	Carbohydrazide	13	P12888	4,10	1,93
R4	Methallyl alcohol	0	P12889	4,34	1,77
R4	Methallyl alcohol	1	P12890	4,32	
R4	Methallyl alcohol	4	P12891	4,04	
R4	Methallyl alcohol	10	P12892	3,75	
R4	Methallyl alcohol	13	P12893	3,60	1,68
R5	Na triphosphate	0	P12894	4,37	1,79
R5	Na triphosphate	1	P12895	4,34	
R5	Na triphosphate	4	P12896	4,19	
R5	Na triphosphate	10	P12897	4,04	
R5	Na triphosphate	13	P12898	3,98	1,89

Table 50: Titration data inhibitor screening experiment 5.

Reactor	Additive	Day	ID	Amine concentration [mol/kg]	CO2- concentration [mol/kg]
R1	Citric acid + Carbohydrazide	0	P121035	4,12	1,66
R1	Citric acid + Carbohydrazide	1	P121036	4,03	
R1	Citric acid + Carbohydrazide	4	P121037	3,93	
R1	Citric acid + Carbohydrazide	9	P121038	3,78	
R1	Citric acid + Carbohydrazide	13	P121039	3,68	1,75
R2	Na triphosphate + Carbohydrazide	0	P121040	4,25	1,71
R2	Na triphosphate + Carbohydrazide	1	P121041	4,15	
R2	Na triphosphate + Carbohydrazide	4	P121042	4,01	
R2	Na triphosphate + Carbohydrazide	9	P121043	3,79	
R2	Na triphosphate + Carbohydrazide	13	P121044	3,64	1,56
R3	HEDP + Carbohydrazide	0	P121045	4,14	1,65
R3	HEDP + Carbohydrazide	1	P121046	4,12	
R3	HEDP + Carbohydrazide	4	P121047	4,02	
R3	HEDP + Carbohydrazide	9	P121048	3,94	
R3	HEDP + Carbohydrazide	13	P121049	3,84	1,79
R4	Metal mix, 98%	0	P121050	4,43	1,79
R4	Metal mix, 98%	1	P121051	4,31	
R4	Metal mix, 98%	4	P121052	4,13	
R4	Metal mix, 98%	9	P121053	3,95	
R4	Metal mix, 98%	13	P121054	3,81	1,76
R5	MEKO	0	P121055	4,38	1,79
R5	MEKO	1	P121056	4,32	
R5	MEKO	4	P121057	4,18	
R5	MEKO	9	P121058	4,02	
R5	MEKO	13	P121059	3,89	1,81

Appendix F: Total alkalinity- and CO_2-titration circulative experiment

Table 51: Titration data circulative experiment with hydrazine.

Reactor	Additive	Day	ID	Amine concentration [mol/kg]	CO2-concentration [mol/kg]
Circulative	Hydrazine	0	P121060	4,23	1,73
Circulative	Hydrazine	1	P121061	4,18	
Circulative	Hydrazine	2	P121062	4,12	
Circulative	Hydrazine	4	P121063	4,05	
Circulative	Hydrazine	7	P121064	3,96	
Circulative	Hydrazine	11	P121065	3,79	
Circulative	Hydrazine	15	P121066	3,67	
Circulative	Hydrazine	19	P121067	3,56	
Circulative	Hydrazine	21	P121068	3,47	1,45

Appendix G: Total alkalinity- and CO_2-titration thermal experiments

Table 52: Titration data thermal experiments; citric acid and potassium sodium tartrate.

Additive	Cylinder material	Day	Amine concentration [mol/kg]	CO2- concentration [mol/kg]
Citric acid	Metal	0	4,30	2,15
Citric acid	Metal	7	3,90	
Citric acid	Metal	14	3,48	
Citric acid	Metal	21	3,08	
Citric acid	Metal	28	2,77	
Citric acid	Metal	35	2,48	1,25
Citric acid	Glass	0	4,30	2,15
Citric acid	Glass	7	3,95	
Citric acid	Glass	14	3,62	
Citric acid	Glass	21	3,26	
Citric acid	Glass	28	2,93	
Citric acid	Glass	35	2,66	1,40
K Na tartrate	Metal	0	4,38	2,20
K Na tartrate	Metal	7	4,05	
K Na tartrate	Metal	14	3,59	
K Na tartrate	Metal	21	3,23	
K Na tartrate	Metal	28	2,89	
K Na tartrate	Metal	35	2,58	1,31
K Na tartrate	Glass	0	4,38	2,20
K Na tartrate	Glass	7	4,05	
K Na tartrate	Glass	14	3,70	
K Na tartrate	Glass	21	3,36	
K Na tartrate	Glass	28	3,05	
K Na tartrate	Glass	35	2,73	1,40

Table 53: Titration data thermal experiments; HEDP and sodium triphosphate

Additive	Material	Day	Amine concentration [mol/kg]	CO2-concentration [mol/kg]
HEDP	Metal	0	4,25	4,25
HEDP	Metal	7	3,91	
HEDP	Metal	14	3,51	
HEDP	Metal	21	3,15	
HEDP	Metal	28	-	
HEDP	Metal	35	2,55	1,30
HEDP	Glass	0	4,25	2,14
HEDP	Glass	7	3,96	
HEDP	Glass	14	3,65	
HEDP	Glass	21	3,30	
HEDP	Glass	28	2,95	
HEDP	Glass	35	2,82	1,31
Na triphosphate	Metal	0	4,33	2,15
Na triphosphate	Metal	7	3,99	
Na triphosphate	Metal	14	3,57	
Na triphosphate	Metal	21	3,14	
Na triphosphate	Metal	28	2,87	
Na triphosphate	Metal	35	2,59	1,37
Na triphosphate	Glass	0	4,33	2,15
Na triphosphate	Glass	7	4,05	
Na triphosphate	Glass	14	3,67	
Na triphosphate	Glass	21	3,31	
Na triphosphate	Glass	28	3,01	
Na triphosphate	Glass	35	2,75	1,44

Table 54: Titration data thermal experiments; sodium sulfite, methallyl alcohol, hydroquinone and DEHA.

Additive	Material	Day	Amine concentration [mol/kg]	CO2-concentration [mol/kg]
Na sulfite	Metal	0	4,36	2,17
Na sulfite	Metal	7	4,03	
Na sulfite	Metal	14	3,64	
Na sulfite	Metal	21	3,26	
Na sulfite	Metal	28	2,95	
Na sulfite	Metal	35	2,62	1,31
Methallyl alcohol	Metal	0	4,25	2,14
Methallyl alcohol	Metal	7	3,90	
Methallyl alcohol	Metal	14	3,49	
Methallyl alcohol	Metal	21	3,15	
Methallyl alcohol	Metal	28	2,83	
Methallyl alcohol	Metal	35	2,50	1,26
Hydroquinone	Metal	0	-	-
Hydroquinone	Metal	7	3,96	
Hydroquinone	Metal	14	3,54	
Hydroquinone	Metal	21	3,15	
Hydroquinone	Metal	28	2,90	
Hydroquinone	Metal	35	2,54	1,28
DEHA	Metal	0	4,28	2,15
DEHA	Metal	7	3,96	
DEHA	Metal	14	3,58	
DEHA	Metal	21	3,19	
DEHA	Metal	28	2,93	
DEHA	Metal	35	2,63	1,30

Table 55: Titration data thermal experiments for MEKO, erythorbic acid and carbohydrazide.

Additive	Material	Day	Amine concentration [mol/kg]	CO2-concentration [mol/kg]
MEKO	Metal	0	4,21	2,12
MEKO	Metal	7	3,93	
MEKO	Metal	14	3,54	
MEKO	Metal	21	3,18	
MEKO	Metal	28	2,89	
MEKO	Metal	35	2,59	1,29
Erythorbic acid	Metal	0	4,11	2,09
Erythorbic acid	Metal	7	3,77	
Erythorbic acid	Metal	14	3,41	
Erythorbic acid	Metal	21	3,05	
Erythorbic acid	Metal	28	2,72	
Erythorbic acid	Metal	35	2,44	1,29
Carbohydrazide	Metal	0	4,04	1,99
Carbohydrazide	Metal	7	3,80	
Carbohydrazide	Metal	14	3,48	
Carbohydrazide	Metal	21	3,14	
Carbohydrazide	Metal	28	2,84	
Carbohydrazide	Metal	35	2,61	1,30

Appendix H: LC-MS MEA thermal experiments

Table 56: LC-MS quantification of MEA for selected samples from the thermal degradation.

Additive	Week	Journal ID	MEA	Unit	MEA	Unit
Citric acid	0	P121085	4,78	mol/L	0,00	mol/kg
Citric acid	1	P121069	3,99	mol/L	3,63	mol/kg
Citric acid	2	P121070	3,08	mol/L	2,80	mol/kg
Citric acid	3	P121071	2,88	mol/L	2,63	mol/kg
Citric acid	4	P121072	2,54	mol/L	2,33	mol/kg
Citric acid	5	P121073	2,15	mol/L	1,96	mol/kg
Citric acid	0	P121085	4,78	mol/L	4,38	mol/kg
Citric acid	1	P121074	4,05	mol/L	3,72	mol/kg
Citric acid	2	P121075	3,59	mol/L	3,27	mol/kg
Citric acid	3	P121076	3,08	mol/L	2,81	mol/kg
Citric acid	4	P121077	2,67	mol/L	2,45	mol/kg
Citric acid	5	P121078	2,34	mol/L	2,15	mol/kg
Carbohydrazide	0	P121084	4,45	mol/L	4,09	mol/kg
Carbohydrazide	1	P121079	3,78	mol/L	3,46	mol/kg
Carbohydrazide	2	P121080	3,30	mol/L	3,04	mol/kg
Carbohydrazide	3	P121081	2,88	mol/L	2,67	mol/kg
Carbohydrazide	4	P121082	2,46	mol/L	2,27	mol/kg
Carbohydrazide	5	P121083	2,16	mol/L	1,98	mol/kg

Appendix I: IC-EC raw data

Table 57: IC-EC raw data for experiment 1.

				Concentration (ppm)					
Reactor	Additive		Pnr	Glycolate	Formate	Nitrite	Oxalate	Nitrate	Sulphate
R1	Metal mix, 6%	0	P12626	<25	<27	<22	<23	<23	41,3
R1	Metal mix, 6%	1	P12627	<25	<27	<22	<23	<23	39,0
R1	Metal mix, 6%	4	P12628	<25	35,2	27,9	<23	<23	40,8
R1	Metal mix, 6%	8	P12629	<25	77,1	67,7	<23	34,2	43,7
R1	Metal mix, 6%	13	P12630	<25	106,2	82,7	<23	48,6	42,5
R1	Metal mix, 6%	21	P12631	<25	207,0	151,2	28,9	86,6	42,1
R1	Metal mix, 6%	25	P12632	<25	259,7	168,5	37,7	115,6	43,4
R2	Metal mix, 6%	0	P12633	<25	30,2	<22	<23	<23	46,1
R2	Metal mix, 6%	1	P12634	<25	25,9	<22	<23	<23	41,0
R2	Metal mix, 6%	4	P12635	<25	57,1	23,1	<23	32,3	43,0
R2	Metal mix, 6%	8	P12636	<25	130,8	56,2	<23	53,8	42,7
R2	Metal mix, 6%	13	P12637	<25	245,3	71,9	24,1	85,9	44,5
R2	Metal mix, 6%	21	P12638	<25	477,3	135,7	47,0	165,7	44,5
R2	Metal mix, 6%	25	P12639	<25	678,0	200,1	70,0	235,1	42,5
R3	Metal mix, 6%	0	P12640	<25	<27	<22	<23	<23	40,6
R3	Metal mix, 6%	1	P12641	<25	<27	<22	<23	<23	41,0
R3	Metal mix, 6%	4	P12642	<25	38,6	22,7	<23	24,0	44,7
R3	Metal mix, 6%	8	P12643	<25	73,6	54,6	<23	36,9	40,9
R3	Metal mix, 6%	13	P12644	<25	123,1	72,8	<23	55,1	42,5
R3	Metal mix, 6%	21	P12645	<25	235,9	126,8	31,0	102,2	46,4
R3	Metal mix, 6%	25	P12646	<25	350,3	188,9	42,5	152,1	46,0
R4	Metal mix, 6%	0	P12647	<25	<27	<22	<23	<23	40,2
R4	Metal mix, 6%	1	P12648	<25	<27	<22	<23	<23	39,1
R4	Metal mix, 6%	4	P12649	<25	38,1	<22	<23	<23	38,8
R4	Metal mix, 6%	8	P12650	<25	82,7	46,9	25,0	34,8	41,4
R4	Metal mix, 6%	13	P12651	<25	115,4	53,1	<23	45,9	39,9
R4	Metal mix, 6%	21	P12652	<25	236,1	104,3	27,5	89,7	47,0
R4	Metal mix, 6%	25	P12653	<25	295,4	126,1	35,8	115,8	41,5
R5	Metal mix, 6%	0	P12654	<25	<27	<22	<23	<23	44,8
R5	Metal mix, 6%	1	P12655	<25	<27	<22	<23	<23	40,4
R5	Metal mix, 6%	4	P12656	<25	38,6	<22	<23	<23	38,9
R5	Metal mix, 6%	8	P12657	<25	75,0	42,6	<23	32,7	41,2
R5	Metal mix, 6%	13	P12658	<25	128,1	56,4	<23	48,1	42,2
R5	Metal mix, 6%	21	P12659	<25	244,0	98,7	28,8	85,5	41,5
R5	Metal mix, 6%	25	P12660	<25	344,7	131,1	38,8	121,1	40,8

Table 58: IC-EC raw data for experiment 2.

				Concentration [mg/kg]				
Reactor	**Additive**	**Days**	**Sample**	**Formate**	**Nitrite**	**Nitrate**	**Sulphate**	**Oxalate**
R1	Metal mix, 98 %	0	P12735	<52	<227	<225	1222	<228
R1	Metal mix, 98 %	1	P12736	<50	276	<223	1237	<226
R1	Metal mix, 98 %	4	P12737	157	707	<223	1271	<226
R1	Metal mix, 98 %	9	P12738	364	1227	348	1369	<226
R1	Metal mix, 98 %	13	P12739	587	1636	502	1463	<226
R2	Metal mix, 98 %	0	P12740	<51	<227	<224	1072	<228
R2	Metal mix, 98 %	1	P12741	105	374	<222	1107	<226
R2	Metal mix, 98 %	4	P12742	528	1150	405	1315	<224
R2	Metal mix, 98 %	9	P12743	1697	2540	957	1475	<222
R2	Metal mix, 98 %	13	P12744	3124	3418	1546	1707	323
R3	Metal mix, 98 %	0	P12745	<51	<238	<236	1281	<239
R3	Metal mix, 98 %	1	P12746	51	242	<223	1243	<226
R3	Metal mix, 98 %	4	P12747	197	666	230	1245	<225
R3	Metal mix, 98 %	9	P12748	464	1216	396	1278	<226
R3	Metal mix, 98 %	13	P12749	728	1560	540	1261	<225
R4	None	0	P12750	<51	<47	<47	1169	<47
R4	None	1	P12751	<49	<46	<46	1175	<46
R4	None	4	P12752	78	103	<46	1239	<47
R4	None	9	P12753	208	197	61	1340	<47
R4	None	13	P12754	347	275	83	1396	<47
R5	Metal mix, 98 %	0	P12755	<50	<224	<222	1008	<225
R5	Metal mix, 98 %	1	P12756	57	291	<220	1022	<223
R5	Metal mix, 98 %	4	P12757	212	825	250	1110	<227
R5	Metal mix, 98 %	9	P12758	535	1449	452	1133	<236
R5	Metal mix, 98 %	13	P12759	938	2056	695	1230	125

Table 59: IC-EC raw data for experiment 3.

Reactor	Additive	Day	Prøve	Dilution	Formate [mg/kg]	Nitrate [mg/kg]	Sulphate [mg/kg]	Oxalate [mg/kg]	Nitrite [mg/kg]
R1	K Na tartrate	0	P12817	1/500	<135	<130	1238,2	<183	<134
R1	K Na tartrate	1	P12818	1/500	<135	<130	1298,1	<183	<134
R1	K Na tartrate	4	P12819	1/500	180,7	<130	1248,8	<183	<134
R1	K Na tartrate	9	P12820	1/500	270,9	278,2	1065,2	<183	541,2
R1	K Na tartrate	13	P12821	1/500	506,5	568,3	1348,4	<183	1031,8
R2	Na sulfite	0	P12822	1/500	<135	<130	2627,4	<183	<134
R2	Na sulfite	1	P12823	1/500	<135	<130	4408,8	<183	<134
R2	Na sulfite	4	P12824	1/500	<135	<130	4987,0	<183	<134
R2	Na sulfite	9	P12825	1/500	474,3	264,6	5106,2	<183	<134
R2	Na sulfite	13	P12826	1/500	810,7	429,9	4783,1	<183	<134
R3	Citric acid	0	P12827	1/500	<135	<130	946,0	<183	<134
R3	Citric acid	1	P12828	1/500	<135	<130	1135,5	<183	<134
R3	Citric acid	4	P12829	1/500	<135	<130	1080,8	<183	<134
R3	Citric acid	9	P12830	1/500	232,4	169,6	1155,2	<183	<134
R3	Citric acid	13	P12831	1/500	359,7	255,8	1151,8	<183	510,7
R4	HEDP	0	P12832	1/500	<135	<130	1345,4	<183	<134
R4	HEDP	1	P12833	1/500	<135	<130	1496,9	<183	<134
R4	HEDP	4	P12834	1/500	<135	<130	1347,3	<183	<134
R4	HEDP	9	P12835	1/500	198,8	<130	1409,7	<183	<134
R4	HEDP	13	P12836	1/500	300,1	<130	1443,6	<183	<134
R5	Hydroquinone	0	P12837	1/500	<135	<130	1046,7	<183	<134
R5	Hydroquinone	1	P12838	1/500	<135	<130	954,5	<183	<134
R5	Hydroquinone	4	P12839	1/500	294,1	330,2	1051,2	<183	921,8
R5	Hydroquinone	9	P12840	1/500	852,1	483,4	987,9	<183	1358,8
R5	Hydroquinone	13	P12841	1/500	1140,2	670,8	982,3	186,3	1664,3

Table 60: IC-EC raw data for experiment 4.

Reactor	Additive	Day	Prøve	Fortynning	Formate [mg/kg]	Nitrate [mg/kg]	Sulphate [mg/kg]	Oxalate [mg/kg]	Nitrite [mg/kg]
R1	DEHA	0	P12874	1/500	<213	<246	684	<164	<128
R1	DEHA	1	P12875	1/500	<213	<246	633	<164	<128
R1	DEHA	4	P12876	1/500	<213	<246	676	<164	287
R1	DEHA	10	P12877	1/500	<213	<246	652	<164	568
R1	DEHA	13	P12878	1/500	228	295	681	<164	619
R2	Erythorbic acid	0	P12879	1/500	<213	<246	626	<164	<128
R2	Erythorbic acid	1	P12880	1/500	<213	<246	602	<164	<128
R2	Erythorbic acid	4	P12881	1/500	<213	<246	593	170	<128
R2	Erythorbic acid	10	P12882	1/500	598	345	637	348	<128
R2	Erythorbic acid	13	P12883	1/500	1002	569	622	447	182
R3	Carbohydrazide	0	P12884	1/500	<213	<246	564	<164	<128
R3	Carbohydrazide	1	P12885	1/500	<213	<246	627	<164	<128
R3	Carbohydrazide	4	P12886	1/500	<213	<246	687	<164	<128
R3	Carbohydrazide	10	P12887	1/500	<213	<246	696	<164	145
R3	Carbohydrazide	13	P12888	1/500	299	267	697	<164	209
R4	Methallyl alcohol	0	P12889	1/500	<213	<246	657	<164	<128
R4	Methallyl alcohol	1	P12890	1/500	<213	<246	653	<164	<128
R4	Methallyl alcohol	4	P12891	1/500	<213	<246	638	<164	188
R4	Methallyl alcohol	10	P12892	1/500	364	276	583	<164	491
R4	Methallyl alcohol	13	P12893	1/500	627	398	638	<164	674
R5	Na triphosphate	0	P12894	1/500	<213	<246	666	<164	<128
R5	Na triphosphate	1	P12895	1/500	<213	<246	607	<164	<128
R5	Na triphosphate	4	P12896	1/500	<213	<246	635	<164	<128
R5	Na triphosphate	10	P12897	1/500	<213	<246	583	<164	129
R5	Na triphosphate	13	P12898	1/500	259	<246	581	<164	147

Table 61:IC-EC raw data for experiment 5.

Reactor	Additive	Days	Prøve	Fortynning	Formate [mg/kg]	Nitrate [mg/kg]	Sulphate [mg/kg]	Oxalate [mg/kg]	Nitrite [mg/kg]
R1	Citric acid + Carbohydrazide	0	P121035	1/500	<135	<130	643,4	<183	<134
R1	Citric acid + Carbohydrazide	1	P121036	1/500	<135	<130	667,7	<183	<134
R1	Citric acid + Carbohydrazide	4	P121037	1/500	<135	<130	623,5	<183	178,2
R1	Citric acid + Carbohydrazide	9	P121038	1/500	149,6	184,8	644,5	<183	582,6
R1	Citric acid + Carbohydrazide	13	P121039	1/500	238,5	257,1	668,3	<183	890,2
R2	Na triphosphate + Carbohydrazide	0	P121040	1/500	<135	<130	652,3	<183	<134
R2	Na triphosphate + Carbohydrazide	1	P121041	1/500	<135	<130	623,0	<183	<134
R2	Na triphosphate + Carbohydrazide	4	P121042	1/500	202,1	170,5	672,0	<183	<134
R2	Na triphosphate + Carbohydrazide	9	P121043	1/500	570,3	293,3	679,5	<183	381,0
R2	Na triphosphate + Carbohydrazide	13	P121044	1/500	927,6	387,5	690,3	<183	617,0
R3	HEDP + Carbohydrazide	0	P121045	1/500	<135	<130	631,3	<183	<134
R3	HEDP + Carbohydrazide	1	P121046	1/500	<135	<130	726,1	<183	<134
R3	HEDP + Carbohydrazide	4	P121047	1/500	<135	<130	691,4	<183	<134
R3	HEDP + Carbohydrazide	9	P121048	1/500	156,8	131,6	749,7	<183	390,3
R3	HEDP + Carbohydrazide	13	P121049	1/500	247,7	158,7	760,5	<183	682,5
R4	Metal mix, 98%	0	P121050	1/500	<135	<130	630,6	<183	<134
R4	Metal mix, 98%	1	P121051	1/500	<135	<130	716,7	<183	<134
R4	Metal mix, 98%	4	P121052	1/500	<135	155,8	715,9	<183	140,8
R4	Metal mix, 98%	9	P121053	1/500	249,9	227,5	650,9	<183	323,4
R4	Metal mix, 98%	13	P121054	1/500	417,8	335,8	694,3	<183	481,5
R5	MEKO	0	P121055	1/500	<135	<130	713,2	<183	<134
R5	MEKO	1	P121056	1/500	<135	<130	686,6	<183	<134
R5	MEKO	4	P121057	1/500	<135	219,6	765,0	<183	207,2
R5	MEKO	9	P121058	1/500	176,0	302,8	725,9	<183	340,7
R5	MEKO	13	P121059	1/500	264,3	366,6	699,6	<183	496,7

Table 62:IC-EC raw data circulative experiment with hydrazine.

Reactor	Additive	Day	Sample	Formate [mg/kg]	Nitrite [mg/kg]	Nitrate [mg/kg]	Sulfate [mg/kg]	Oxalate [mg/kg]
Circulative	Hydrazine	0	P121060	<218	<139	<256	<242	<172
Circulative	Hydrazine	1	P121061	<218	<139	<256	<242	<172
Circulative	Hydrazine	2	P121062	<218	<139	<256	<242	<172
Circulative	Hydrazine	4	P121063	<218	<139	<256	<242	<172
Circulative	Hydrazine	7	P121064	<218	<139	<256	<242	<172
Circulative	Hydrazine	11	P121065	383	<139	<256	<242	<172
Circulative	Hydrazine	15	P121066	652	258	<256	<242	<172
Circulative	Hydrazine	19	P121067	1094	149	<256	<242	<172
Circulative	Hydrazine	23	P121068	1312	211	<256	<242	<172

Table 63: IC-EC raw data for quantification of chelating agents from experiments on the inhibitor screening apparatus.

Inhibitor	P. nr.	Dilutions	Signal inhibitor	Concentration inhibitor [mg/kg]	Detection limit
	P12817	0,00220886	0,3036	1215	317
	P12818	0,00220891	0,2865	1142	317
Potassium	P12819	0,00235683	0,2628	974	297
sodium	P12820	0,00232398	0,1616	575	301
tartrate	P12821	0,00221561	0,1358	492	316
	P12827	0,00231931	0,7093	3926	367
	P12828	0,00222006	0,7795	4525	384
	P12829	0,0023334	0,6472	3545	365
	P12830	0,00220888	0,4625	2625	386
Citric acid	P12831	0,00221111	0,3035	1658	385
	P12832	0,00243228	no signal	-	-
	P12833	0,00220666	no signal	-	-
	P12834	0,00224457	no signal	-	-
	P12835	0,00244695	no signal	-	-
HEDP	P12836	0,00233573	no signal	-	-
	P12894	0,00219757	0,642	2737	434
	P12895	0,00244193	0,5891	2270	391
	P12896	0,00226034	0,5957	2478	422
Sodium	P12897	0,00260423	0,4568	1676	366
triphosphate	P12898	0,00249897	0,4043	1560	382

Table 64: IC-EC raw data for the quantification of chelating agents from the experiments conducted at thermal conditions.

Inhibitor	Cylinder material	Week	Concentration [mg/kg]
Potassium sodium tartrate	-	0	1343
	Metal	1	509
	Metal	2	402
	Metal	3	363
	Metal	4	309
	Metal	5	<274
	Glass	1	591
	Glass	2	519
	Glass	3	467
	Glass	4	403
	Glass	5	357
Citric acid	-	0	4520
	Metal	1	<354
	Metal	2	<354
	Metal	3	<354
	Metal	4	<354
	Metal	5	<354
	Glass	1	<354
	Glass	2	<354
	Glass	3	<354
	Glass	4	<354
	Glass	5	<354
HEDP	-	0	818
	Metal	1	891
	Metal	2	1078
	Metal	3	949
	Metal	4	-
	Metal	5	887
	Glass	1	1013
	Glass	2	930
	Glass	3	942
	Glass	4	991
	Glass	5	975
Sodium triphosphate	-	0	2361
	Metal	1	<412
	Metal	2	<412
	Metal	3	<412
	Metal	4	<412
	Metal	5	<412
	Glass	1	<412
	Glass	2	<412
	Glass	3	<412
	Glass	4	<412
	Glass	5	<412

Appendix J: Calculated concentrations of inhibitors

Table 65: Calculated concentrations for the inhibitors added in the experiments on the inhibitor screening apparatus.

Inhibitor	C inhibitor [wt%]	C inhibitor [mg/kg]	C inhibitor [mol/kg]
Potassium sodium tartrate	0,25	2535	0,009
Sodium sulfite	0,59	5929	0,047
Citric acid	0,46	4598	0,024
HEDP	0,18	1823	0,008
Hydroquinone	0,12	1158	0,011
Methallyl alcohol	0,35	3544	0,049
Sodium triphosphate	0,37	3727	0,01
DEHA	0,4	3962	0,044
MEKO	0,41	4064	0,047
Erythorbic acid	0,89	8939	0,051
Carbohydrazide	0,45	4467	0,05
Carbohydrazide	0,45	4491	0,05
HEDP	0,2	1982	0,009
Carbohydrazide	0,43	4340	0,048
Citric acid	0,48	4788	0,025
Carbohydrazide	0,43	4345	0,048
Sodium triphosphate	0,36	3623	0,01

Table 66: Calculated concentrations for the inhibitors added in the experiments at thermal conditions.

Inhibitor	C inhibitor [wt%]	C inhibitor [mg/kg]	C inhibitor [mol/kg]
Potassium sodium tartrate	0,28	2778	0,010
Sodium sulfite	0,71	7094	0,056
Citric acid	0,50	4968	0,026
HEDP	0,19	1915	0,009
Hydroquinone	0,12	1178	0,011
Methallyl alcohol	0,37	3659	0,051
Sodium triphosphate	0,36	3583	0,010
DEHA	0,48	4820	0,054
MEKO	0,44	4386	0,050
Erythorbic acid	0,88	8758	0,050
Carbohydrazide	0,47	4692	0,052

Table 67: Calculated concentration of hydrazine in the experiment screening hydrazine on the circulative closed loop apparatus.

Inhibitor	C inhibitor [wt%]	C inhibitor [mg/kg]	C inhibitor [mol/kg]
Hydrazine hydrate 50-60%	0,29	2928	0,05

Appendix K: Degradation products

Table 68: Specification of degradation products and analytical methods for their quantification in this thesis.

Name	Abbreviation	Structure	Cas. No.	Analytical method
N, N'-bis(2-hydroxyethyl) oxalamide	BHEOX	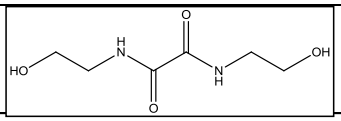	1871-89-2	LC-MS
-	Formate	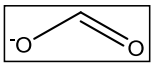	-	IC-EC
N-(2-hydroxyethyl) acetamide	HEA	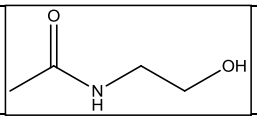	142-26-7	LC-MS
N-(2-hydroxyethyl)formamide	HEF	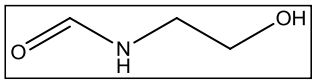	693-26-1	LC-MS
N-(2-hydroxyethyl)glycine	HeGly	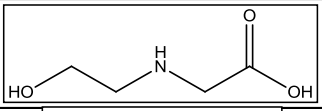	-	LC-MS
N-(2-hydroxyethyl)imidazole	HEI	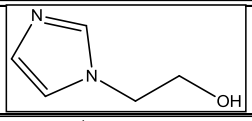	1615-14-1	LC-MS
4-(2-hydroxyethyl)piperazin-2-one	HEPO	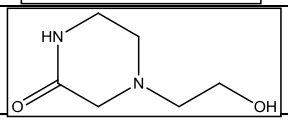	23936-04-1	LC-MS
-	Nitrate	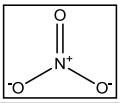		IC-EC
-	Nitrite	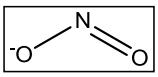		IC-EC
-	Oxalate	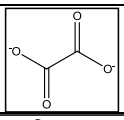		IC-EC
2-oxazolidinone	OZD	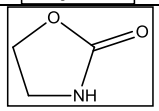	497-25-6	LC-MS
-	Sulfate	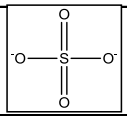		IC-EC

Table of figures

List of tables